

Flavor phenomenology of an extended 2HDM with inverse seesaw mechanism

N. T. Duy* and D. T. Huong†

Institute of Physics, VAST, 10 Dao Tan, Ba Dinh, Hanoi, Vietnam

A. E. Cárcamo Hernández‡

Universidad Técnica Federico Santa María, Casilla 110-V, Valparaíso, Chile

Centro Científico-Tecnológico de Valparaíso, Casilla 110-V, Valparaíso, Chile and

Millennium Institute for Subatomic physics at high energy frontier - SAPHIR, Fernandez Concha 70 Santiago, Chile

(Dated: April 15, 2025)

We perform a detailed and comprehensive study of several flavor physics observables in both lepton and quark sectors within the framework of an extended 2HDM theory where the inverse seesaw mechanism is implemented to generate the SM fermion mass hierarchy. In that theory, the SM gauge symmetry is supplemented by the local $U(1)_X$ and discrete $Z_4 \times Z_2$ groups. In particular, we find that the leptonic flavor observables specifically, the branching ratios of charged lepton flavor violating decays $\mu \rightarrow e\gamma, \tau \rightarrow e(\mu)\gamma$ as well as the anomalous magnetic moments $\Delta a_{e(\mu)}$ strongly depend on the couplings of the neutral CP even(odd) Higgses with exotic charged lepton E_1 , whereas other observables involving three-body leptonic decays $\text{BR}(l \rightarrow 3l')$, $\text{Mu}-\overline{\text{Mu}}$ transition and coherent conversion $\mu \rightarrow e$ in a muonic atom are predicted to be less than several orders of magnitude compared to the corresponding experimental limits. Regarding the quark flavor observables, the most stringent limits arising from the flavor changing neutral currents (FCNC) are those involving the down type quark $d_a \rightarrow d_b$ ($a = 1, 2, 3$) transitions and including the branching ratios of inclusive decay $\text{BR}(\bar{B} \rightarrow X_s\gamma)$, pure leptonic decay of B_s meson $\text{BR}(B_s \rightarrow \mu^+\mu^-)$, and meson mixing $\Delta m_{K, B_s, B_d}$. Considering the obtained constraints from these observables, the new physics contributions to other processes such as $\text{BR}(B_s \rightarrow \tau^+\mu^-)$, $\text{BR}(B^+ \rightarrow K^+\tau^+\tau^-)$, $\text{BR}(B^+ \rightarrow K^+\tau^+\mu^-)$, as well as FCCC $b \rightarrow c$ transition, specifically LFUV ratios $R_{D^{(*)}}$ are shown to be remarkably small. Regarding the observables in the up type quark transitions, the FCNC top quark processes $t \rightarrow u(c)\gamma$ and $t \rightarrow u(c)h$ have branching ratios consistent with the experimental limits. Additionally, observables related to SM-like Higgs boson decays, such as LFV decays $\text{BR}(h \rightarrow \bar{l}l)$ and modified couplings $a_{h\bar{f}f}$ are also discussed.

I. INTRODUCTION

Without a doubt, the Standard Model (SM) is not complete, regardless of its incredible theoretical and phenomenological successes as indicated by the experimental confirmation of its predictions. However, the SM falls short in addressing unsolved puzzles in both theory and experiment. One such puzzle is the unnatural hierarchy observed in the SM fermion masses, which is extended by five orders of magnitude from the electron mass up to the top quark mass. This mass discrepancy widens to thirteen orders of magnitude when considering the neutrino sector. Neutrino oscillation experiments have revealed that active neutrinos have very tiny masses many orders of magnitude smaller than the scale of spontaneous breaking of electroweak symmetry [1–12]. Moreover, the SM fails to account for the substantial disparity between the patterns of quark and lepton mixings. While the mixing angles are small in the quark sector, suggesting that the quark mixing matrix is very close to the identity matrix, the lepton sector exhibits two large mixing angles are large and one small angle, which implies that the leptonic mixing matrix significantly deviates from the identity matrix [13]. Additionally, the SM lacks an explanation of why there are three generations of fermions and the absence of viable Dark Matter (DM) [14, 15] and is unable to accommodate the observed baryon asymmetry of the Universe (BAU) [13, 16]. Furthermore, there are some recent experimental results for low-energy processes induced by flavor-changing neutral currents (FCNCs), such as $b \rightarrow s$, $b \rightarrow c$ transitions, including angular observables, branching ratios of $b \rightarrow ll$ decays [17–21]; as well as lepton flavor universality violating (LFUV) ratios $R_{D^{(*)}}$ [22], which exhibit tensions compared with their corresponding SM values. These tensions have a confidence

*Electronic address: ntduy@iop.vast.vn (Corresponding author)

†Electronic address: dthuong@iop.vast.vn

‡Electronic address: antonio.carcamo@usm.cl

level less than 5σ , often called flavor anomalies.¹ Therefore, these signals could potentially indicate the emergence of new physics (NP). However, it is important to emphasize that these tensions are still controversial since they can be triggered by the lack of efficient calculation for the long distance (LD) effect in SM or issues related to the analysis background of the experiment [25]. In general, we need more efforts to improve the LD calculation in SM for these processes and the analysis technique in measurements to confirm or exclude the possibility of NP in these $b \rightarrow s$ or $b \rightarrow c$ observables. In this work, we choose the scenario where these tensions are potentially caused by NP interactions.

To address the aforementioned issues, many NP models have been proposed by extending the SM including enlarged symmetries, [26],[27–33], expanding particle content [34–41]. Among these NP models, the Two-Higgs-Doublet model (2HDM) [42–45] is one of the most motivated BSM theories. Recently, the authors in Ref. [46] have extended the 2HDM with the inclusion of the $U(1)_X \times Z_4 \times Z_2$ symmetry and new particles including gauge singlet scalars, charged vector-like fermions, right-handed Majorana neutrinos. In that theory, the local $U(1)_X$ and the discrete Z_4 symmetries are spontaneously broken, whereas the Z_2 symmetry is preserved. Within this setup, the model can explain the hierarchy of SM fermion masses via the inverse seesaw mechanism which is implemented in both charged fermion and neutrino sectors. Specifically, the second and first families of SM charged fermions obtain masses from an inverse seesaw mechanism at the tree level and one-loop level, respectively. On the other hand, one of the Higgs doublets, namely ϕ_1 generates the top quark mass, whereas the other one, i.e., ϕ_2 contributes to the generation of the masses of the bottom quark and tau lepton. The tiny masses of active neutrinos are caused by an inverse seesaw mechanism at a two-loop level, whose radiative nature is ensured by the preserved Z_2 symmetry. To the best of our knowledge, this model is the first one explaining the mass hierarchy of the charged fermion sector by an inverse seesaw mechanism. Besides, the model provides stable scalar and fermionic DM candidates due to the preserved Z_2 symmetry. Furthermore, BAU is discussed via the leptogenesis mechanism. The flavor observables data such as meson oscillations $\Delta m_{K, B_s, B_d}$ and electron (muon) anomalous magnetic moments $\Delta a_e, \Delta a_\mu$ are shown to be consistent with the model predictions.

In the model, it is important to note that both charged and neutral CP-even (odd) Higgs bosons couple with the SM and new fermions at the tree level. Furthermore, non-universal assignments between the (first and second) and third quark generations exist under the extended local $U(1)_X$ symmetry. This implies the existence of tree level FCNC interactions between the SM up (down) type quarks, mediated by the exchange of the new neutral gauge boson Z' . Consequently, the model provides rich sources for numerous flavor-violating processes in both lepton and quark sectors at both tree and loop levels. It is worth noting that in Ref. [46], the authors just considered a few flavor phenomenological studies within simplified assumptions of the scalar spectrum and couplings.

In this study, we aim at investigating a variety of flavor phenomenologies related to both leptonic and quark sectors with all possible NP contributions associated with heavy neutral gauge boson Z' and several Higgs bosons (CP-even, CP-odd, and charged Higgs). For the lepton flavor observables, we study the lepton flavor violating (LFV) decays of SM-like Higgs boson $h \rightarrow \bar{l}l$ as well as the modified couplings between h and SM fermions $a_{h\bar{f}f} = \frac{(a_{h\bar{f}f})_{\text{theory}}}{(a_{h\bar{f}f})_{\text{SM}}}$. We investigate the branching ratios for LFV decays of charged leptons $\text{BR}(l \rightarrow l'\gamma)$, three body leptonic decays ($l \rightarrow 3l'$), as well as the transition probability between the muonium (Mu : μ^+e^-) and antimuonium ($\bar{\text{Mu}} : \mu^-e^+$), and $\mu \rightarrow e$ conversion in a muonic atom in detail. In addition, we revise the anomalous magnetic moments for electron and muon $\Delta a_{e(\mu)}$ with all NP contributions. It should be noted that in the previous work [46], $\Delta a_{e(\mu)}$ was only studied under a simplifying benchmark scenario, including few scalar contributions. Moving to the quark sector, we focus on the analysis of flavor observables related with FCNCs in down-type quark transitions. These contain the branching ratios of leptonic decay $\text{BR}(B_s \rightarrow \mu^+\mu^-)$, $\text{BR}(B_s \rightarrow \tau^+\mu^-)$, the inclusive decay $\text{BR}(\bar{B} \rightarrow X_s\gamma)$, semileptonic decays $\text{BR}(B^+ \rightarrow K^+\tau^+\tau^-)$, $\text{BR}(B^+ \rightarrow K^+\tau^+\mu^-)$. The meson oscillation parameters $\Delta m_{K, B_s, B_d}$ are also reconsidered with full NP contributions, as well as $\Delta a_{e(\mu)}$. Furthermore, the FCCC $b \rightarrow c$ transitions, namely the lepton flavor universality violating (LFUV) ratios $R_{D^{(*)}}$, are of great interest. We also study the up-type quark flavor observables, including FCNC top quark decays $t \rightarrow u(c)h$ and radiative decays $t \rightarrow u(c)\gamma$. We would like to notice that this work is not only the update for flavor phenomenologies studies, which were not fully considered in the previous paper [46], but also attempts to investigate in much more detail many classes of flavor observables.

The paper is structured as follows: In Sec. II, we revisit the particle spectrum of the model. Next, in Sec. III, we obtain the benchmark points that satisfy the lepton masses and mixing spectrum. Sec. IV investigates the scalar potential spectrum in detail. We provide analytical expressions for lepton and quark flavor observables in the following section, and then carry out the numerical studies in Sec. VI. Finally, we summarize the main results in the conclusion

¹ The most recent reports by LHCb for LFUV ratios in $b \rightarrow s$ transitions $R_{K^{(*)}}^{\text{LHCb}}$ show the agreement with SM predictions, $R_{K^{(*)}}^{\text{LHCb}} \simeq R_{K^{(*)}}^{\text{SM}} \simeq 1$ [23, 24], therefore the signals of LFUV in $b \rightarrow s$ presently disappear.

	$SU(3)_C$	$SU(2)_L$	$U(1)_Y$	$U(1)_X$	Z_2	Z_4
ϕ_1	1	2	$\frac{1}{2}$	$\frac{1}{3}$	0	-1
ϕ_2	1	2	$\frac{1}{2}$	$\frac{2}{3}$	0	1
σ	1	1	0	$\frac{1}{3}$	0	-1
χ	1	1	0	$\frac{2}{3}$	0	-2
η	1	1	0	-1	0	-1
ρ	1	1	0	2	0	0
κ	1	1	0	2	0	-2
S	1	1	0	0	0	1
ζ_1^+	1	1	1	$\frac{2}{3}$	0	1
ζ_2^+	1	1	1	1	0	0
φ_1	1	1	0	1	1	0
φ_2	1	1	0	0	1	1

Table I: Scalar assignments under $SU(3)_C \times SU(2)_L \times U(1)_Y \times U(1)_X \times Z_2 \times Z_4$.

	$SU(3)_C$	$SU(2)_L$	$U(1)_Y$	$U(1)_X$	Z_2	Z_4
q_{nL}	3	2	$\frac{1}{6}$	0	0	-2
q_{3L}	3	2	$\frac{1}{6}$	$\frac{1}{3}$	0	0
u_{iR}	3	1	$\frac{2}{3}$	$\frac{2}{3}$	0	-1
d_{iR}	3	1	$-\frac{1}{3}$	$-\frac{1}{3}$	0	-1
U_L	3	1	$\frac{2}{3}$	$\frac{1}{3}$	0	0
U_R	3	1	$\frac{2}{3}$	$\frac{2}{3}$	0	-1
T_L	3	1	$\frac{2}{3}$	$-\frac{1}{3}$	0	2
T_R	3	1	$\frac{2}{3}$	$-\frac{1}{3}$	0	2
D_{1L}	3	1	$-\frac{1}{3}$	0	0	-2
D_{1R}	3	1	$-\frac{1}{3}$	$-\frac{1}{3}$	0	-1
D_{2L}	3	1	$-\frac{1}{3}$	0	1	-1
D_{2R}	3	1	$-\frac{1}{3}$	$-\frac{1}{3}$	0	0
B_L	3	1	$-\frac{1}{3}$	$\frac{2}{3}$	0	0
B_R	3	1	$-\frac{1}{3}$	$\frac{2}{3}$	0	0

Table II: Quark assignments under $SU(3)_C \times SU(2)_L \times U(1)_Y \times U(1)_X \times Z_2 \times Z_4$. Here $i = 1, 2, 3$ and $n = 1, 2$.

section.

II. THE REVIEW OF MODEL

In this section, we briefly review the extended 2HDM model with the universal inverse seesaw mechanism. The model is based on the $SU(3)_C \times SU(2)_L \times U(1)_Y \times U(1)_X$ gauge symmetry supplemented by the discrete group $Z_4 \times Z_2$. The spontaneous breaking of the $SU(3)_C \times SU(2)_L \times U(1)_Y \times U(1)_X \times Z_4$ symmetry allows the radiative inverse seesaw mechanism at two-loop level, resulting in the tiny masses of active neutrinos, while the Z_2 symmetry remains preserved. The scalar sector of the model consists of two Higgs doublets ϕ_1 and ϕ_2 , with different charges under $U(1)_X$ and Z_4 symmetries, along with 10 gauge singlets. The particle spectrum of the model and their transformations under the group $SU(3)_C \times SU(2)_L \times U(1)_Y \times U(1)_X \times Z_2 \times Z_4$ are displayed in Tables I, III, II. With the previously specified

	$SU(3)_C$	$SU(2)_L$	$U(1)_Y$	$U(1)_X$	Z_2	Z_4
l_{iL}	1	2	$-\frac{1}{2}$	$-\frac{1}{3}$	0	0
l_{nR}	1	1	-1	-1	0	2
l_{3R}	1	1	-1	-1	0	-1
E_{1L}	1	1	-1	-1	0	1
E_{1R}	1	1	-1	-1	0	-1
E_{2L}	1	1	-1	1	0	1
E_{2R}	1	1	-1	1	0	1
ν_{iR}^C	1	1	0	$-\frac{1}{3}$	0	-1
N_{iR}	1	1	0	0	0	-2
Ψ_{nR}	1	1	0	1	1	2
Ω_{nR}	1	1	0	-1	0	-1

Table III: Lepton assignments under $SU(3)_C \times SU(2)_L \times U(1)_Y \times U(1)_X \times Z_2 \times Z_4$. Here $i = 1, 2, 3$ and $n = 1, 2$.

particle content and symmetries, the following quark and leptonic Yukawa interactions arise:

$$\begin{aligned}
-\mathcal{L}_Y^{(q)} = & \sum_{i=1}^3 y_i^{(u)} \bar{q}_{3L} \tilde{\phi}_1 u_{iR} + \sum_{i=1}^3 y_i^{(d)} \bar{q}_{3L} \phi_2 d_{iR} + \sum_{n=1}^2 x_n^{(U)} \bar{q}_{nL} \tilde{\phi}_2 U_R + \sum_{n=1}^2 x_n^{(D)} \bar{q}_{nL} \phi_1 D_{1R} \\
& + z_D \bar{D}_{2L} \sigma D_{2R} + \sum_{i=1}^3 x_i^{(u)} \bar{U}_L \sigma^* u_{iR} + z_T \bar{U}_L \chi T_R + z_U \bar{T}_L \eta U_R + m_T \bar{T}_L T_R \\
& + \sum_{i=1}^3 x_i^{(d)} \bar{D}_{1L} \sigma d_{iR} + z_B \bar{D}_{1L} \chi^* B_R + z_D \bar{B}_L \eta^* D_{1R} + m_B \bar{B}_L B_R \\
& + \sum_{i=1}^3 w_i^{(u)} \bar{D}_{1L} \zeta_1^- u_{iR} + \sum_{i=1}^3 w_i^{(d)} \bar{U}_L \zeta_1^+ d_{iR} + H.c., \tag{1}
\end{aligned}$$

$$\begin{aligned}
-\mathcal{L}_Y^{(l)} = & \sum_{i=1}^3 y_i^{(l)} \bar{l}_{iL} \phi_2 l_{3R} + \sum_{i=1}^3 y_i^{(E)} \bar{l}_{iL} \phi_2 E_{1R} + \sum_{n=1}^2 x_n^{(l)} \bar{E}_{1L} S^* l_{nR} + y_E \bar{E}_{1L} \rho^* E_{2R} + x_E \bar{E}_{2L} \kappa E_{1R} + m_E \bar{E}_{2L} E_{2R} \\
& + \sum_{i=1}^3 \sum_{j=1}^3 y_{ij}^{(\nu)} \bar{l}_{iL} \tilde{\phi}_2 \nu_{jR} + \sum_{i=1}^3 \sum_{n=1}^2 z_{in}^{(l)} \bar{N}_{iR}^C \zeta_2^+ l_{nR} + \sum_{i=1}^3 \sum_{j=1}^3 y_{ij}^{(N)} \nu_{iR} \sigma^* \bar{N}_{jR}^C + \sum_{i=1}^3 \sum_{n=1}^2 (x_N)_{in} \bar{N}_{iR} \Psi_{nR}^C \varphi_1 \\
& + \sum_{n=1}^2 \sum_{m=1}^2 (x_\Psi)_{nm} \bar{\Psi}_{nR} \varphi_2 \Omega_{mR}^C + \sum_{n=1}^2 \sum_{m=1}^2 (y_\Omega)_{nm} \bar{\Omega}_{nR} \Omega_{mR}^C \kappa^* + H.c.. \tag{2}
\end{aligned}$$

We would like to note that some of Lagrangian Yukawa terms in previous work [46] are not invariant under Z_4 symmetry if the Z_4 charges of particles are assigned as shown in this reference. For example, the first term in Eq. (1) and the fourth, and fifth terms in Eq. (2) are not invariant concerning Z_4 symmetry. Therefore, in the present work, we redefine the charges of particle content, as given in the Tables I, II and III, so that the structure of the Yukawa Lagrangian terms for quark and lepton is maintained. In particular, the Z_4 charge of the new singlet charged scalar ζ_1^\pm is assigned as +1, instead of -1 as in [46], thus giving it the same quantum numbers as the charged singlet ζ_3^\pm . Consequently, one of these charged singlets can be removed; for instance, we choose to remove ζ_3^\pm . However, the new neutral singlet κ is proposed to ensure that the fourth and fifth terms in the first line of Eq. (2) are invariant. Therefore, the total number of scalar fields remains unchanged, and the results of previous work remain valid.

III. THE CHARGED LEPTON SECTOR

In Ref. [46], a detailed numerical analysis of the quark masses and mixing was performed, and the corresponding benchmark point that successfully reproduces the quark masses and CKM mixing parameters were provided. However,

the benchmark point that successfully accommodates the lepton masses and mixings was not provided in [46] In this section, we perform a numerical analysis of lepton masses and mixings. From the charged lepton Yukawa interactions, it is found in [46] that the mass matrix for SM charged leptons takes the form:

$$\widetilde{M}_E = C_E + \frac{m_E}{X_E Y_E} F_E G_E^T + \Delta_E. \quad (3)$$

where

$$M_E = \begin{pmatrix} C_E + \Delta_E & F_E & 0_{3 \times 1} \\ G_E^T & 0 & X_E \\ 0_{1 \times 3} & Y_E & m_E \end{pmatrix}, \quad (F_E)_i = y_i^{(E)} \frac{v_2}{\sqrt{2}}, \quad (G_E^T)_n = x_n^{(l)} \frac{v_S}{\sqrt{2}}, \quad (G_E^T)_3 = 0, \\ C_E = \begin{pmatrix} 0 & 0 & y_1^{(l)} \\ 0 & 0 & y_2^{(l)} \\ 0 & 0 & y_3^{(l)} \end{pmatrix} \frac{v_2}{\sqrt{2}}, \quad X_E = y_E \frac{v_\rho}{\sqrt{2}}, \quad Y_E = x_E \frac{v_\kappa}{\sqrt{2}}, \quad i = 1, 2, 3, \quad n = 1, 2, \quad (4)$$

and

$$\Delta_E = \frac{m_{\widetilde{E}}}{16\pi^2} \sum_{i=1}^3 \begin{pmatrix} r_{1i}^{(E)} w_{1i}^{(E)} & r_{1i}^{(E)} w_{2i}^{(E)} & 0 \\ r_{2i}^{(E)} w_{1i}^{(E)} & r_{2i}^{(E)} w_{2i}^{(E)} & 0 \\ r_{1i}^{(E)} w_{3i}^{(E)} & r_{2i}^{(E)} w_{3i}^{(E)} & 0 \end{pmatrix} \frac{m_{H_i^\pm}^2}{m_{H_i^\pm}^2 - m_{\widetilde{E}}^2} \ln \left(\frac{m_{H_i^\pm}^2}{m_{\widetilde{E}}^2} \right). \quad (5)$$

The first term in Eq. (3) provides the dominant contribution to the SM charged lepton mass matrix and arises from the renormalizable Yukawa interaction involving the $SU(2)_L$ scalar doublet ϕ_2 . resulting in the tau lepton mass. Conversely, the second and third terms of Eq. (3) stem from the inverse seesaw mechanism at the tree and one loop levels, respectively, contributing to the masses of muon and electron. By solving the eigenvalue problem of the SM charged lepton mass matrix, we successfully reproduce the experimental values for charged lepton masses, [13, 47] with the following benchmark point:

$$v_S \simeq 6 \text{ TeV}, \quad v_\rho = v_\kappa \simeq 1 \text{ TeV}, \quad m_E \simeq 1.12653 \text{ GeV}, \quad m_{\widetilde{E}} \simeq 4.243 \text{ TeV}, \quad (6)$$

$$y_1^{(l)} \simeq 0.0707, \quad y_2^{(l)} \simeq -0.0066, \quad y_3^{(l)} \simeq 0.0117, \quad y_1^{(E)} \simeq 0.086, \quad y_2^{(E)} \simeq -0.05, \quad y_3^{(E)} \simeq -0.0364 \\ x_1^{(l)} \simeq 0.0645, \quad x_2^{(l)} \simeq -0.113, \quad y_E = x_E \simeq 1.3131, \quad r_{1j}^{(E)} \simeq -0.0961, \quad r_{2j}^{(E)} \simeq -0.0331, \\ w_{1j}^{(E)} \simeq -0.1, \quad w_{2j}^{(E)} \simeq 0.0538, \quad w_{3j}^{(E)} \simeq -0.0915. \quad (7)$$

IV. SCALAR SECTOR

The full scalar potential of the model which is invariant under the gauge and discrete symmetries can be split as follows following summation

$$V = V_\phi + V_{\text{neutral singlets}} + V_{\text{charged singlets}} + V_{\text{odd } Z_2 \text{ singlets}} + V_{\text{mix}}, \quad (8)$$

where $V_\phi, V_{\text{neutral singlets}}, V_{\text{charged singlets}}, V_{\text{odd } Z_2 \text{ singlets}}, V_{\text{mix}}$ correspond to the scalar potential of two doublets $\phi_{1,2}$, 6 neutral singlets $\sigma, \chi, \eta, \rho, \kappa, S$, 2 charge singlets $\zeta_{1,2}^\pm$, and two odd Z_2 singlets $\varphi_{1,2}$ and mixing between them, respectively. These different contributions are given by:

$$V_\phi = \sum_{j=1}^2 (|\phi_j|^2 + \lambda_j |\phi_j|^4) + \lambda_{12} |\phi_1|^2 |\phi_2|^2 + \tilde{\lambda}_{12} (\phi_1^\dagger \phi_2) (\phi_2^\dagger \phi_1) + \lambda'_{12} [\epsilon_{ab} \epsilon_{cd} (\phi_1)^a (\phi_2)^b (\phi_1^\dagger)^c (\phi_2^\dagger)^d + H.c.], \quad (9)$$

$$V_{\text{neutral singlets}} = \sum_{j=\sigma}^{\kappa} (\mu_j^2 |s_j|^2 + \lambda_j |s_j|^4) + |\sigma|^2 \sum_{j=\chi}^{\kappa} \lambda_{\sigma j} |s_j|^2 + |\chi|^2 \sum_{j=\eta}^{\kappa} \lambda_{\chi j} |s_j|^2 + |\eta|^2 \sum_{j=\rho}^{\kappa} \lambda_{\eta j} |s_j|^2 \\ + |\rho|^2 \sum_{j=S}^{\kappa} \lambda_{\rho j} |s_j|^2 + \lambda_{S\kappa} |S|^2 |\kappa|^2, \quad (10)$$

$$V_{\text{charged singlets}} = \sum_{j=1}^2 [\mu_{cj}^2 \zeta_i^+ \zeta_i^- + \lambda_{cj} (\zeta_i^+ \zeta_i^-)^2] + \lambda_{\zeta_{12}} (\zeta_1^- \zeta_1^+) (\zeta_2^- \zeta_2^+), \quad (11)$$

$$V_{\text{odd } Z_2 \text{ singlets}} = \sum_{j=1}^2 (\mu_{oj}^2 |\varphi_j|^2 + \lambda_{oj} |\varphi_j|^4) + \tilde{\lambda}_{o2} \varphi_2^4 + 2\lambda_{\varphi_{12}} |\varphi_1|^2 |\varphi_2|^2, \quad (12)$$

$$\begin{aligned} V_{\text{mix}} = & \sum_{j=1}^2 \sum_{k=1}^2 \alpha_{jk} |\phi_j|^2 (\zeta_k^+ \zeta_k^-) + \sum_{j=\sigma}^{\kappa} \sum_{k=1}^2 \beta_{jk} |s_j|^2 (\zeta_k^+ \zeta_k^-) + \sum_{j=1}^2 \sum_{k=1}^2 \gamma_{jk} \varphi_j^2 (\zeta_k^+ \zeta_k^-) \\ & + \sum_{j=1}^2 \sum_{k=\sigma}^{\kappa} \varkappa_{jk} |\phi_j|^2 |s_k|^2 + \sum_{j=1}^2 \sum_{k=1}^2 \varsigma_{jk} |\phi_j|^2 |\varphi_k|^2 + \sum_{j=1}^2 \sum_{k=\sigma}^{\kappa} \varrho_{jk} |\varphi_j|^2 |s_k|^2 \\ & + B_1 (\sigma \chi \eta + H.c.) + B_2 (\zeta_1^+ \zeta_2^- \sigma + H.c.) + B_3 (\epsilon_{ab} \phi_1^a \phi_2^b \zeta_2^- + H.c.) + B_4 (\eta^2 \kappa + H.c.) + B_5 (\sigma^2 \chi^* + H.c.) \\ & + f_1 (\epsilon_{ab} \phi_1^a \phi_2^b \zeta_1^- \sigma^* + H.c.) + f_2 (\phi_1^\dagger \phi_2 \sigma^* S + H.c.) + f_3 (\zeta_1^- \zeta_2^+ \eta \chi + H.c.) + f_4 (\sigma^3 \eta + H.c.) \\ & + f_5 (\chi^2 \sigma^* \eta + H.c.) + f_6 (\zeta_1^- \zeta_2^+ \chi^* \sigma + H.c.) + f_7 (S^4 + H.c.) + f_8 (\sigma \chi \eta^* \kappa^* + H.c.) \\ & + f_9 (\rho \kappa^* S^2 + H.c.) + f_{10} (\rho \kappa^* S^{*2} + H.c.) + f_{11} (\rho^2 \kappa^{*2} + H.c.) + f_{12} (\chi^3 \kappa^* + H.c.) \\ & + f_{13} (\varphi_1^* \varphi_2 \eta \rho + H.c.), \end{aligned} \quad (13)$$

where s_j denotes the neutral singlets $\sigma, \chi, \eta, \rho, S, \kappa$, respectively. It is important to note that the couplings B_i , ($i = 1, \dots, 5$) have mass dimension, whereas f_j , ($j = 1, \dots, 13$) are dimensionless. Expanding the even Z_2 Higgs multiplets around their minimum, excepting $\varphi_{1,2}$ since they are charged under Z_2 symmetry, we have

$$\begin{aligned} \phi_{1,2} &= \begin{pmatrix} \phi_{1,2}^+ \\ \frac{v_{1,2} + \phi_{1,2R}^0 + i\phi_{1,2I}^0}{\sqrt{2}} \end{pmatrix}, \quad s = \frac{v_s + s_R + i s_I}{\sqrt{2}}, \quad s = \sigma, \dots, \kappa, \\ \varphi_{1,2} &= \frac{\varphi_{9,10R} + i\varphi_{9,10I}}{\sqrt{2}} \end{aligned} \quad (14)$$

From the minimization conditions of the scalar potential, we obtain the following relations

$$\begin{aligned} \mu_1^2 &= -\frac{1}{2} \left(\frac{f_2 v_2 v_S v_\sigma}{v_1} + 2\lambda_1 v_1^2 + (\tilde{\lambda}_{12} + \lambda'_{12}) v_2^2 + \sum_{j=\sigma}^S \varkappa_{1j} v_j^2 \right), \\ \mu_2^2 &= -\frac{1}{2} \left(\frac{f_2 v_1 v_S v_\sigma}{v_2} + 2\lambda_2 v_2^2 + (\tilde{\lambda}_{12} + \lambda'_{12}) v_1^2 + \sum_{j=\sigma}^S \varkappa_{2j} v_j^2 \right), \\ \mu_\sigma^2 &= -\frac{1}{2} \left(\frac{f_2 v_2 v_1 v_S}{v_\sigma} + 3f_4 v_\eta v_\sigma + 2\lambda_\sigma v_\sigma^2 + \frac{v_\eta v_\chi (\sqrt{2} B_1 + f_8 v_\kappa + f_5 v_\chi)}{v_\sigma} + 2\sqrt{2} B_5 v_\chi + \sum_{j=1}^2 \varkappa_{j\sigma} v_j^2 + \sum_{j=\chi, \eta, \rho, S, \kappa} \lambda_{\sigma j} v_j^2 \right), \\ \mu_\eta^2 &= -\frac{1}{2} \left(2\sqrt{2} B_4 v_\kappa + \frac{f_4 v_\sigma^3}{v_\eta} + 2\lambda_\eta v_\eta^2 + \lambda_{\sigma\eta} v_\sigma^2 + \frac{v_\sigma v_\chi (\sqrt{2} B_1 + f_8 v_\kappa + f_5 v_\chi)}{v_\eta} + \sum_{j=1}^2 \varkappa_{j\eta} v_j^2 + \sum_{j=\sigma, \chi, \rho, S, \kappa} \lambda_{\eta j} v_j^2 \right), \\ \mu_\chi^2 &= -\frac{1}{2} \left(\frac{\sqrt{2} v_\sigma (B_1 v_\eta + B_5 v_\sigma)}{v_\chi} + \frac{f_8 v_\sigma v_\eta v_\kappa}{v_\chi} + 2f_5 v_\eta v_\sigma + 3f_{12} v_\kappa v_\chi + 2\lambda_\chi v_\chi^2 + \sum_{j=1}^2 \varkappa_{j\chi} v_j^2 + \sum_{j=\sigma, \eta, \rho, S, \kappa} \lambda_{\chi j} v_j^2 \right), \\ \mu_\rho^2 &= -\frac{1}{2} \left(\frac{(f_{10} + f_9) v_S^2 v_\kappa}{v_\rho} + 2\lambda_\rho v_\rho^2 + 2f_{11} v_\kappa^2 + \sum_{j=1}^2 \varkappa_{j\rho} v_j^2 + \sum_{j=\sigma, \chi, \eta, S, \kappa} \lambda_{\rho j} v_j^2 \right), \\ \mu_S^2 &= -\frac{1}{2} \left(\frac{f_2 v_1 v_2 v_\sigma}{v_S} + 2v_S^2 (\lambda_S + 2f_7) + 2(f_9 + f_{10}) v_\rho v_\kappa + \sum_{j=1}^2 \varkappa_{jS} v_j^2 + \sum_{j=\sigma, \chi, \eta, \rho, \kappa} \lambda_{Sj} v_j^2 \right), \\ \mu_\kappa^2 &= -\frac{1}{2} \left(\frac{\sqrt{2} B_4 v_\eta^2}{v_\kappa} + \frac{(f_{10} + f_9) v_S^2 v_\rho}{v_\kappa} + \frac{f_8 v_\eta v_\sigma v_\chi + f_{12} v_\chi^3}{v_\kappa} + 2\lambda_\kappa v_\kappa^2 + 2f_{11} v_\rho^2 + \sum_{j=1}^2 \varkappa_{j\kappa} v_j^2 + \sum_{j=\sigma, \chi, \eta, \rho, S} \lambda_{\kappa j} v_j^2 \right). \end{aligned} \quad (15)$$

A. Charged sector

From the scalar potential and taking into account its minimization conditions, we find that the squared mass matrix for the electrically charged scalar fields in the basis $(\phi_1^+ \phi_2^+ \zeta_1^+ \zeta_2^+)^T$ is given by:

$$M_c^2 = \begin{pmatrix} -\frac{v_2(f_2 v_S v_\sigma + v_1 v_2(\tilde{\lambda}_{12} - 2\lambda'_{12}))}{2v_1} & \frac{f_2 v_S v_\sigma + v_1 v_2(\tilde{\lambda}_{12} - 2\lambda'_{12})}{2} & \frac{f_1 v_2 v_\sigma}{2} & \frac{B_3 v_2}{\sqrt{2}} \\ \frac{f_2 v_S v_\sigma + v_1 v_2(\tilde{\lambda}_{12} - 2\lambda'_{12})}{2} & -\frac{v_1(f_2 v_S v_\sigma + v_1 v_2(\tilde{\lambda}_{12} - 2\lambda'_{12}))}{2v_2} & -\frac{f_1 v_1 v_\sigma}{2} & -\frac{B_3 v_1}{\sqrt{2}} \\ \frac{f_1 v_2 v_\sigma}{2} & -\frac{f_1 v_1 v_\sigma}{2} & (M_c^2)_{33} & \frac{\sqrt{2} B_2 v_\sigma + f_3 v_\eta v_\chi + f_6 v_\sigma v_\chi}{2} \\ \frac{B_3 v_2}{\sqrt{2}} & -\frac{B_3 v_1}{\sqrt{2}} & \frac{\sqrt{2} B_2 v_\sigma + f_3 v_\eta v_\chi + f_6 v_\sigma v_\chi}{2} & (M_c^2)_{44} \end{pmatrix}, \quad (16)$$

where the 33 and 44 matrix elements are defined as

$$\begin{aligned} (M_c^2)_{33} &= \mu_{\zeta_1}^2 + \frac{1}{2} \left(\sum_{j=1}^2 \alpha_{j1} v_j^2 + \sum_{j=\sigma}^{\kappa} \beta_{j1} v_j^2 \right), \\ (M_c^2)_{44} &= \mu_{\zeta_2}^2 + \frac{1}{2} \left(\sum_{j=1}^2 \alpha_{j2} v_j^2 + \sum_{j=\sigma}^{\kappa} \beta_{j2} v_j^2 \right). \end{aligned} \quad (17)$$

This matrix contains one vanishing eigenvalue, corresponding to the SM Goldstone bosons G_{W^\pm} associated with the longitudinal components of the W_μ^\pm bosons. The remaining eigenstates are massive and depend on the new physics scales $v_\sigma, \dots, v_\kappa$, which generally have very complicated forms. However, we can use the perturbation method to approximately diagonalize this matrix in the limit $v_{1,2} \ll v_\sigma, \dots, v_\kappa$ and $B_i \sim \mathcal{O}(10^{-3} - 10^{-2})$ TeV $\ll v = \sqrt{v_1^2 + v_2^2} \sim 0.246$ TeV, $f_i \sim \mathcal{O}(10^{-3} - 10^{-2}) \ll 1$, assuming that all mass dimension(less) couplings B_i and f_i are the same for different indices i . Additionally, we assume that the couplings between the doublet scalars $\phi_{1,2}$ with charged singlets $\zeta_{1,2}^\pm$ satisfy $\alpha_{11} \sim \alpha_{12}, \alpha_{21} \sim \alpha_{22}$. Therefore, the original matrix can be split into two parts such as $M_c^2 = M_{c_0}^2 + M_{c_p}^2$ where $M_{c_0}^2$ is the leading matrix obtained in the limit $B, v \rightarrow 0$, and inversely $M_{c_p}^2$ contains B, v terms. At the first-order in $\mathcal{O}(v^2/v_{\sigma, \dots, \kappa}^2)$, we find that the physical masses and states of electrically charged scalars are given as follows:

$$\begin{aligned} m_{G_W^\pm}^2 &= 0, \quad m_{H^\pm}^2 \simeq -\frac{f v_S v_\sigma}{s_{2\alpha}} - \frac{v^2(\tilde{\lambda}_{12} - 2\lambda'_{12})}{2}, \\ m_{H_{1,2}^\pm}^2 &\simeq \frac{1}{2} \left\{ \left(\mu_{\zeta_1}^2 + \mu_{\zeta_2}^2 + \sum_{j=\sigma}^{\kappa} \frac{(\beta_{j1} + \beta_{j2}) v_j^2}{2} \right) \right. \\ &\quad \mp \sqrt{\left(\mu_{\zeta_1}^2 - \mu_{\zeta_2}^2 + \sum_{j=\sigma}^{\kappa} \frac{(\beta_{j1} - \beta_{j2}) v_j^2}{2} \right)^2 + [f v_\chi (v_\eta + v_\sigma)]^2} \\ &\quad \left. + \frac{v^2[\alpha_{12} + \alpha_{22} + (\alpha_{12} - \alpha_{22})c_{2\alpha}]}{4} \pm \frac{B v_\sigma s_{2\theta}}{\sqrt{2}} \right\}, \end{aligned} \quad (18)$$

where the coupling f satisfies $f < 0$ to ensure that the squared masses are positive. The physical eigenstates are related to the gauge eigenstates of charged scalars by the following relation:

$$(G_W^\pm \ H^\pm \ H_1^\pm \ H_2^\pm)^T = U_c (\phi_1^\pm \ \phi_2^\pm \ \zeta_1^\pm \ \zeta_2^\pm)^T, \quad (20)$$

where the mixing matrix U_c is given by

$$U_c \simeq \begin{pmatrix} c_\alpha & -s_\alpha & 0 & 0 \\ s_\alpha & c_\alpha & \frac{v[f v_\sigma (\epsilon_1 + \epsilon_2) - (\epsilon_1 - \epsilon_2)(f v_\sigma c_{2\theta} + \sqrt{2} B s_\theta)]}{4\epsilon_1 \epsilon_2} & \frac{v[\sqrt{2} B (\epsilon_1 + \epsilon_2) + (\epsilon_1 - \epsilon_2)(-f v_\sigma s_{2\theta} + \sqrt{2} B c_{2\theta})]}{4\epsilon_1 \epsilon_2} \\ \frac{v s_\alpha (f v_\sigma c_\theta + \sqrt{2} B s_\theta)}{2\epsilon_1} & -\frac{v c_\alpha (f v_\sigma c_\theta + \sqrt{2} B s_\theta)}{2\epsilon_1} & c_\theta - \frac{B v_\sigma c_{2\theta} s_\theta}{\sqrt{2}(\epsilon_1 - \epsilon_2)} & s_\theta + \frac{B v_\sigma c_{2\theta} c_\theta}{\sqrt{2}(\epsilon_1 - \epsilon_2)} \\ \frac{v s_\alpha (-f v_\sigma s_\theta + \sqrt{2} B c_\theta)}{2\epsilon_2} & \frac{v c_\alpha (f v_\sigma s_\theta - \sqrt{2} B c_\theta)}{2\epsilon_2} & -s_\theta - \frac{B v_\sigma c_{2\theta} c_\theta}{\sqrt{2}(\epsilon_1 - \epsilon_2)} & c_\theta - \frac{B v_\sigma c_{2\theta} s_\theta}{\sqrt{2}(\epsilon_1 - \epsilon_2)} \end{pmatrix} \quad (21)$$

and the mixing angles α, θ and terms ϵ_1, ϵ_2 defined as

$$t_\alpha = \frac{v_2}{v_1}, \quad t_{2\theta} = \frac{fv_\chi(v_\eta + v_\sigma)}{\mu_{\zeta_1}^2 - \mu_{\zeta_2}^2 + \sum_{j=\sigma}^{\kappa} (\beta_{j1} - \beta_{j2})v_j^2/2}, \quad (22)$$

$$\begin{aligned} \epsilon_{1,2} &= m_{H_{1,2}^\pm}^2 - m_{H^\pm}^2 = \frac{1}{2} \left\{ \left(\mu_{\zeta_1}^2 + \mu_{\zeta_2}^2 + \sum_{j=\sigma}^{\kappa} \frac{(\beta_{j1} + \beta_{j2})v_j^2}{2} \right) \right. \\ &\quad \mp \sqrt{\left(\mu_{\zeta_1}^2 - \mu_{\zeta_2}^2 + \sum_{j=\sigma}^{\kappa} \frac{(\beta_{j1} - \beta_{j2})v_j^2}{2} \right)^2 + [fv_\chi(v_\eta + v_\sigma)]^2} \left. \right\} + \frac{fv_S v_\sigma}{s_{2\alpha}}. \end{aligned} \quad (23)$$

B. CP odd sector

The squared mass matrix of the CP-odd scalar fields in the basis $(\phi_{1I}^0 \phi_{2I}^0 \sigma_I \eta_I \chi_I \rho_I S_I \kappa_I)^T$ can be written as:

$$M_A^2 = \begin{pmatrix} M_{A_1}^2 & (M_{A_2}^2)^T \\ M_{A_2}^2 & M_{A_3}^2 \end{pmatrix}, \quad (24)$$

where the submatrices $M_{A_{1,2,3}}^2$ are given by

$$\begin{aligned} M_{A_1}^2 &= \begin{pmatrix} -\frac{f_2 v_2 v_S v_\sigma}{2v_1} & \frac{f_2 v_S v_\sigma}{2} \\ \frac{f_2 v_S v_\sigma}{2} & -\frac{f_2 v_1 v_S v_\sigma}{2v_2} \end{pmatrix}, \quad M_{A_2}^2 = \begin{pmatrix} -\frac{f_2 v_2 v_S}{2} & \frac{f_2 v_1 v_S}{2} \\ 0 & 0 \\ 0 & 0 \\ 0 & 0 \\ \frac{f_2 v_2 v_\sigma}{2} & -\frac{f_2 v_1 v_\sigma}{2} \\ 0 & 0 \end{pmatrix}, \\ M_{A_3}^2 &= \begin{pmatrix} (m_{A_3}^2)_{11} & (m_{A_3}^2)_{12} & (m_{A_3}^2)_{13} & 0 & \frac{f_2 v_1 v_2}{2} & \frac{f_8 v_\eta v_\chi}{2} \\ (m_{A_3}^2)_{12} & (m_{A_3}^2)_{22} & (m_{A_3}^2)_{23} & 0 & 0 & (m_{A_3}^2)_{26} \\ (m_{A_3}^2)_{13} & (m_{A_3}^2)_{23} & (m_{A_3}^2)_{33} & 0 & 0 & \frac{f_8 v_\sigma v_\eta + 3f_{12} v_\chi^2}{2} \\ 0 & 0 & 0 & (m_{A_3}^2)_{44} & (f_{10} - f_9)v_S v_\kappa & (m_{A_3}^2)_{46} \\ \frac{f_2 v_1 v_2}{2} & 0 & 0 & (f_{10} - f_9)v_S v_\kappa & (M_{A_3}^2)_{55} & (-f_{10} + f_9)v_S v_\rho \\ \frac{f_8 v_\eta v_\chi}{2} & (M_{A_3}^2)_{26} & \frac{f_8 v_\sigma v_\eta + 3f_{12} v_\chi^2}{2} & (m_{A_3}^2)_{46} & (-f_{10} + f_9)v_S v_\rho & (m_{A_3}^2)_{66} \end{pmatrix}, \end{aligned} \quad (25)$$

with some matrix elements of $M_{A_3}^2$ defined as follows

$$\begin{aligned}
(m_{A_3}^2)_{11} &= -\frac{f_2 v_1 v_2 v_S + 9f_4 v_\eta v_\sigma^2 + 4\sqrt{2}B_5 v_\sigma v_\chi + v_\eta v_\chi(\sqrt{2}B_1 + f_8 v_\kappa + f_5 v_\chi)}{2v_\sigma}, \\
(m_{A_3}^2)_{12} &= \frac{-3f_4 v_\sigma^2 + v_\chi(-\sqrt{2}B_1 + f_8 v_\kappa + f_5 v_\chi)}{2}, \\
(m_{A_3}^2)_{13} &= \sqrt{2}B_5 v_\sigma - \frac{v_\eta(\sqrt{2}B_1 + f_8 v_\kappa - 2f_5 v_\chi)}{2}, \\
(m_{A_3}^2)_{22} &= -2\sqrt{2}B_4 v_\kappa - \frac{v_\sigma[f_4 v_\sigma^2 + v_\chi(\sqrt{2}B_1 + f_8 v_\kappa + f_5 v_\chi)]}{2v_\eta}, \\
(m_{A_3}^2)_{23} &= -\frac{v_\sigma(\sqrt{2}B_1 - f_8 v_\kappa + 2f_5 v_\chi)}{2}, \\
(m_{A_3}^2)_{26} &= -\sqrt{2}B_4 v_\eta - \frac{f_8 v_\sigma v_\chi}{2}, \\
(m_{A_3}^2)_{33} &= -\frac{\sqrt{2}B_1 v_\eta v_\sigma + f_8 v_\eta v_\sigma v_\kappa + \sqrt{2}B_5 v_\sigma^2 + 4f_5 v_\eta v_\sigma v_\chi + 9f_{12} v_\kappa v_\chi^2}{2v_\chi}, \\
(m_{A_3}^2)_{44} &= -2f_{11} v_\kappa^2 - \frac{(f_{10} + f_9)v_S^2 v_\kappa}{2v_\rho}, \\
(m_{A_3}^2)_{46} &= 2f_{11} v_\kappa v_\rho + \frac{(f_{10} + f_9)v_S^2}{2}, \\
(m_{A_3}^2)_{55} &= -8f_7 v_S^2 - 2(f_{10} + f_9)v_\kappa v_\rho - \frac{f_2 v_1 v_2 v_\sigma}{2v_S}, \\
(m_{A_3}^2)_{66} &= -\frac{\sqrt{2}B_4 v_\eta^2 + v_\rho[(f_{10} + f_9)v_S^2 + 4f_{11} v_\kappa v_\rho] + f_8 v_\eta v_\sigma v_\kappa + f_{12} v_\chi^3}{2v_\kappa}. \tag{26}
\end{aligned}$$

The matrix M_A^2 will be perturbatively diagonalized by a similar method used in the diagonalization of M_c^2 , i.e we split this matrix into leading and perturbative parts as $M_A^2 = M_{A_0}^2 + M_{A_p}^2$, where $M_{A_0}^2$ is obtained in the limit $B, v \rightarrow 0$. It should be noted that we have obtained all values of VEVs from the fermion mass and mixing spectrum studies, namely $v_S = v_\sigma = 6$ TeV, $v_\eta = v_\chi = 5$ TeV, $v_\rho = v_\kappa = 1$ TeV. Replacing all values of VEVs and at the leading order, the CP odd squared mass matrix can be diagonalized as follows

$$U_{A^0} M_{A^0}^2 U_{A^0}^T = (M_{A^0}^{\text{diag}})^2 \simeq f \times \text{diag}(0, 0, -30.76, -86, -148.7, -162.5, -206, -293) [\text{TeV}^2], \tag{27}$$

where the mixing matrix U_{A^0} is defined by

$$U_{A^0} \simeq \begin{pmatrix} 0.993 & 0.122 & 0. & 0. & 0. & 0. & 0. & 0. \\ 0. & 0. & -0.288 & 0.721 & -0.481 & -0.288 & 0. & -0.288 \\ 0. & 0. & -0.11 & 0.354 & -0.053 & 0.911 & 0. & 0.174 \\ 0. & 0. & -0.002 & 0.535 & 0.771 & -0.215 & 0. & 0.271 \\ -0.122 & 0.993 & 0. & 0. & 0. & 0. & 0. & 0. \\ 0. & 0. & 0.95 & 0.261 & -0.166 & 0.009 & 0. & -0.03 \\ 0. & 0. & -0.039 & 0.01 & -0.38 & -0.203 & 0. & 0.901 \\ 0. & 0. & 0. & 0. & 0. & 0. & -1. & 0. \end{pmatrix}. \tag{28}$$

This matrix shows the relations between physical and gauge eigenstates as follows

$$(G_Z \ G_{Z'} \ \mathcal{A}_3 \ \mathcal{A}_4 \ \mathcal{A}_5 \ \mathcal{A}_6 \ \mathcal{A}_7 \ \mathcal{A}_8)^T = U_{A^0}(\phi_{1I} \ \phi_{2I} \ \sigma_I \ \eta_I \ \chi_I \ \rho_I \ S_I \ \kappa_I)^T. \tag{29}$$

It should be noted that here the squared masses for the CP odd scalars are expressed in units of TeV^2 . For instance, if $f \sim -10^{-2}$, $B \sim 10^{-3}$ TeV, we obtain the range of masses for the CP odd scalars as $M_A \sim (0, 0, 0.554, 0.927, 1.219, 1.271, 4.28, 1.705)$ TeV. The mass spectrum of CP odd scalars shows that two massless states correspond to two Goldstone bosons G_Z and $G_{Z'}$ associated with the longitudinal components of the SM Z , and new

heavy neutral Z' gauge bosons, respectively.² When considering next-to-leading order via the matrix $M_{A_p}^2 \sim \mathcal{O}(Bv)$, the physical squared masses and states of CP odd scalars are slightly modified as follows

$$\delta M_A^2 \simeq B[\text{TeV}] \times \text{diag}(0, 0, -2.027, -14.245, 0, -19.027, -15.692, 0) [\text{TeV}]. \quad (30)$$

For $B \sim 10^{-3}$ TeV, these corrections for CP odd Higgs squared masses are of the order $\sim \mathcal{O}(10^{-3} - 10^{-2})$ TeV², which is significantly 2 to 3 orders of magnitude lower compared with the leading order results in Eq. (27). Similarly, the physical states are also slightly shifted when considering the first order. Thus, we can safely ignore the very subleading second-order correction and use only the leading first-order result.

C. CP even sector

The squared mass matrix for CP even scalar fields in the basis $(\phi_{1R}^0 \phi_{2R}^0 \sigma_R \eta_R \chi_R \rho_R S_R \kappa_R)^T$ have the following form:

$$M_S^2 = \begin{pmatrix} M_{S_1}^2 & (M_{S_2}^2)^T \\ M_{S_2}^2 & M_{S_3}^2 \end{pmatrix}, \quad (31)$$

where the submatrices $M_{S_{1,2,3}}^2$ are given by:

$$M_{S_2}^2 = \begin{pmatrix} \frac{f_2 v_2 v_S}{2} + \lambda_{1\sigma} v_1 v_\sigma & \frac{f_2 v_1 v_S}{2} + \lambda_{2\sigma} v_2 v_\sigma \\ \lambda_{1\eta} v_1 v_\eta & \lambda_{2\eta} v_2 v_\eta \\ \lambda_{1\chi} v_1 v_\chi & \lambda_{2\chi} v_2 v_\chi \\ \lambda_{1\rho} v_1 v_\rho & \lambda_{2\rho} v_2 v_\rho \\ \frac{f_2 v_2 v_\sigma}{2} + \lambda_{1S} v_1 v_S & \frac{f_2 v_1 v_\sigma}{2} + \lambda_{2S} v_2 v_S \\ \lambda_{1\kappa} v_1 v_\kappa & \lambda_{2\kappa} v_2 v_\kappa \end{pmatrix},$$

$$M_{S_1}^2 = \begin{pmatrix} -\frac{f_2 v_2 v_S v_\sigma}{2v_1} + 2\lambda_1 v_1^2 & \frac{f_2 v_S v_\sigma}{2} + v_1 v_2 (\lambda_{12} + \tilde{\lambda}_{12}) \\ \frac{f_2 v_S v_\sigma}{2} + v_1 v_2 (\lambda_{12} + \tilde{\lambda}_{12}) & -\frac{f_2 v_1 v_S v_\sigma}{2v_2} + 2\lambda_2 v_2^2 \end{pmatrix}, \quad (32)$$

$$M_{S_3}^2 = \begin{pmatrix} (m_{S_3}^2)_{11} & (m_{S_3}^2)_{12} & (m_{S_3}^2)_{13} & \lambda_{\sigma\rho} v_\sigma v_\rho & \lambda_{\sigma S} v_\sigma v_S + \frac{f_2 v_1 v_2}{2} & \lambda_{\sigma\kappa} v_\sigma v_\kappa + \frac{f_8 v_\eta v_\chi}{2} \\ (m_{S_3}^2)_{12} & (m_{S_3}^2)_{22} & (m_{S_3}^2)_{23} & \lambda_{\eta\rho} v_\eta v_\rho & \lambda_{\eta S} v_\eta v_S & (m_{S_3}^2)_{26} \\ (m_{S_3}^2)_{13} & (m_{S_3}^2)_{23} & (m_{S_3}^2)_{33} & \lambda_{\chi\rho} v_\chi v_\rho & \lambda_{\chi S} v_\chi v_S & (m_{S_3}^2)_{36} \\ \lambda_{\sigma\rho} v_\sigma v_\rho & \lambda_{\eta\rho} v_\eta v_\rho & \lambda_{\chi\rho} v_\chi v_\rho & (m_{S_3}^2)_{44} & (m_{S_3}^2)_{45} & (m_{S_3}^2)_{46} \\ \lambda_{\sigma S} v_\sigma v_S + \frac{f_2 v_1 v_2}{2} & \lambda_{\eta S} v_\eta v_S & \lambda_{\chi S} v_\chi v_S & \lambda_{\rho S} v_\rho v_S + (f_9 + f_{10}) v_S v_\kappa & (m_{S_3}^2)_{55} & (m_{S_3}^2)_{56} \\ \lambda_{\sigma\kappa} v_\sigma v_\kappa + \frac{f_8 v_\eta v_\chi}{2} & (m_{S_3}^2)_{26} & (m_{S_3}^2)_{36} & (m_{S_3}^2)_{46} & (m_{S_3}^2)_{56} & (m_{S_3}^2)_{66} \end{pmatrix},$$

² We want to emphasize that the full matrix M_A^2 has exactly two vanishing eigenvalues corresponding to two Goldstone bosons $G_{Z,Z'}$. These two massless states will not receive masses even when we consider corrections arising from higher order terms in the perturbative expansion.

with some matrix elements of $M_{S_3}^2$ defined as:

$$\begin{aligned}
(m_{S_3}^2)_{11} &= -\frac{f_2 v_1 v_2 v_S - 3f_4 v_\eta v_\sigma^2 + v_\eta v_\chi (\sqrt{2}B_1 + f_8 v_\kappa + f_5 v_\chi) - 4\lambda_\sigma v_\sigma^3}{2v_\sigma}, \\
(m_{S_3}^2)_{12} &= -\frac{3f_4 v_\sigma^2}{2} + \frac{v_\chi (\sqrt{2}B_1 + f_8 v_\kappa + f_5 v_\chi)}{2} + \lambda_{\sigma\eta} v_\sigma v_\eta, \\
(m_{S_3}^2)_{13} &= \frac{B_1 v_\eta}{\sqrt{2}} + \frac{f_8 v_\eta v_\kappa}{2} + \sqrt{2}B_5 v_\sigma + f_5 v_\eta v_\chi + \lambda_{\sigma\chi} v_\sigma v_\chi, \\
(m_{S_3}^2)_{26} &= \sqrt{2}B_4 v_\eta + \lambda_{\eta\kappa} v_\eta v_\kappa + \frac{f_8 v_\sigma v_\chi}{2}, \\
(m_{S_3}^2)_{55} &= 4f_7 v_S^2 + 2\lambda_S v_S^2 - \frac{f_2 v_1 v_2 v_\sigma}{2v_S}, \\
(m_{S_3}^2)_{56} &= \lambda_{\kappa S} v_\kappa v_S + (f_9 + f_{10}) v_S v_\rho, \\
(m_{S_3}^2)_{66} &= -\frac{\sqrt{2}B_4 v_\eta^2 + (f_9 + f_{10}) v_S^2 v_\rho + f_8 v_\eta v_\sigma v_\chi + f_{12} v_\chi^3 - 4\lambda_\kappa v_\kappa^3}{2v_\kappa}.
\end{aligned} \tag{33}$$

We continue to approximately diagonalize the given CP even squared mass matrix under the assumption that $B \ll v \ll v_{\sigma, \dots, \kappa}$, using a similar procedure employed in the diagonalization of M_A^2 and M_c^2 . However, this matrix contains more parameters, such as λ_{ij} , $\varkappa_{1i, 2i}$, compared to M_A^2 , M_c^2 , thus we will made several assumptions regarding these parameters. Our first assumption concerns the λ_i couplings of four new singlets i , ($i = \sigma, \dots, \kappa$). We consider a benchmark scenario where $v_\sigma = v_S = 6$ TeV, $v_\rho = v_\kappa = 1$ TeV, $v_\eta = v_\chi = 5$ TeV, with the following conditions

$$\lambda_\sigma = \lambda_S = \lambda, \quad \lambda_\rho = \lambda_\kappa \sim \lambda \frac{v_\rho}{v_\sigma}, \quad \lambda_\eta = \lambda_\chi \sim \lambda \frac{v_\chi}{v_\sigma}. \tag{34}$$

Furthermore, we set the couplings λ_{ij} between new singlets i and j relating to λ as

$$\lambda_{ij} \sim \lambda \mathcal{O}\left(\frac{v_i v_j}{v_\sigma^2}\right), \tag{35}$$

and for $\varkappa_{1, 2i}$ are couplings between two doublets $\phi_{1, 2}$ with new singlets i , we assume for the sake of simplicity that

$$\varkappa_{1, 2i} \sim \lambda_{1, 2} \mathcal{O}\left(\frac{v_{1, 2}}{v_i}\right) \ll 1. \tag{36}$$

Due to these assumptions, the matrix M_S^2 can be decomposed as

$$M_S^2 = M_{S_0}^2 + M_{S_p}^2. \tag{37}$$

At the leading order, we obtain the physical masses

$$U_{S_0} M_{S_0}^2 U_{S_0}^T \simeq f \times \text{diag}(0, -20.95, -44.46, -144.12, -148.73, -221.55, -228.5, -548.54) [\text{TeV}^2], \tag{38}$$

where the matrix U_{S_0} is given by

$$U_{S_0} \simeq \begin{pmatrix} 0.993 & 0.122 & 0. & 0. & 0. & 0. & 0. & 0. \\ 0. & 0. & -0.259 & -0.192 & 0.204 & 0.805 & 0.378 & 0.253 \\ 0. & 0. & -0.405 & -0.326 & 0.267 & -0.536 & 0.605 & -0.075 \\ 0. & 0. & -0.038 & 0.155 & 0.605 & -0.202 & -0.303 & 0.689 \\ -0.122 & 0.993 & 0. & 0. & 0. & 0. & 0. & 0. \\ 0. & 0. & 0.545 & -0.739 & -0.18 & -0.074 & 0.023 & 0.343 \\ 0. & 0. & -0.129 & 0.35 & -0.632 & -0.135 & 0.333 & 0.576 \\ 0. & 0. & 0.674 & 0.405 & 0.297 & 0.01 & 0.537 & -0.076 \end{pmatrix}, \tag{39}$$

and the physical states are determined by

$$(H_1 \ H_2 \ H_3 \ H_4 \ H_5 \ H_6 \ H_7 \ H_8)^T = U_{S_0} (\phi_{1R} \ \phi_{2R} \ \sigma_R \ \eta_R \ \chi_R \ \rho_R \ S_R \ \kappa_R)^T. \tag{40}$$

We see that at the leading order, there is a physical state H_1 with zero mass which is composed of real components of doublets ϕ_{1R} and ϕ_{2R} . This state will be identified as an SM-like Higgs boson h discovered by the LHC. Furthermore, there are seven heavy CP even scalars with masses that are proportional to coupling f and are on the TeV scale. When considering the next-to-leading order, the SM-like Higgs boson gains a small mass through the perturbative expansion

$$\delta m_{H_1 \equiv h}^2 \simeq 0.1175\lambda_1 + 2.675 \times 10^{-5}\lambda_2 + 1.773 \times 10^{-3}(\lambda_{12} + \bar{\lambda}_{12}) [\text{TeV}^2] \simeq 0.1175\lambda_1 [\text{TeV}^2]. \quad (41)$$

We comment that the SM-like Higgs boson mass is at the electroweak scale, and to assign its mass 125 GeV, as measured by the ATLAS and CMS experiments [13], the coupling $\lambda_1 \sim 0.133$. As for the remaining seven heavy scalars $H_{2,\dots,8}$, their masses are shifted by

$$\delta m_H^2 \simeq B[\text{TeV}] \times (-3.803, -3.763, -10.21, 0, -13.25, -7.55, 4.366)[\text{TeV}]. \quad (42)$$

For $B \sim \mathcal{O}(10^{-3})$ TeV, we obtain $\delta m_H^2 \sim \mathcal{O}(10^{-3} - 10^{-2})$ TeV², which is much smaller compared with leading order ones given in Eq. (38). Similarly, their eigenstates are also slightly changed. Consequently, we will adopt the leading order results, as in the CP odd scalar sector.

V. FLAVOR PHENOMENOLOGY

With the Yukawa terms shown in Eqs. (1,2), we find that the model under consideration contains several couplings of both charged and neutral CP even(odd) Higgs bosons with SM and new exotic fermions. Besides that, the different $U(1)_X$ charges of the third and two first quark generations causes quark flavor-changing $\bar{q}_i q_j Z'$ interactions mediated by new neutral gauge boson Z' at tree-level. Consequently, these couplings give rise to quark flavor-violating observables at tree or one-loop level. In this section, we study these processes in detail.

A. Lepton flavor phenomenology

From the leptonic Yukawa interactions of Eq. (2), we get the following terms describing the lepton flavor violating (LFV) processes

$$\begin{aligned} -\mathcal{L}_{\text{lepton}} = & \sum_{i=1}^3 y_i^{(l)} \bar{l}_{iL} \frac{v_2 + \phi_{2R}^0 + i\phi_{2I}^0}{\sqrt{2}} l_{3R} + \sum_{i=1}^3 y_i^{(l)} \bar{\nu}_{iL} \phi_2^+ l_{3R} \\ & + \sum_{i=1}^3 y_i^{(E)} \bar{l}_{iL} \frac{v_2 + \phi_{2R}^0 + i\phi_{2I}^0}{\sqrt{2}} E_{1R} + \sum_{n=1}^2 x_n^{(E)} \bar{E}_{1L} \frac{v_S + S_R - iS_I}{\sqrt{2}} l_{nR} \\ & - \sum_{i=1}^3 \sum_{j=1}^3 y_{ij}^{(\nu)} \bar{l}_{iL} \phi_2^- \nu_{jR} + \sum_{i=1}^3 \sum_{n=1}^2 z_{in}^{(l)} \bar{N}_{iR}^C \zeta_2^+ l_{nR} + H.c.. \end{aligned} \quad (43)$$

We work based on physical states of charged leptons $e'_{aL(R)}$, which are related to the flavor states $e_{iL(R)}$ via the following transformations:

$$e_{iL(R)} = (V_{eL(R)})_{ia} e'_{aL(R)}, \quad (44)$$

where $V_{eL(R)}$ are mixing matrix of the left (right)-handed lepton fields. We want to emphasize that there is barely any mixing between mass states of active neutrinos ν_L and heavy neutrinos ν_R, N_R via the inverse seesaw mechanism. For simplicity, we assume this mixing is suppressed and ignored, and only active neutrinos are mixed between themselves via the 3×3 matrix V_{ν_L} which is defined by the relation $V_{\nu_L}^\dagger V_{eL} = V_{\text{PMNS}}$, and the flavor states are related with the physical states as follows

$$\nu_{iL} = (V_{\nu_L})_{ia} \nu'_{aL}. \quad (45)$$

Furthermore, we assume the flavor states of right-handed neutrino ν_{iR}, N_{iR} are related to physical states via matrices V_{ν_R} and V_{N_R}

$$\nu_{iR} = (V_{\nu_R})_{ia} \nu'_{aR}, \quad N_{iR} = (V_{N_R})_{ia} N'_{aR}. \quad (46)$$

Besides that, using the relations between physical and gauge eigenstates of charged, CP odd and CP even scalars shown in Eqs. (20,29,40), the leptonic Yukawa interactions can be rewritten as follows:

$$\begin{aligned}
-\mathcal{L}_{\text{lepton}} = & \bar{\nu}'_{aL} g_R^{H^+ \bar{\nu}_{aL} l_b} P_R l'_b H^+ + \overline{N'_{aR}{}^C} g_R^{H^+ \bar{N}_{aL} l_b} P_R l'_b H^+ + \bar{\nu}'_{aR} g_R^{H^+ \bar{\nu}_{aR} l} P_L l'_b H^+ \\
& + \bar{\nu}'_{aL} g_R^{H_{1,2}^+ \bar{\nu}_{aL} l_b} P_R l'_b H_{1,2}^+ + \overline{N'_{aR}{}^C} g_R^{H_{1,2}^+ \bar{N}_{aL} l_b} P_R l'_b H_{1,2}^+ + \bar{\nu}'_{aR} g_R^{H_{1,2}^+ \bar{\nu}_{aR} l} P_L l'_b H_{1,2}^+ \\
& + \sum_{p=1}^8 \overline{E'_1} (g_L^{H_p \bar{E}_1 l_b} P_L + g_R^{H_p \bar{E}_1 l_b} P_R) l'_b H_p + i \sum_{p=3}^8 \overline{E'_1} (g_L^{\mathcal{A}_p \bar{E}_1 l_b} P_L + g_R^{\mathcal{A}_p \bar{E}_1 l_b} P_R) l'_b \mathcal{A}_p \\
& + \sum_{p=1}^8 \bar{l}'_a g_R^{H_p \bar{l}'_a l_b} P_R l'_b H_p + i \sum_{p=3}^8 \bar{l}'_a g_R^{\mathcal{A}_p \bar{l}'_a l_b} P_R l'_b \mathcal{A}_p + H.c., \tag{47}
\end{aligned}$$

with the coefficients given explicitly in Appendix A. Here the index p is taken from 3 to 8 for interactions of CP odd Higgs \mathcal{A} since we only care about the physical fields. Let's discuss the roles of each term in the equation provided above. The terms in first line of Eq. (47) contribute to the radiative decays $l_{b_1} \rightarrow l_{b_2} \gamma$ with the one loop level exchange of charged Higgs $H^+, H_{1,2}^+$ and active neutrinos ν_{aL} , right-handed neutrinos N_{aR}^c, ν_{aR} running in the internal lines, respectively. Furthermore, the second and third lines contain terms describing radiative decays mediated by the neutral CP even (odd) Higgs $H(\mathcal{A})$ and new exotic lepton E_1 or ordinary charged leptons l_a . The Feynman diagrams for such observables are shown in subfigures (a,b) in Fig. (1). Additionally, the last line provides sources for tree-level lepton flavor violating decays of the SM like Higgs boson $H_1 \equiv h$ if index $p = 1$, $h \rightarrow \bar{l}_a l_b$, and potentially the tree-level three leptonic body decays $l \rightarrow 3l'$ via the CP even (odd) Higgs bosons $H(\mathcal{A})$, demonstrates in subfigures (c,d) in Fig. (1). These LFV terms also trigger other processes, namely the coherent $\mu \rightarrow e$ conversion in a muonic atom and the transition between muonium Mu to antimuonium $\overline{\text{Mu}}$ state, see in subfigures (e) and (f) of Fig. (1).

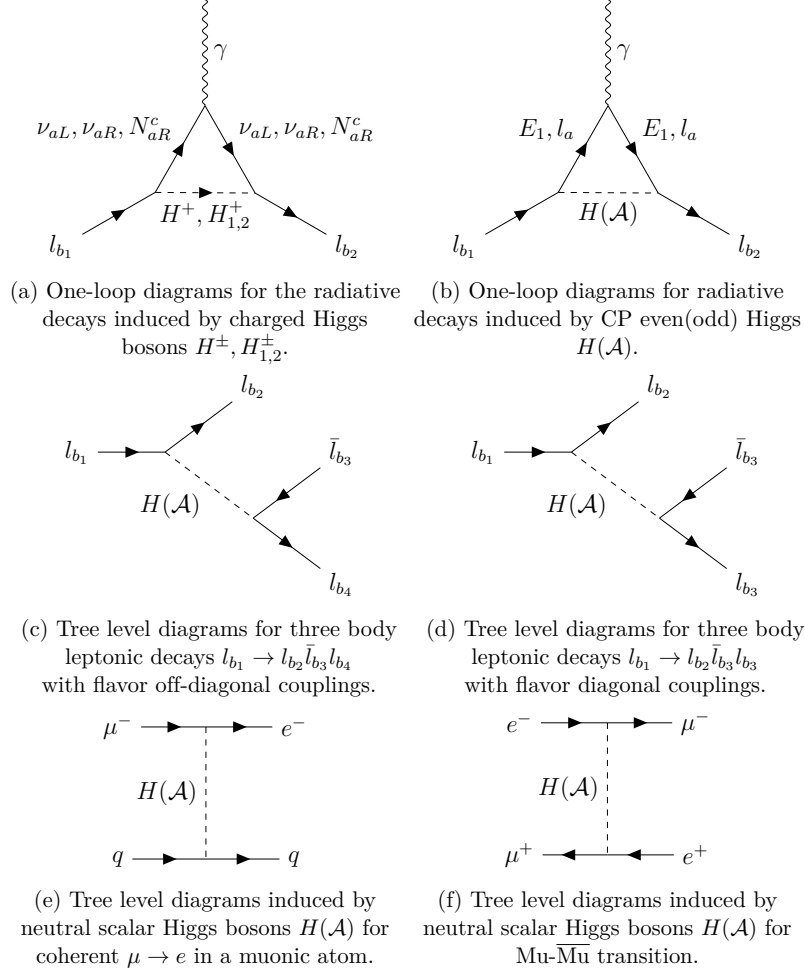


Figure 1: Feynman diagrams for leptonic observables.

1. LFV decays

The radiative cLFV observables $l_{b_1} \rightarrow l_{b_2} \gamma$ with $l_{b_1} = \{\mu, \tau\}$, $l_{b_2} = \{e, \mu\}$ and $l_{b_1} \neq l_{b_2}$ can be described via the effective Hamiltonian contributing by new charged Higgs and neutral CP even (odd) Higgs at the one-loop levels

$$\mathcal{H}_{\text{eff}}^{\text{lepton}} = \bar{e}_{b_2} \sigma_{\mu\nu} [(C_L)_{b_2 b_1} P_L + (C_R)_{b_2 b_1} P_R] e_{b_1} F^{\mu\nu}, \quad (48)$$

where the coefficients $(C_{L,R})_{b_2 b_1}$ are determined by evaluating one-loop diagrams involving charged Higgs $H^\pm, H_{1,2}^\pm$, neutral CP even (odd) Higgs $H(\mathcal{A})$, and the SM charged gauge boson W_μ^\pm as follows

$$\begin{aligned} (C_L)_{b_2 b_1} &= (C_L^{H^+ \bar{\nu}_L l})_{b_2 b_1} + (C_{L,R}^{H^+ \bar{N} l})_{b_2 b_1} + (C_{L,R}^{H_{1,2}^+ \bar{\nu}_L l})_{b_2 b_1} + (C_{L,R}^{H_{1,2}^+ \bar{N} l})_{b_2 b_1} + (C_L^{H_p(\mathcal{A}_p) \bar{E}_1 l})_{b_2 b_1} \\ &\quad + (C_L^{H_p(\mathcal{A}_p) \bar{l} l})_{b_2 b_1}, \\ (C_R)_{b_2 b_1} &= (C_R^{W^+ \bar{\nu}_L l})_{b_2 b_1} + (C_R^{H^+ \bar{\nu}_R l})_{b_2 b_1} + (C_R^{H_{1,2}^+ \bar{\nu}_R l})_{b_2 b_1} + (C_R^{H_p(\mathcal{A}_p) \bar{E}_1 l})_{b_2 b_1}. \end{aligned} \quad (49)$$

Besides, these coefficients are obtained in the limit that the external mass of daughter lepton m_{b_2} is very small in compared with the mass of decaying lepton m_{b_1} , i.e $m_{b_2} \ll m_{b_1}$, $m_{b_2} \sim 0$. Therefore, we have the following expressions

for $(C_{L,R})_{b_2 b_1}$

$$\begin{aligned}
(C_R^{W^+ \bar{\nu}_L l})_{b_2 b_1} &= \frac{-em_{b_1}}{32\pi^2 m_{W^\pm}^2} \sum_{a=1}^3 (g_L^{W^+ \bar{\nu}_a l b_2})^* g_L^{W^+ \bar{\nu}_a l b_1} f_\gamma \left(\frac{m_{\nu_{aL}}^2}{m_{W^+}^2} \right), \\
(C_L^{H^+ \bar{\nu}_L l})_{b_2 b_1} &= \frac{-em_{b_1}}{32\pi^2 m_{H_{1,2}^\pm}^2} \sum_{a=1}^3 (g_R^{H^+ \bar{\nu}_a l b_2})^* g_R^{H^+ \bar{\nu}_a l b_1} f_\gamma \left(\frac{m_{\nu_{aL}}^2}{m_{H^+}^2} \right), \\
(C_L^{H^+ \bar{N} l})_{b_2 b_1} &= \frac{-em_{b_1}}{32\pi^2 m_{H_{1,2}^\pm}^2} \sum_{a=1}^3 (g_R^{H^+ \bar{N}_a l b_2})^* g_R^{H^+ \bar{N}_a l b_1} f_\gamma \left(\frac{m_{N_a}^2}{m_{H^+}^2} \right), \\
(C_R^{H^+ \bar{\nu}_R l})_{b_2 b_1} &= \frac{-em_{b_1}}{32\pi^2 m_{H_{1,2}^\pm}^2} \sum_{a=1}^3 (g_L^{H^+ \bar{\nu}_a R l b_2})^* g_L^{H^+ \bar{\nu}_a R l b_1} f_\gamma \left(\frac{m_{\nu_{aR}}^2}{m_{H^+}^2} \right), \\
(C_L^{H_{1,2}^+ \bar{\nu}_L l})_{b_2 b_1} &= \frac{-em_{b_1}}{32\pi^2 m_{H_{1,2}^\pm}^2} \sum_{a=1}^3 (g_R^{H_{1,2}^+ \bar{\nu}_a l b_2})^* g_R^{H_{1,2}^+ \bar{\nu}_a l b_1} f_\gamma \left(\frac{m_{\nu_{aL}}^2}{m_{H_{1,2}^+}^2} \right), \\
(C_L^{H_{1,2}^+ \bar{N} l})_{b_2 b_1} &= \frac{-em_{b_1}}{32\pi^2 m_{H_{1,2}^\pm}^2} \sum_{a=1}^3 (g_R^{H_{1,2}^+ \bar{N}_a l b_2})^* g_R^{H_{1,2}^+ \bar{N}_a l b_1} f_\gamma \left(\frac{m_{N_a}^2}{m_{H_{1,2}^+}^2} \right), \\
(C_R^{H_{1,2}^+ \bar{\nu}_R l})_{b_2 b_1} &= \frac{-em_{b_1}}{32\pi^2 m_{H_{1,2}^\pm}^2} \sum_{a=1}^3 (g_L^{H_{1,2}^+ \bar{\nu}_a R l b_2})^* g_L^{H_{1,2}^+ \bar{\nu}_a R l b_1} f_\gamma \left(\frac{m_{\nu_{aR}}^2}{m_{H_{1,2}^+}^2} \right), \\
(C_R^{H_p \bar{E}_1 l})_{b_2 b_1} &= \sum_{p=1}^8 \frac{em_{b_1}}{32\pi^2 m_{H_p}^2} \left[(g_L^{H_p \bar{E}_1 l b_2})^* g_L^{H_p \bar{E}_1 l b_1} f_\gamma \left(\frac{m_{E_1}^2}{m_{H_p}^2} \right) + (g_R^{H_p \bar{E}_1 l b_2})^* g_R^{H_p \bar{E}_1 l b_1} \frac{m_{E_1}}{m_{b_1}} h'_\gamma \left(\frac{m_{E_1}^2}{m_{H_p}^2} \right) \right], \\
(C_L^{H_p \bar{E}_1 l})_{ab} &= \sum_{p=1}^8 \frac{em_{b_1}}{32\pi^2 m_{H_p}^2} \left[(g_R^{H_p \bar{E}_1 l b_2})^* g_R^{H_p \bar{E}_1 l b_1} f_\gamma \left(\frac{m_{E_1}^2}{m_{H_p}^2} \right) + (g_L^{H_p \bar{E}_1 l b_2})^* g_L^{H_p \bar{E}_1 l b_1} \frac{m_{E_1}}{m_{b_1}} h'_\gamma \left(\frac{m_{E_1}^2}{m_{H_p}^2} \right) \right], \\
(C_R^{A_p \bar{E}_1 l})_{b_2 b_1} &= \sum_{p=3}^8 \frac{em_{b_1}}{32\pi^2 m_{A_p}^2} \left[(g_L^{A_p \bar{E}_1 l b_2})^* g_L^{A_p \bar{E}_1 l b_1} f_\gamma \left(\frac{m_{E_1}^2}{m_{A_p}^2} \right) + (g_R^{A_p \bar{E}_1 l b_2})^* g_R^{A_p \bar{E}_1 l b_1} \frac{m_{E_1}}{m_{b_1}} h'_\gamma \left(\frac{m_{E_1}^2}{m_{A_p}^2} \right) \right], \\
(C_L^{A_p \bar{E}_1 l})_{b_2 b_1} &= \sum_{p=1}^8 \frac{em_{b_1}}{32\pi^2 m_{A_p}^2} \left[(g_R^{A_p \bar{E}_1 l b_2})^* g_R^{A_p \bar{E}_1 l b_1} f_\gamma \left(\frac{m_{E_1}^2}{m_{A_p}^2} \right) + (g_L^{A_p \bar{E}_1 l b_2})^* g_L^{A_p \bar{E}_1 l b_1} \frac{m_{E_1}}{m_{b_1}} h'_\gamma \left(\frac{m_{E_1}^2}{m_{A_p}^2} \right) \right], \\
(C_L^{H_p \bar{l} l})_{b_2 b_1} &= \sum_{a=1}^3 \sum_{p=1}^8 \frac{em_{b_1}}{32\pi^2 m_{H_p}^2} (g_R^{H_p \bar{l}_a l b_2})^* (g_R^{H_p \bar{l}_a l b_1}) f'_\gamma \left(\frac{m_{l_a}^2}{m_{H_p}^2} \right), \\
(C_L^{A_p \bar{l} l})_{b_2 b_1} &= \sum_{a=1}^3 \sum_{p=3}^8 \frac{em_{b_1}}{32\pi^2 m_{A_p}^2} (g_R^{A_p \bar{l}_a l b_2})^* (g_R^{A_p \bar{l}_a l b_1}) f'_\gamma \left(\frac{m_{l_a}^2}{m_{A_p}^2} \right), \tag{50}
\end{aligned}$$

where the couplings of SM gauge boson W are given as : $g_L^{W^+ \bar{\nu}_a l b_1(2)} = \sum_{i=1}^3 (V_{\nu L}^*)_{ia} (V_{eL})_{ib_1(2)}$. Besides, the loop functions $f_\gamma^W, h'_\gamma, f_\gamma^{(')}$ are defined in Appendix B. The formulas of the branching ratio of cLFV decays are expressed by

$$\text{BR}(l_{b_1} \rightarrow l_{b_2} \gamma) = \frac{m_{b_1}^3}{4\pi \Gamma_{l_{b_1}}} (|(C_L)_{b_2 b_1}|^2 + |(C_R)_{b_2 b_1}|^2), \tag{51}$$

where $\Gamma_{l_{b_1}}$ is the total decay width of decaying lepton l_{b_1} . For LFV decays of SM like Higgs boson $h \rightarrow \bar{l}_a l_b$, their branching ratio are given as follows

$$\text{BR}(h \rightarrow \bar{l}_a l_b) = \frac{m_h}{8\pi \Gamma_h^{\text{SM}}} (|g_R^{h \bar{l}_a l_b}|^2 + |(g_R^{h \bar{l}_a l_b})^*|^2), \tag{52}$$

where $\Gamma_h^{\text{SM}} \simeq 4.1$ MeV is the total width of SM Higgs boson h .

Besides, the LFV couplings in the last line of Eq. (47) can also cause the three body leptonic decays. The expressions for their branching ratios read

$$\begin{aligned}
\text{BR}(\tau \rightarrow 3\mu) &= R \left\{ \sum_{p=1}^8 \left[2 \left| \frac{g_R^{H_p \bar{l}_2 l_3} g_R^{H_p \bar{l}_2 l_2}}{m_{H_p}^2} \right|^2 + 2 \left| \frac{(g_R^{H_p \bar{l}_3 l_2})^* (g_R^{H_p \bar{l}_2 l_2})^*}{m_{H_p}^2} \right|^2 + \left| \frac{g_R^{H_p \bar{l}_2 l_3} (g_R^{H_p \bar{l}_2 l_2})^*}{m_{H_p}^2} \right|^2 + \left| \frac{(g_R^{H_p \bar{l}_3 l_2})^* g_R^{H_p \bar{l}_2 l_2}}{m_{H_p}^2} \right|^2 \right] \right. \\
&\quad \left. + \sum_{p=3}^8 \left[2 \left| \frac{g_R^{A_p \bar{l}_2 l_3} g_R^{A_p \bar{l}_2 l_2}}{m_{A_p}^2} \right|^2 + 2 \left| \frac{(g_R^{A_p \bar{l}_3 l_2})^* (g_R^{A_p \bar{l}_2 l_2})^*}{m_{A_p}^2} \right|^2 + \left| \frac{g_R^{A_p \bar{l}_2 l_3} (g_R^{A_p \bar{l}_2 l_2})^*}{m_{A_p}^2} \right|^2 + \left| \frac{(g_R^{A_p \bar{l}_3 l_2})^* g_R^{A_p \bar{l}_2 l_2}}{m_{A_p}^2} \right|^2 \right] \right\}, \\
\text{BR}(\tau \rightarrow \mu e \mu) &= R \left\{ \sum_{p=1}^8 \left[2 \left| \frac{g_R^{H_p \bar{l}_2 l_3} g_R^{H_p \bar{l}_2 l_1}}{m_{H_p}^2} \right|^2 + 2 \left| \frac{(g_R^{H_p \bar{l}_3 l_2})^* (g_R^{H_p \bar{l}_1 l_2})^*}{m_{H_p}^2} \right|^2 + \left| \frac{g_R^{H_p \bar{l}_2 l_3} (g_R^{H_p \bar{l}_1 l_2})^*}{m_{H_p}^2} \right|^2 + \left| \frac{(g_R^{H_p \bar{l}_3 l_2})^* g_R^{H_p \bar{l}_2 l_1}}{m_{H_p}^2} \right|^2 \right] \right. \\
&\quad \left. + \sum_{p=3}^8 \left[2 \left| \frac{g_R^{A_p \bar{l}_2 l_3} g_R^{A_p \bar{l}_2 l_1}}{m_{A_p}^2} \right|^2 + 2 \left| \frac{(g_R^{A_p \bar{l}_3 l_2})^* (g_R^{A_p \bar{l}_1 l_2})^*}{m_{A_p}^2} \right|^2 + \left| \frac{g_R^{A_p \bar{l}_2 l_3} (g_R^{A_p \bar{l}_1 l_2})^*}{m_{A_p}^2} \right|^2 + \left| \frac{(g_R^{A_p \bar{l}_3 l_2})^* g_R^{A_p \bar{l}_2 l_1}}{m_{A_p}^2} \right|^2 \right] \right\}, \\
\text{BR}(\tau \rightarrow e \mu \mu) &= R \sum_{p=1}^8 \left[\left| \frac{g_R^{H_p \bar{l}_1 l_3} g_R^{H_p \bar{l}_2 l_2}}{m_{H_p}^2} + \frac{g_R^{H_p \bar{l}_2 l_3} g_R^{H_p \bar{l}_1 l_2}}{m_{H_p}^2} \right|^2 + \left| \frac{(g_R^{H_p \bar{l}_3 l_1})^* (g_R^{H_p \bar{l}_2 l_2})^*}{m_{H_p}^2} + \frac{(g_R^{H_p \bar{l}_3 l_2})^* (g_R^{H_p \bar{l}_2 l_1})^*}{m_{H_p}^2} \right|^2 \right. \\
&\quad \left. + \left| \frac{(g_R^{H_p \bar{l}_3 l_1})^* g_R^{H_p \bar{l}_2 l_2}}{m_{H_p}^2} \right|^2 + \left| \frac{(g_R^{H_p \bar{l}_3 l_2})^* g_R^{H_p \bar{l}_1 l_2}}{m_{H_p}^2} \right|^2 \right] \\
&\quad + R \sum_{p=3}^8 \left[\left| \frac{g_R^{A_p \bar{l}_1 l_3} g_R^{A_p \bar{l}_2 l_2}}{m_{A_p}^2} + \frac{g_R^{A_p \bar{l}_2 l_3} g_R^{A_p \bar{l}_1 l_2}}{m_{A_p}^2} \right|^2 + \left| \frac{(g_R^{A_p \bar{l}_3 l_1})^* (g_R^{A_p \bar{l}_2 l_2})^*}{m_{A_p}^2} + \frac{(g_R^{A_p \bar{l}_3 l_2})^* (g_R^{A_p \bar{l}_2 l_1})^*}{m_{A_p}^2} \right|^2 \right. \\
&\quad \left. + \left| \frac{(g_R^{A_p \bar{l}_3 l_1})^* g_R^{A_p \bar{l}_2 l_2}}{m_{A_p}^2} \right|^2 + \left| \frac{(g_R^{A_p \bar{l}_3 l_2})^* g_R^{A_p \bar{l}_1 l_2}}{m_{A_p}^2} \right|^2 \right], \tag{53}
\end{aligned}$$

where $R = \frac{m_\tau^5}{1536\pi^3\Gamma_\tau}$ is the overall factor. Similarly, we can obtain the branching ratios of the other three body leptonic decays such as $\mu \rightarrow 3e$, $\tau \rightarrow 3e$, and $\tau \rightarrow e\mu e$ by replacing appropriate indices.

We would like to emphasize that the model includes contributions to the anomalous magnetic moments for electron or muon, denoted as $\Delta a_{e,\mu}$ respectively, as studied in previous work [46]. However, as aforementioned, the paper considered the observables within a framework of a very simplifying benchmark scenario containing few scalar contributions. Therefore, in this work, we revisit $\Delta a_{e,\mu}$ in a more comprehensive manner, considering all possible contributions. The expressions for $\Delta a_{e,\mu}$ are written as follows

$$\begin{aligned}
\Delta a_{e(\mu)} &= -\frac{4m_{e\mu}}{e} \text{Re}[(C_R)_{b_1 b_1 (b_2 b_2)}], \\
(C_R)_{b_1 b_1 (b_2 b_2)} &= (C_R^{H^+ \bar{\nu}_R l})_{b_1 b_1 (b_2 b_2)} + (C_R^{H_{1,2}^+ \bar{\nu}_R l})_{b_1 b_1 (b_2 b_2)} + (C_R^{H(A)ll})_{b_1 b_1 (b_2 b_2)}. \tag{54}
\end{aligned}$$

To close this section, we offer a concise qualitative discussion on how our model impacts the electric dipole moment of the neutron. Following the considerations given in [48, 49], the neutron's electric dipole moment in multi-Higgs doublet models like the one considered in this work originates from various factors. Firstly, there's the tree-level exchange of CP-violating scalars, resulting in four-fermion operators involving both up- and down-type quarks. Secondly, there's the CP-violating three-gluon operator, known as the Weinberg operator, along with Barr-Zee type two-loop diagrams. These contribute to the electric dipole moment and chromoelectric dipole moments of both up- and down-type quarks. Notably, the contributions from the first and third sources are diminished due to the small masses of the light quarks [48, 49].

Consequently, it is expected that the main contribution to the electric dipole moment of the neutron in the extended 2HDM theory considered in this work will arise from the CP violating two loop level self-gluon trilinear interaction involving the exchange of charged scalars along with top and bottom quarks through virtual processes as in Refs. [48, 49]. Thus, the upper limit on the electric dipole moment of the neutron $|d_e| \leq 1.1 \times 10^{-29} e \text{ cm}$ [50] can set constraints on the ratio between CP-violating parameter combinations and squared charged scalar masses, as discussed in detail in Ref. [48]. Some recent detailed studies of the consequences of multi Higgs doublet models

in the electric dipole moment of the neutron are done in Refs. [49, 51, 52]. A detailed numerical analysis of the constraints arising from the upper experimental bound on the electric dipole moment of the neutron in our model under consideration goes beyond the scope of the present work and is deferred for future work.

2. $Mu - \overline{Mu}$ transition

The LFV couplings of CP odd(even) Higgs $H(\mathcal{A})$ in the last line of Eq. (47) also cause another process, called the muonium (Mu: μ^+e^-) to antimuonium (\overline{Mu} : μ^-e^+) transition. This process can be induced via the following effective Lagrangian

$$\mathcal{L}_{\text{eff}}^{\text{Mu}-\overline{Mu}} = - \sum_{i=1,2} \frac{\mathcal{G}_i}{\sqrt{2}} \mathcal{Q}_i, \quad (55)$$

where the coefficients and corresponding operators are defined as follows

$$\begin{aligned} \mathcal{Q}_1 &= [\bar{\mu}(1 - \gamma_5)e][\bar{\mu}(1 - \gamma_5)e], & \mathcal{G}_1 &= \sum_{p=1}^8 \frac{[(g_R^{H_p \bar{l}_1 l_2})^*]^2}{4\sqrt{2}m_{H_p}^2} + \sum_{p=3}^8 \frac{[(g_R^{A_p \bar{l}_1 l_2})^*]^2}{4\sqrt{2}m_{\mathcal{A}_p}^2} \\ \mathcal{Q}_2 &= [\bar{\mu}(1 + \gamma_5)e][\bar{\mu}(1 + \gamma_5)e], & \mathcal{G}_2 &= \sum_{p=1}^8 \frac{(g_R^{H_p \bar{l}_2 l_1})^2}{4\sqrt{2}m_{H_p}^2} + \sum_{p=3}^8 \frac{(g_R^{A_p \bar{l}_2 l_1})^2}{4\sqrt{2}m_{\mathcal{A}_p}^2}. \end{aligned} \quad (56)$$

The $Mu - \overline{Mu}$ transition probability in the presence of external magnetic field B is given by [53]

$$P(\text{Mu} \rightarrow \overline{\text{Mu}}) = 2\tau^2 \left(|c_{0,0}|^2 |\mathcal{M}_{0,0}^B|^2 + |c_{1,0}|^2 |\mathcal{M}_{1,0}^B|^2 + \sum_{m=\pm 1} |c_{1,m}|^2 \frac{|M_{1,m}|^2}{1 + (\tau \Delta E)^2} \right), \quad (57)$$

where $\tau \sim 2.2 \times 10^{-6} s$ is the expected lifetime of the Mu system. Additionally, $|c_{0,0}|^2 = 0.32$, $|c_{1,0}|^2 = 0.18$ are the population of Mu states. ΔE is the energy splitting between the $(1, 1)$ and $(1, -1)$ states caused by external magnetic field B . The factor $X = 0.631$ is for a magnetic field $B = 0.1$ Tesla. It should be noted that the transition probability for $(1, \pm 1)$ states is suppressed for the case $B \geq \mathcal{O}(10^{-6})$ Tesla. The transition probability in this case reads

$$P(\text{Mu} \rightarrow \overline{\text{Mu}}) \simeq 5.74 \times 10^{-7} \frac{|\mathcal{G}_1 + \mathcal{G}_2|^2}{G_F^2}. \quad (58)$$

The PSI experiment for $Mu - \overline{Mu}$ transition reported that $P(\text{Mu} \rightarrow \overline{\text{Mu}}) < 8.3 \times 10^{-11}$ [54], which implies

$$|\mathcal{G}_1 + \mathcal{G}_2| < 1.2 \times 10^{-2} G_F. \quad (59)$$

3. $\mu \rightarrow e$ coherent conversion

On the one hand, the LFV couplings of neutral Higgs boson $H(\mathcal{A})$ can also induce the coherent $\mu \rightarrow e$ conversion in a muonic atom. Specifically, μ^- is captured by atomic nuclei target and subsequently converts into e^- without emitting a neutrino due to the influence of the nuclear field, as described in the Feynman diagram (e) of Fig. (1). In this work, the $\mu \rightarrow e$ conversion arises from the non-photonic contribution and can be described via the effective Lagrangian at the quark level as follows

$$\mathcal{L}_{\text{eff}}^{\mu \rightarrow e} = -G_F m_\mu m_N \sum_{q=u,d,s} [C_{SL}^q (\bar{e} P_L \mu) + C_{SR}^q (\bar{e} P_R \mu)] (\bar{q} q) + H.c., \quad (60)$$

where the operators $\bar{q} \gamma_5 q$ do not contribute to the coherent conversion process [55], therefore we do not include them. m_μ and m_N are the masses of muon and nuclei N , respectively. The coefficients C_{SL}^q, C_{SR}^q are given by

$$\begin{aligned} C_{SL}^q &= \sum_{p=1}^8 \frac{(g_R^{H_p \bar{l}_2 l_1})^* \text{Re}(g_R^{H_p \bar{q} q})}{m_{H_p}^2} + \sum_{p=3}^8 \frac{(g_R^{A_p \bar{l}_2 l_1})^* \text{Im}(g_R^{A_p \bar{q} q})}{m_{\mathcal{A}_p}^2}, \\ C_{SR}^q &= \sum_{p=1}^8 \frac{g_R^{H_p \bar{l}_1 l_2} \text{Re}(g_R^{H_p \bar{q} q})}{m_{H_p}^2} + \sum_{p=3}^8 \frac{g_R^{A_p \bar{l}_1 l_2} \text{Im}(g_R^{A_p \bar{q} q})}{m_{\mathcal{A}_p}^2}, \end{aligned} \quad (61)$$

where coefficients $g^{H_p(A_p)\bar{q}q}$, ($q = u, d, s$) are defined below in the Section. (VB). To evaluate the rate of $\mu \rightarrow e$ transition in a nuclei, we should transform the above Lagrangian from the quark to nucleon level

$$\mathcal{L}_{\text{eff}}^{\mu N \rightarrow e N} = - \sum_{N=p,n} [C_{SL}^N(\bar{e}P_L\mu) + C_{SR}^N(\bar{e}P_R\mu)](\bar{\psi}_N\psi_N) + H.c., \quad (62)$$

with ψ_N is defined as the nucleon field, whereas the coefficients are rewritten as

$$C_{SL(R)}^{p(n)} = \sum_{q=u,d,s} C_{SL(R)}^q f_{S_{p(n)}}^q, \quad (63)$$

$$f_{S_{p(n)}}^u = \frac{m_u}{m_u + m_d} \frac{\sigma_{\pi N}}{m_p} (1 \pm \xi), \quad f_{S_{p(n)}}^d = \frac{m_d}{m_u + m_d} \frac{\sigma_{\pi N}}{m_p} (1 \mp \xi), \quad f_{S_p}^s = \frac{m_s}{m_u + m_d} \frac{\sigma_{\pi N}}{m_p} y,$$

where the nucleon matrix elements $\sigma_{\pi N} = 39.8$ MeV, $\xi = 0.18$ and $y = 0.09$. $m_{u,d,s}$ are the quark masses evaluated at the scale of 2 GeV [13, 56]. Then the branching ratio of $\mu \rightarrow e$ conversion in a target of atomic nuclei N is given by

$$\text{BR}(\mu N \rightarrow e N) = \frac{4G_F^2 m_\mu^7}{\Gamma_{\text{capt}}^N} [|m_p C_{SR}^p S_N^p + m_n C_{SR}^n S_N^n|^2 + |m_p C_{SL}^p S_N^p + m_n C_{SL}^n S_N^n|^2], \quad (64)$$

where Γ_{capt}^N is the total capture rate, $S_N^{p,n}$ are the overlap integrals of atomic nuclei N . For instance, we consider the $\mu \rightarrow e$ transition captured by Gold (Au) nuclei, we have $S_{\text{Au}}^p = 0.0614$, $S_{\text{Au}}^n = 0.0918$ [55], $\Gamma_{\text{capt}}^{\text{Au}} \simeq 8.7 \times 10^{-18}$ GeV [57]. The predicted branching ratio in Eq. (64) will be compared to the experimental limit reported by SINDRUM-II [58].

All the above-mentioned leptonic observables should be compared with the corresponding upper experimental limits shown in Table. IV. Here we require the consistency with the 3σ experimentally allowed range for the observable $\Delta a_{e(\mu)}$ by the following reason. The first and second charged fermion families of the model, i.e., the electron and muon receive tree and loop-level masses, respectively, from the inverse seesaw mechanism. This makes the interactions of the first and second generations of fermions with other particles quite suppressed, therefore we will compare the predictions with the 3σ experimentally allowed ranges of $\Delta a_{e(\mu)}$. For other observables related to electron or muon, we apply this setup.

LFV Observables	Experimental limits	LFV Observables	Experimental constraints
BR($\mu \rightarrow e\gamma$)	$\leq 4.2 \times 10^{-13}$ [58–60]	BR($h \rightarrow e\mu$)	$< 6.1 \times 10^{-5}$ [13]
BR($\tau \rightarrow e\gamma$)	$\leq 3.3 \times 10^{-8}$ [58–60]	BR($h \rightarrow e\tau$)	$< 2.2 \times 10^{-3}$ [13]
BR($\tau \rightarrow \mu\gamma$)	$\leq 4.4 \times 10^{-8}$ [58–60]	BR($h \rightarrow \mu\tau$)	$< 1.5 \times 10^{-3}$ [13]
BR($\mu^- \rightarrow e^- e^+ e^-$)	$\leq 1.0 \times 10^{-12}$ [13]	BR($\tau^- \rightarrow \mu^- e^+ \mu^-$)	$\leq 9.8 \times 10^{-9}$ [13]
BR($\tau^- \rightarrow e^- e^+ e^-$)	$\leq 1.4 \times 10^{-8}$ [13]	BR($\tau^- \rightarrow e^- \mu^+ e^-$)	$\leq 8.4 \times 10^{-9}$ [13]
BR($\tau^- \rightarrow e^- \mu^+ \mu^-$)	$\leq 1.6 \times 10^{-8}$ [13]	BR($\tau^- \rightarrow \mu^- \mu^+ \mu^-$)	$\leq 1.1 \times 10^{-8}$ [13]
BR($\tau^- \rightarrow \mu^+ \mu^-$)	$\leq 1.6 \times 10^{-8}$ [13]	P(Mu – $\bar{\text{M}}\bar{\text{u}}$)	$< 8.3 \times 10^{-11}$ [54]
BR($\mu^- \text{Au} \rightarrow e^- \text{Au}$)	$\leq 7.0 \times 10^{-13}$ [58]	Δa_e^{Rb}	$0.48(30) \times 10^{-12}$ [13]
Δa_μ	$249(48) \times 10^{-11}$ [61]		

Table IV: Experimental constraints for leptonic flavor observables.

B. Quark flavor phenomenology

The Yukawa terms contributing to the down type quark transitions, such as $b \rightarrow s(d)$, are obtained from Eq. (1) as follows

$$-\mathcal{L}_{\text{quark}}^{d_a \rightarrow d_b} = \sum_{i=1}^3 y_i^{(d)} \bar{u}_{3L} \phi_2^+ d_{iR} + \sum_{i=1}^3 y_i^{(d)} \bar{d}_{3L} \frac{v_2 + \phi_{2R}^0 + i\phi_{2I}^0}{\sqrt{2}} d_{iR} + \sum_{i=1}^3 w_1^{(d)} \bar{U}_L \zeta_1^+ d_{iR} + \sum_{i=1}^3 x_i^{(d)} \bar{D}_{1L} \frac{v_\sigma + \sigma_R + i\sigma_I}{\sqrt{2}} d_{iR}$$

$$- \sum_{i=1}^3 y_i^{(u)} \bar{d}_{3L} \phi_1^- u_{iR} - \sum_{n=1}^2 x_n^{(U)} \bar{d}_{nL} \phi_2^- U_R + \sum_{n=1}^2 x_n^{(D)} \bar{d}_{nL} \frac{v_1 + \phi_{1R}^0 + i\phi_{1I}^0}{\sqrt{2}} D_{1R} + H.c.. \quad (65)$$

For the observables related to the up-type quark transitions such as $t \rightarrow (u, c)$, we have the following Yukawa interactions: -

$$\begin{aligned} \mathcal{L}_{\text{quark}}^{u_a \rightarrow u_b} &= \sum_{i=1}^3 y_i^{(u)} \bar{u}_{3L} \frac{v_1 + \phi_{1R}^0 + i\phi_{1I}^0}{\sqrt{2}} u_{iR} + \sum_{n=1}^2 x_n^{(U)} \bar{u}_{nL} \frac{v_2 + \phi_{2R}^0 + i\phi_{2I}^0}{\sqrt{2}} U_R \\ &+ \sum_{n=1}^2 x_n^{(D)} \bar{u}_{nL} \phi_1^+ D_{1R} + \sum_{i=1}^3 w_i^{(u)} \bar{D}_{1L} \zeta_1^- u_{iR} + \sum_{i=1}^3 x_i^{(u)} \bar{U}_L \frac{v_\sigma + \sigma_R - i\sigma_I}{\sqrt{2}} u_{iR} + H.c.. \end{aligned} \quad (66)$$

We now rewrite the above-given quark Yukawa interactions in a physical basis taking into account that the physical quark eigenstates u'_L, d'_L are related with the quark interaction eigenstates by the following transformations

$$u_{iL(R)} = (V_{u_{L(R)}})_{ia} u'_{aL(R)}, \quad d_{iL(R)} = (V_{d_{L(R)}})_{ia} d'_{aL(R)}, \quad (67)$$

where $V_{u(d)_{L,R}}$ are the mixing matrices of left(right) of up(type) quarks, respectively. Furthermore, the physical states of scalar fields are similar as pointed out in the lepton flavor sector. The quark Yukawa terms of Eqs. (65,66) are then be rewritten as follows

$$\begin{aligned} -\mathcal{L}^{d_a \rightarrow d_b} &= \bar{u}'_a (g_L^{H^+ \bar{u}_a d_b} P_L + g_R^{H^+ \bar{u}_a d_b} P_R) d'_b H^+ + \bar{u}'_a (g_L^{H_{1,2}^+ \bar{u}_a d_b} P_L + g_R^{H_{1,2}^+ \bar{u}_a d_b} P_R) d'_b H_{1,2}^+ \\ &+ \bar{U}' (g_L^{H^+ \bar{U} d_b} P_L + g_R^{H^+ \bar{U} d_b} P_R) d'_b H^+ + \bar{U}' (g_L^{H_{1,2}^+ \bar{U} d_b} P_L + g_R^{H_{1,2}^+ \bar{U} d_b} P_R) d'_b H_{1,2}^+ \\ &+ \sum_{p=1}^8 \bar{D}'_1 (g_L^{H_p \bar{D}_1 d_b} P_L + g_R^{H_p \bar{D}_1 d_b} P_R) d'_b H_p + i \sum_{p=3}^8 \bar{D}'_1 (g_L^{A_p \bar{D}_1 d_b} P_L + g_R^{H_p \bar{D}_1 d_b} P_R) d'_b \mathcal{A}_p \\ &+ \sum_{p=1}^8 \bar{d}'_a (g_R^{H_p \bar{d}_a d_b} P_R) d'_b H_p + i \sum_{p=3}^8 \bar{d}'_a (g_L^{A_p \bar{d}_a d_b} P_R) d'_b \mathcal{A}_p + H.c., \end{aligned} \quad (68)$$

$$\begin{aligned} -\mathcal{L}^{u_a \rightarrow u_b} &= \bar{D}'_1 (g_L^{H^- \bar{D}_1 u_b} P_L + g_R^{H^- \bar{D}_1 u_b} P_R) u'_b H^- + \bar{D}'_1 (g_L^{H_{1,2}^- \bar{D}_1 u_b} P_L + g_R^{H_{1,2}^- \bar{D}_1 u_b} P_R) u'_b H_{1,2}^- \\ &+ \sum_{p=1}^8 \bar{U}' (g_L^{H_p \bar{U} u_b} P_L + g_R^{H_p \bar{U} u_b} P_R) u'_b H_p + i \sum_{p=3}^8 \bar{U}' (g_L^{A_p \bar{U} u_b} P_L + g_R^{H_p \bar{U} u_b} P_R) u'_b \mathcal{A}_p \\ &+ \sum_{p=1}^8 \bar{u}'_a (g_R^{H_p \bar{u}_a u_b} P_R) u'_b H_p + i \sum_{p=3}^8 \bar{u}'_a (g_R^{A_p \bar{u}_a u_b} P_R) u'_b \mathcal{A}_p + H.c., \end{aligned} \quad (69)$$

where the coefficients in Eqs. (68,69) are defined in Appendix A. Here, we will clarify in detail the roles of each term in the above given Yukawa interactions. The terms in the first and second lines of Eq. (68) contribute to flavor-changing neutral current processes (FCNC), such as the inclusive decay branching ratio $\text{BR}(\bar{B} \rightarrow X_s \gamma)$ at one-loop level. This process involves the virtual exchange of charged Higgs $H^\pm, H_{1,2}^\pm$ and up type quarks (both SM u or new exotic ones U) in the internal lines of the loops, as illustrated in subfigure (a) in Fig. (2). The terms of the third line similarly contribute to such processes, but through the one-loop level exchange of neutral CP even (odd) Higgs bosons $H(\mathcal{A})$ and new exotic down type quark D_1 , as shown in (subfigure (b) in Fig. (2)). The observables are also influenced by the one-loop exchange of the same neutral Higgs, but with the internal quarks in the loop being the SM ones d , rather than the new quark D_1 , shown in the last line of Eq. (68). Otherwise, the terms in Eq. (69) contribute to observables in up type quark transition $u_a \rightarrow u_b$, such as the branching ratios of FCNC top quark decays, i.e $\text{BR}(t \rightarrow u(c)\gamma)$, $\text{BR}(t \rightarrow h(u, c))$ (see the subfigure (c) and (d) in Fig. (2).) Furthermore, we want to emphasize that the terms in the last line of Eq. (68) and Eq. (69) trigger the meson mixing $K^0 - \bar{K}^0, B_{s,d}^0 - \bar{B}_{s,d}^0$ and $D^0 - \bar{D}^0$ at the tree-level via the exchange of CP even(odd) Higgs bosons $H(\mathcal{A})$ (see the subfigure (e)). Particularly, for the index $p = 1$, the terms also describe the tree-level flavor violating decays of SM-like Higgs boson $h \rightarrow \bar{d}_a d_b, h \rightarrow \bar{u}_a u_b$.

It is important to note that when combining the lepton flavor conserving (violating) interactions by $H(\mathcal{A})$ in Eq. (47), the model provides the tree-level contributions to several observables, namely the branching ratio of leptonic decays $\text{BR}(B_s \rightarrow l^+ l^-)$, $\text{BR}(B_s \rightarrow \tau^+ \mu^-)$; semileptonic decays $\text{BR}(B \rightarrow K \tau^+ \tau^-)$, $\text{BR}(B^+ \rightarrow K^+ \tau^+ \mu^-)$, the lepton flavor universality violating (LFUV) ratios $R_{K^{(*)}} = \frac{\text{BR}(B \rightarrow K^{(*)} \mu^+ \mu^-)}{\text{BR}(B \rightarrow K^{(*)} e^+ e^-)}$ (shown in subfigure (f)). Additionally, the terms in the first line also contribute to the observables related to flavor-changing charged currents (FCCCs) at the tree-level ($b \rightarrow c \bar{\nu} \nu_\tau$), such as LFUV ratios $R_{D^{(*)}} = \frac{\text{BR}(\bar{B} \rightarrow D^{(*)} \tau \bar{\nu}_\tau)}{\text{BR}(\bar{B} \rightarrow D^{(*)} l \bar{\nu}_l)}$, $l = e, \mu$, shown in subfigure (g) in Fig. (2).

Besides the above-mentioned contributions, the model also provides other contributions arising from the new neutral gauge boson Z' with quark flavor violating couplings $Z'\bar{q}_{iL}q_{jL}$ at tree-level, due to the different $U(1)_X$ charges of left-handed third quark q_{3L} generation compared to the first and second ones $q_{(1,2)L}$. This kind of contribution not only yields new physics contributions to meson mass splittings $\Delta m_{K, B_s, B_d}$ at tree-level as pointed out in the previous work [46] but also give rise to other FCNC observables such as $\text{BR}(\bar{B} \rightarrow X_s \gamma)$ at one-loop level (with Z' and SM down type quark d_i are internal lines), $\text{BR}(B_s \rightarrow l^+ l^-)$ at the tree-level (subfigure (h) in Fig. (2)). However, the contribution of this Z' to the inclusive decay $\text{BR}(\bar{B} \rightarrow X_s \gamma)$ is negligible, in comparison with contributions of charged Higgs bosons [62]. All of these contributions will be analyzed in detail in the section on numerical studies.

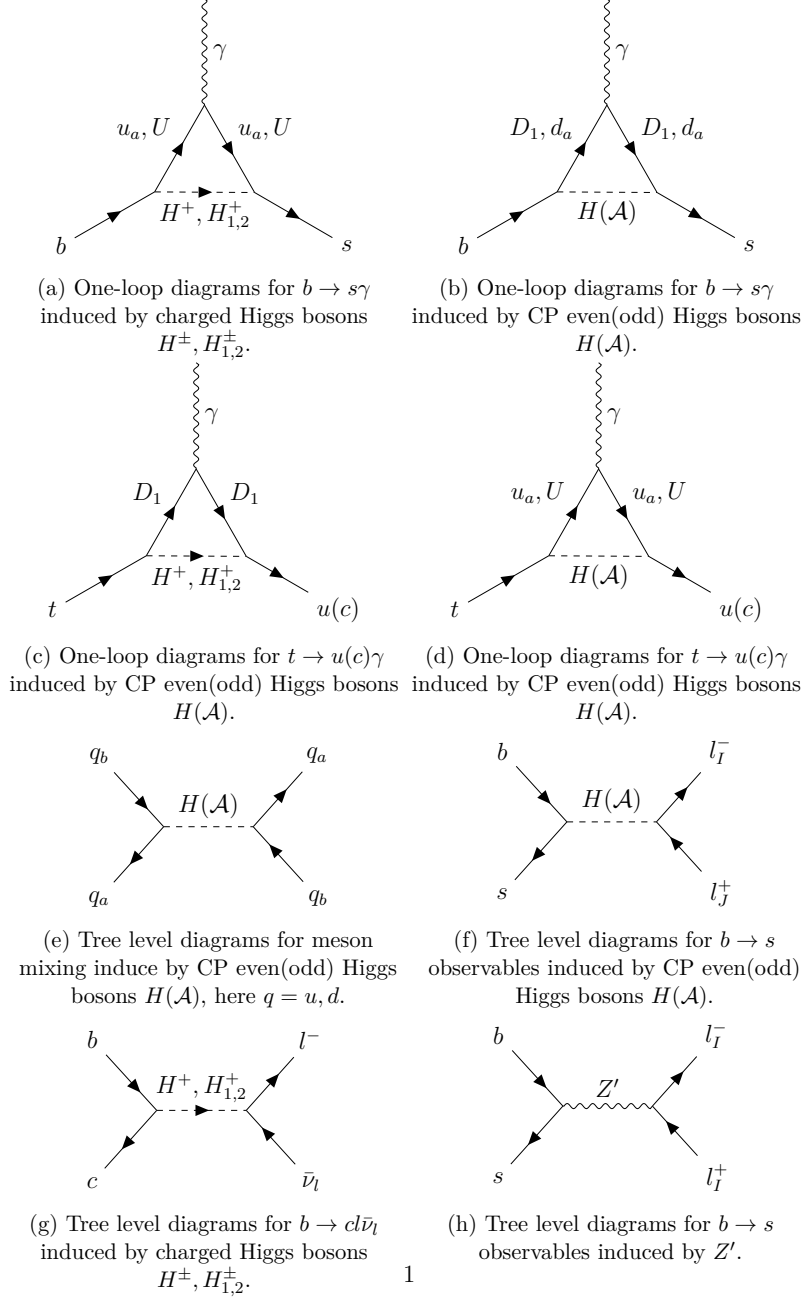


Figure 2: Feynman diagrams for $b \rightarrow s$, $b \rightarrow c$ and $t \rightarrow u(c)$ quark transitions.

1. FCNC $d_a \rightarrow d_b$ observables

Firstly, we study the FCNC $d_a \rightarrow d_b$ observables which can be described via the general effective Hamiltonian

$$\mathcal{H}_{\text{eff}} = -\frac{4G_F}{\sqrt{2}}V_{ts}^*V_{tb} \left\{ \sum_{i=7,8,9,10} [C_i(\mu)\mathcal{O}_i(\mu) + C'_i(\mu)\mathcal{O}'_i(\mu)] + \sum_{i=S,P} [C_i^{IJ}(\mu)\mathcal{O}_i^{IJ}(\mu) + C_i'^{IJ}(\mu)\mathcal{O}'_i{}^{IJ}(\mu)] \right\}, \quad (70)$$

where $C_i^{(\prime)}(\mu)$ are the Wilson coefficients (WCs) corresponding to the effective operators $\mathcal{O}_i^{(\prime)}$ for $b \rightarrow s$ observables at the scale $\mu = \mathcal{O}(m_b)$. The indices I, J denote different lepton flavors in WCs $C_{S,P}^{(\prime)}$ since the model contains lepton flavor violating coupling related to CP even(odd) Higgs bosons³. All WCs are defined as follows

$$\mathcal{O}_7^{(\prime)} = \frac{e}{16\pi^2}m_b(\bar{s}\sigma^{\mu\nu}P_{R(L)}b)F_{\mu\nu}, \quad \mathcal{O}_8^{(\prime)} = \frac{g_s}{16\pi^2}m_b(\bar{s}\sigma^{\mu\nu}T^aP_{R(L)}b)G_{\mu\nu}^a, \quad (71)$$

$$\mathcal{O}_9^{(\prime)} = \frac{e^2}{16\pi^2}(\bar{s}\gamma^\mu P_{L(R)}b)(\bar{l}\gamma_\mu l), \quad \mathcal{O}_{10}^{(\prime)} = \frac{e^2}{16\pi^2}(\bar{s}\gamma^\mu P_{L(R)}b)(\bar{l}\gamma_\mu\gamma_5 l), \quad (72)$$

$$\mathcal{O}_S^{IJ(\prime)} = \frac{e^2}{16\pi^2}(\bar{s}P_{L(R)}b)(\bar{l}_I l_J), \quad \mathcal{O}_P^{IJ(\prime)} = \frac{e^2}{16\pi^2}(\bar{s}P_{L(R)}b)(\bar{l}_I\gamma_5 l_J). \quad (73)$$

The primed WCs C'_i, \tilde{C}'_S corresponding to the operators $\mathcal{O}'_i, \tilde{\mathcal{O}}'_S$ are obtained by flipping the chirality. It is important to emphasize that the quark mixing matrix $V_q = V_{u_L}^\dagger V_{d_L}$ obtained from the diagonalization of the low energy up and down type quark mass matrices is found to be unitary. Its magnitude $|V|$ is consistent with the absolute entry value constraints of the CKM matrix given in [13], as shown in Sec (VI A). However, the matrix itself V has the different entries $(V_q)_{ij}$ compared to corresponding CKM ones defined by the "standard" parametrization with three mixing angles and one CP violation phase [13]. Therefore, the SM WCs in our model are modified by $C_{7,8,9,10}^{\text{SM}} \rightarrow C_{7,8,9,10}^{\text{SM}} \frac{(V_q^*)_{32}(V_q)_{33}}{V_{ts}^*V_{tb}}$. We can split the WCs as combination of both SM and NP, i.e. $C_{7,8,9,10}^{(\prime)} = C_{7,8,9,10}^{\text{SM}} \frac{(V_q^*)_{32}(V_q)_{33}}{V_{ts}^*V_{tb}} + C_i^{(\prime)\text{NP}}$, where $C_{7,8,9,10}^{\text{SM}}$ have been calculated in SM [63–65], whereas $C_{S,P}^{\text{SM}}$ are absent. For WCs of NP $C_{7,8,9,10,S,P}^{(\prime)\text{NP}}$, we can write them as the summation of different NP contributions as follows

$$\begin{aligned} C_{7,8}^{\text{NP}}(\mu) &= C_{7,8}^{H^+ \bar{u}d}(\mu) + C_{7,8}^{H_{1(2)}^+ \bar{u}d}(\mu) + C_{7,8}^{H^+ \bar{U}d}(\mu) + C_{7,8}^{H_{1(2)}^+ \bar{U}d}(\mu) + C_{7,8}^{H_p \bar{D}_1 d}(\mu) + C_{7,8}^{A_p \bar{D}_1 d}(\mu), \\ C_{7,8}^{\prime\text{NP}}(\mu) &= C_{7,8}^{\prime H^+ \bar{u}d}(\mu) + C_{7,8}^{\prime H_{1(2)}^+ \bar{u}d}(\mu) + C_{7,8}^{\prime H^+ \bar{U}d}(\mu) + C_{7,8}^{\prime H_{1(2)}^+ \bar{U}d}(\mu) + C_{7,8}^{\prime H_p \bar{D}_1 d}(\mu) + C_{7,8}^{\prime A_p \bar{D}_1 d}(\mu) \\ &\quad + C_{7,8}^{\prime H_p \bar{d}d}(\mu) + C_{7,8}^{\prime A_p \bar{d}d}(\mu), \\ C_9^{\text{NP}}(\mu) &= C_9^{Z'}(\mu), \quad C_{10}^{\text{NP}}(\mu) = C_{10}^{Z'}(\mu), \quad C_{9,10}^{\prime\text{NP}}(\mu) = 0, \\ C_S^{(\prime)IJ}(\mu) &= \sum_{p=1}^8 (C_S^{(\prime)H_p \bar{d}_2 d_3})_{IJ}(\mu), \quad C_P^{(\prime)IJ}(\mu) = \sum_{p=3}^8 (C_P^{(\prime)A_p \bar{d}_2 d_3})_{IJ}(\mu). \end{aligned} \quad (74)$$

It should be noted that the WCs depend on the energy scale. The model contains several energy scales namely masses of the new Higgses as well as the Z' gauge boson mass. Because the QCD running effect is negligible at high energy, we can assume that these scales are approximately the same $\mu_H \sim \mathcal{O}(m_H)$, thus implying that the WCs only depend on a single energy scale $\mu = \mu_H$. For simplicity, we calculate the loop contributions at on-shell, i.e., $q^2 = 0$, $p_s^2 = m_s^2$, and $p_b^2 = m_b^2$. Because $m_s \ll m_b$, we set the s quark mass to be zero, $m_s = 0$, and keep the mass of b quark at the linear order, i.e. $m_b^2 = 0$. Thus, we have the following expression of WCs at scale $\mu = \mu_H$ for $b \rightarrow s$ transitions as

³ However, the WCs $C_{9,10}$ are only generated by new neutral gauge boson Z' which have the same couplings with three lepton generations, thus these are no lepton flavor universality violations (LFUV) caused by these WCs.

follows

$$\begin{aligned}
C_7^{H^+\bar{u}d}(\mu_H) &= \frac{-\sqrt{2}}{8G_F V_{ts}^* V_{tb} m_{H^\pm}^2} \sum_{a=1}^3 \left[(g_L^{H^+\bar{u}_a d_2})^* g_L^{H^+\bar{u}_a d_3} f_\gamma'' \left(\frac{m_{u_a}^2}{m_{H^+}^2} \right) + (g_L^{H^+\bar{u}_a d_2})^* g_R^{H^+\bar{u}_a d_3} \frac{m_{u_a}}{m_b} h_\gamma'' \left(\frac{m_{u_a}^2}{m_{H^+}^2} \right) \right], \\
C_7^{\prime H^+\bar{u}d}(\mu_H) &= \frac{-\sqrt{2}}{8G_F V_{ts}^* V_{tb} m_{H^\pm}^2} \sum_{a=1}^3 \left[(g_R^{H^+\bar{u}_a d_2})^* g_R^{H^+\bar{u}_a d_3} f_\gamma'' \left(\frac{m_{u_a}^2}{m_{H^+}^2} \right) + (g_R^{H^+\bar{u}_a d_2})^* g_L^{H^+\bar{u}_a d_3} \frac{m_{u_a}}{m_b} h_\gamma'' \left(\frac{m_{u_a}^2}{m_{H^+}^2} \right) \right], \\
C_7^{H_{1(2)}^+\bar{u}d}(\mu_H) &= \frac{-\sqrt{2}}{8G_F V_{ts}^* V_{tb} m_{H_{1(2)}^\pm}^2} \sum_{a=1}^3 \left[(g_L^{H_{1(2)}^+\bar{u}_a d_2})^* g_L^{H_{1(2)}^+\bar{u}_a d_3} f_\gamma'' \left(\frac{m_{u_a}^2}{m_{H_{1(2)}^+}^2} \right) + (g_L^{H_{1(2)}^+\bar{u}_a d_2})^* g_R^{H_{1(2)}^+\bar{u}_a d_3} \frac{m_{u_a}}{m_b} h_\gamma'' \left(\frac{m_{u_a}^2}{m_{H_{1(2)}^+}^2} \right) \right], \\
C_7^{\prime H_{1(2)}^+\bar{u}d}(\mu_H) &= \frac{-\sqrt{2}}{8G_F V_{ts}^* V_{tb} m_{H_{1(2)}^\pm}^2} \sum_{a=1}^3 \left[(g_R^{H_{1(2)}^+\bar{u}_a d_2})^* g_R^{H_{1(2)}^+\bar{u}_a d_3} f_\gamma'' \left(\frac{m_{u_a}^2}{m_{H_{1(2)}^+}^2} \right) + (g_R^{H_{1(2)}^+\bar{u}_a d_2})^* g_L^{H_{1(2)}^+\bar{u}_a d_3} \frac{m_{u_a}}{m_b} h_\gamma'' \left(\frac{m_{u_a}^2}{m_{H_{1(2)}^+}^2} \right) \right], \\
C_7^{H^+\bar{U}d}(\mu_H) &= \frac{-\sqrt{2}}{8G_F V_{ts}^* V_{tb} m_{H^\pm}^2} \left[(g_L^{H^+\bar{U}d_2})^* g_L^{H^+\bar{U}d_3} f_\gamma'' \left(\frac{m_U^2}{m_{H^+}^2} \right) + (g_L^{H^+\bar{U}d_2})^* g_R^{H^+\bar{U}d_3} \frac{m_U}{m_b} h_\gamma'' \left(\frac{m_U^2}{m_{H^+}^2} \right) \right], \\
C_7^{\prime H^+\bar{U}d}(\mu_H) &= \frac{-\sqrt{2}}{8G_F V_{ts}^* V_{tb} m_{H^\pm}^2} \left[(g_R^{H^+\bar{U}d_2})^* g_R^{H^+\bar{U}d_3} f_\gamma'' \left(\frac{m_U^2}{m_{H^+}^2} \right) + (g_R^{H^+\bar{U}d_2})^* g_L^{H^+\bar{U}d_3} \frac{m_U}{m_b} h_\gamma'' \left(\frac{m_U^2}{m_{H^+}^2} \right) \right], \\
C_7^{H_{1(2)}^+\bar{U}d}(\mu_H) &= \frac{-\sqrt{2}}{8G_F V_{ts}^* V_{tb} m_{H_{1(2)}^\pm}^2} \left[(g_L^{H_{1(2)}^+\bar{U}d_2})^* g_L^{H_{1(2)}^+\bar{U}d_3} f_\gamma'' \left(\frac{m_U^2}{m_{H_{1(2)}^+}^2} \right) + (g_L^{H_{1(2)}^+\bar{U}d_2})^* g_R^{H_{1(2)}^+\bar{U}d_3} \frac{m_U}{m_b} h_\gamma'' \left(\frac{m_U^2}{m_{H_{1(2)}^+}^2} \right) \right], \\
C_7^{\prime H_{1(2)}^+\bar{U}d}(\mu_H) &= \frac{-\sqrt{2}}{8G_F V_{ts}^* V_{tb} m_{H_{1(2)}^\pm}^2} \left[(g_R^{H_{1(2)}^+\bar{U}d_2})^* g_R^{H_{1(2)}^+\bar{U}d_3} f_\gamma'' \left(\frac{m_U^2}{m_{H_{1(2)}^+}^2} \right) + (g_R^{H_{1(2)}^+\bar{U}d_2})^* g_L^{H_{1(2)}^+\bar{U}d_3} \frac{m_U}{m_b} h_\gamma'' \left(\frac{m_U^2}{m_{H_{1(2)}^+}^2} \right) \right], \\
C_7^{H_p \bar{D}_1 d}(\mu_H) &= \frac{\sqrt{2}}{24G_F V_{ts}^* V_{tb}} \sum_{p=1}^8 \frac{1}{m_{H_p}^2} \left[(g_L^{H_p \bar{D}_1 d_2})^* g_L^{H_p \bar{D}_1 d_3} f_\gamma' \left(\frac{m_{D_1}^2}{m_{H_p}^2} \right) + (g_L^{H_p \bar{D}_1 d_2})^* g_R^{H_p \bar{D}_1 d_3} \frac{m_{D_1}}{m_b} h_\gamma' \left(\frac{m_{D_1}^2}{m_{H_p}^2} \right) \right], \\
C_7^{\prime H_p \bar{D}_1 d}(\mu_H) &= \frac{\sqrt{2}}{24G_F V_{ts}^* V_{tb}} \sum_{p=1}^8 \frac{1}{m_{H_p}^2} \left[(g_R^{H_p \bar{D}_1 d_2})^* g_R^{H_p \bar{D}_1 d_3} f_\gamma' \left(\frac{m_{D_1}^2}{m_{H_p}^2} \right) + (g_R^{H_p \bar{D}_1 d_2})^* g_L^{H_p \bar{D}_1 d_3} \frac{m_{D_1}}{m_b} h_\gamma' \left(\frac{m_{D_1}^2}{m_{H_p}^2} \right) \right], \\
C_7^{A_p \bar{D}_1 d}(\mu_H) &= \frac{\sqrt{2}}{24G_F V_{ts}^* V_{tb}} \sum_{p=3}^8 \frac{1}{m_{A_p}^2} \left[(g_L^{A_p \bar{D}_1 d_2})^* g_L^{A_p \bar{D}_1 d_3} f_\gamma' \left(\frac{m_{D_1}^2}{m_{A_p}^2} \right) + (g_L^{A_p \bar{D}_1 d_2})^* g_R^{A_p \bar{D}_1 d_3} \frac{m_{D_1}}{m_b} h_\gamma' \left(\frac{m_{D_1}^2}{m_{A_p}^2} \right) \right], \\
C_7^{\prime A_p \bar{D}_1 d}(\mu_H) &= \frac{\sqrt{2}}{24G_F V_{ts}^* V_{tb}} \sum_{p=3}^8 \frac{1}{m_{A_p}^2} \left[(g_R^{A_p \bar{D}_1 d_2})^* g_R^{A_p \bar{D}_1 d_3} f_\gamma' \left(\frac{m_{D_1}^2}{m_{A_p}^2} \right) + (g_R^{A_p \bar{D}_1 d_2})^* g_L^{A_p \bar{D}_1 d_3} \frac{m_{D_1}}{m_b} h_\gamma' \left(\frac{m_{D_1}^2}{m_{A_p}^2} \right) \right], \\
C_7^{\prime H_p \bar{d}d}(\mu_H) &= \frac{\sqrt{2}}{24G_F V_{ts}^* V_{tb}} \sum_{p=1}^8 \frac{1}{m_{H_p}^2} \sum_{a=1}^3 \left[(g_R^{H_p \bar{d}_a d_2})^* g_R^{H_p \bar{d}_a d_3} f_\gamma' \left(\frac{m_{d_a}^2}{m_{H_p}^2} \right) \right], \\
C_7^{\prime A_p \bar{d}d}(\mu_H) &= \frac{\sqrt{2}}{24G_F V_{ts}^* V_{tb}} \sum_{p=3}^8 \frac{1}{m_{A_p}^2} \sum_{a=1}^3 \left[(g_R^{A_p \bar{d}_a d_2})^* g_R^{A_p \bar{d}_a d_3} f_\gamma' \left(\frac{m_{d_a}^2}{m_{A_p}^2} \right) \right], \tag{75}
\end{aligned}$$

where the functions $f_\gamma^{(\prime\prime)}$, $h_\gamma^{(\prime\prime)}$ are given in Appendix B. The WCs $C_8^{(\prime)}$ have similar form as C_7 but replacing functions $f_\gamma^{(\prime\prime)}$, $h_\gamma^{(\prime\prime)}$ by $f_g^{(\prime\prime)}$, $h_g^{(\prime\prime)}$. For the WCs associated Z' boson, there are WCs $C_{9,10}$ as follows

$$C_9^{(Z')}(\mu_H) = \frac{8\sqrt{2}\pi^2 g_X^2}{9e^2 G_F V_{ts}^* V_{tb} m_{Z'}^2} (V_{d_L}^*)_{32} (V_{d_L})_{33}, \quad C_{10}^{(Z')}(\mu_H) = \frac{4\sqrt{2}\pi^2 g_X^2}{9e^2 G_F V_{ts}^* V_{tb} m_{Z'}^2} (V_{d_L}^*)_{32} (V_{d_L})_{33}. \tag{76}$$

Here we denote g_X is the coupling of Z' gauge boson, which is given in [46]. We want to emphasize that WCs $C_{9,10}$ in our model are blinded with lepton flavor, i.e $C_{9,10}^e = C_{9,10}^\mu = C_{9,10}^\tau$ since all three lepton generations are identical under the gauge symmetry group. Furthermore, the LFUV ratios $R_{K^{(*)}}$ mostly depend on $C_{9,10}$, thus making these observable to be nearly identity, which satisfies the current experimental results [66]. On the other hand, the CP even

(odd) Higgs cause scalar and pseudoscalar WCs $C_{S,P}^{(\prime)IJ}$, which have the following expressions

$$(C_S^{H_p \bar{d}_2 d_3})^{IJ}(\mu_H) = \frac{16\pi^2}{e^2} \frac{\sqrt{2}}{4G_F V_{ts}^* V_{tb}} \sum_{p=1}^8 \frac{(g_R^{H_p \bar{d}_3 d_2})^* (g_R^{H_p \bar{l}_1 l_J} + g_R^{H_p \bar{l}_J l_1})}{2m_{H_p}^2}, \quad (77)$$

$$(C_S^{\prime H_p \bar{d}_2 d_3})^{IJ}(\mu_H) = \frac{16\pi^2}{e^2} \frac{\sqrt{2}}{4G_F V_{ts}^* V_{tb}} \sum_{p=1}^8 \frac{g_R^{H_p \bar{d}_2 d_3} (g_R^{H_p \bar{l}_1 l_J} + g_R^{H_p \bar{l}_J l_1})}{2m_{H_p}^2}, \quad (78)$$

$$(C_P^{A_p \bar{d}_2 d_3})^{IJ}(\mu_H) = -\frac{16\pi^2}{e^2} \frac{\sqrt{2}}{4G_F V_{ts}^* V_{tb}} \sum_{p=3}^8 \frac{(g_R^{A_p \bar{d}_3 d_2})^* (g_R^{A_p \bar{l}_1 l_J} + g_R^{A_p \bar{l}_J l_1})}{2m_{A_p}^2}, \quad (79)$$

$$(C_P^{\prime A_p \bar{d}_2 d_3})^{IJ}(\mu_H) = -\frac{16\pi^2}{e^2} \frac{\sqrt{2}}{4G_F V_{ts}^* V_{tb}} \sum_{p=3}^8 \frac{g_R^{A_p \bar{d}_2 d_3} (g_R^{A_p \bar{l}_1 l_J} + g_R^{A_p \bar{l}_J l_1})}{2m_{A_p}^2}. \quad (80)$$

With the definitions of WCs, we have the following formula for the branching ratio $\text{BR}(B_s \rightarrow \mu^+ \mu^-)$ [67],

$$\begin{aligned} \text{BR}(B_s \rightarrow \mu^+ \mu^-) &= \frac{\tau_{B_s}}{64\pi^3} \alpha^2 G_F^2 f_{B_s}^2 |V_{tb} V_{ts}^*|^2 m_{B_s} \sqrt{1 - \frac{4m_\mu^2}{m_{B_s}^2}} \left\{ \left(1 - \frac{4m_\mu^2}{m_{B_s}^2} \right) \left| \frac{m_{B_s}^2}{m_b + m_s} (C_S^{\mu\mu} - C_S^{\prime\mu\mu}) \right|^2 \right. \\ &\quad \left. + \left| 2m_\mu C_{10} + \frac{m_{B_s}^2}{m_b + m_s} (C_P^{\mu\mu} - C_P^{\prime\mu\mu}) \right|^2 \right\}, \end{aligned} \quad (81)$$

where τ_{B_s} is the lifetime of B_s meson, α_{em} is the fine-structure constant. Furthermore, we have to take into account the effect of $B_s - \bar{B}_s$ oscillations, therefore theoretical prediction is related to the experimental value by [68]

$$\text{BR}(B_s \rightarrow \mu^+ \mu^-)_{\text{exp}} \simeq \frac{1}{1 - y_s} \text{BR}(B_s \rightarrow \mu^+ \mu^-), \quad (82)$$

where $y_s = \frac{\Delta\Gamma_{B_s}}{2\Gamma_{B_s}}$ which has numerical values is given Table VI.

For the inclusive decay $\bar{B} \rightarrow X_s \gamma$, we have its branching ratio given by [69, 70]

$$\text{BR}(\bar{B} \rightarrow X_s \gamma) = \frac{6\alpha_{\text{em}}}{\pi C} \left| \frac{V_{ts}^* V_{tb}}{V_{cb}} \right|^2 \left[|C_7(\mu_b)|^2 + |C_7'(\mu_b)|^2 + N(E_\gamma) \right] \text{BR}(\bar{B} \rightarrow X_c e \bar{\nu}), \quad (83)$$

where $N(E_\gamma)$ is a non-perturbative contribution which amounts around 4% of the branching ratio. We compute the leading order contribution to $N(E_\gamma)$ followed the Eq. (3.8) in Ref. [64] and then obtain $N(E_\gamma) \simeq 3.3 \times 10^{-3}$. Additionally, C is the semileptonic phase-space factor, $C = |V_{ub}/V_{cb}|^2 \Gamma(\bar{B} \rightarrow X_c e \bar{\nu}_e) / \Gamma(\bar{B} \rightarrow X_u e \bar{\nu}_e)$, and $\text{BR}(\bar{B} \rightarrow X_c e \bar{\nu})$ is the branching ratio for semileptonic decay. It is necessary to consider the QCD corrections to complete the calculation for such decay. The WCs $C_7^{(\prime)}(\mu_b)$ are evaluated at the matching scale $\mu_b = 2$ GeV by running down from the higher scale μ_H via the renormalization group equations. Its expression can be split as follows

$$C_7(\mu_b) = \frac{(V_q^*)_{32} (V_q)_{33}}{V_{ts}^* V_{tb}} C_7^{\text{SM}}(\mu_b) + C_7^{\text{NP}}(\mu_b), \quad C_7'(\mu_b) = C_7^{\prime\text{NP}}(\mu_b), \quad (84)$$

where $C_7^{\text{SM}}(\mu_b)$ is the SM WC and have been calculated up to next-to-next-leading order of QCD corrections at the scale $\mu_b = 2.0$ GeV [63, 64]. Furthermore, for the NP contributions at the matching scale μ_b , WCs $C_{7,8}$, we have [70]

$$C_7^{(\prime)H^\pm}(\mu_b) = \kappa_7 C_7^{(\prime)H^\pm}(m_{H^\pm}) + \kappa_8 C_8^{(\prime)H^\pm}(m_{H^\pm}), \quad (85)$$

where $\kappa_{7,8}$ are so called "magic numbers" and given in [70].

Besides, we also are interested in other observables which are affected by short-distance effects, such as the branching ratios of decays $B^+ \rightarrow K^+ \tau^+ \tau^-$, $B^+ \rightarrow K^+ \tau^+ \mu^-$, $B_s \rightarrow \tau^+ \mu^-$. These branching ratios are given by [71]

$$10^9 \times \text{BR}(B^+ \rightarrow K^+ \tau^+ \tau^-) = 2.2|C_9|^2 + 6|C_{10}|^2 + 8.3|C_S^{\tau\tau} - C_S^{\prime\tau\tau}|^2 + 8.9|C_P^{\tau\tau} - C_P^{\prime\tau\tau}|^2 \\ + 4.8\text{Re}[(C_S^{\tau\tau} - C_S^{\prime\tau\tau})C_9^*] + 5.9\text{Re}[(C_P^{\tau\tau} - C_P^{\prime\tau\tau})C_{10}^*], \quad (86)$$

$$10^9 \times \text{BR}(B^+ \rightarrow K^+ \tau^+ \mu^-) = 13.58|C_S^{\tau\mu} - C_S^{\prime\tau\mu}|^2 + 14.54|C_P^{\tau\mu} - C_P^{\prime\tau\mu}|^2, \quad (87)$$

$$\begin{aligned} \text{BR}(B_s \rightarrow \tau^- \mu^+) &= \frac{\tau_{B_s}}{64\pi^3} \alpha^2 G_F^2 f_{B_s}^2 |V_{ts}^* V_{tb}|^2 \frac{m_{B_s}^5}{(m_b + m_s)^2} \left(1 - \frac{m_\tau^2}{m_{B_s}^2} \right)^2 \\ &\quad \times (|C_S^{\tau\mu} - C_S^{\prime\tau\mu}|^2 + |C_P^{\tau\mu} - C_P^{\prime\tau\mu}|^2). \end{aligned} \quad (88)$$

We would like to note that the meson mass splittings such as $\Delta m_K, \Delta m_{B_s}$ and Δm_{B_d} were investigated in [46]. However, the authors have just considered these observables in simplified scenarios in which there were only a few Higgs contributions and assumptions real down quark Yukawa couplings. Therefore, in this work, we reconsider the meson mixing in more detail with all Higgs contributions and general Yukawa couplings. The new physics contributions to meson masses differences involve neutral gauge Z' and CP even (odd) Higgs $H(\mathcal{A})$ bosons as given by

$$\begin{aligned} \Delta m_K &\simeq \frac{2}{27} \frac{g_X^2}{m_{Z'}^2} \text{Re} \{ [(V_{dL})_{31}^* (V_{dL})_{32}]^2 \} m_K f_K^2 \\ &+ \frac{5}{48} \text{Re} \left\{ \sum_{p=1}^8 \left[\left(g_R^{H_p \bar{d}_1 d_2} \right)^2 + \left[\left(g_R^{H_p \bar{d}_2 d_1} \right)^* \right]^2 \right] \frac{1}{m_{H_p}^2} \right. \\ &- \sum_{p=3}^8 \left[\left(g_R^{\mathcal{A}_p \bar{d}_1 d_2} \right)^2 + \left[\left(g_R^{\mathcal{A}_p \bar{d}_2 d_1} \right)^* \right]^2 \right] \frac{1}{m_{\mathcal{A}_p}^2} \left. \right\} \left(\frac{m_K}{m_s + m_d} \right)^2 m_K f_K^2 \\ &- \frac{1}{4} \text{Re} \left\{ \sum_{p=1}^8 \left(g_R^{H_p \bar{d}_2 d_1} \right)^* \left(g_R^{H_p \bar{d}_1 d_2} \right) \frac{1}{m_{H_p}^2} + \sum_{p=3}^8 \left(g_R^{\mathcal{A}_p \bar{d}_2 d_1} \right)^* \left(g_R^{\mathcal{A}_p \bar{d}_1 d_2} \right) \frac{1}{m_{\mathcal{A}_p}^2} \right\} \left(\frac{1}{6} + \frac{m_K^2}{(m_s + m_d)^2} \right) m_K f_K^2, \quad (89) \end{aligned}$$

$$\begin{aligned} \Delta m_{B_s} &\simeq \frac{2}{27} \frac{g_X^2}{m_{Z'}^2} \text{Re} \{ [(V_{dL})_{32}^* (V_{dL})_{33}]^2 \} m_{B_s} f_{B_s}^2 \\ &+ \frac{5}{48} \text{Re} \left\{ \sum_{p=1}^8 \left[\left(g_R^{H_p \bar{d}_2 d_3} \right)^2 + \left[\left(g_R^{H_p \bar{d}_3 d_2} \right)^* \right]^2 \right] \frac{1}{m_{H_p}^2} \right. \\ &- \sum_{p=3}^8 \left[\left(g_R^{\mathcal{A}_p \bar{d}_2 d_3} \right)^2 + \left[\left(g_R^{\mathcal{A}_p \bar{d}_3 d_2} \right)^* \right]^2 \right] \frac{1}{m_{\mathcal{A}_p}^2} \left. \right\} \left(\frac{m_{B_s}}{m_s + m_b} \right)^2 m_{B_s} f_{B_s}^2 \\ &- \frac{1}{4} \text{Re} \left\{ \sum_{p=1}^8 \left(g_R^{H_p \bar{d}_2 d_3} \right)^* \left(g_R^{H_p \bar{d}_3 d_2} \right) \frac{1}{m_{H_p}^2} + \sum_{p=3}^8 \left(g_R^{\mathcal{A}_p \bar{d}_2 d_3} \right)^* \left(g_R^{\mathcal{A}_p \bar{d}_3 d_2} \right) \frac{1}{m_{\mathcal{A}_p}^2} \right\} \left(\frac{1}{6} + \frac{m_{B_s}^2}{(m_s + m_b)^2} \right) m_{B_s} f_{B_s}^2, \quad (90) \end{aligned}$$

$$\begin{aligned} \Delta m_{B_d} &\simeq \frac{2}{27} \frac{g_X^2}{m_{Z'}^2} \text{Re} \{ [(V_{dL})_{31}^* (V_{dL})_{33}]^2 \} m_{B_d} f_{B_d}^2 \\ &+ \frac{5}{48} \text{Re} \left\{ \sum_{p=1}^8 \left[\left(g_R^{H_p \bar{d}_1 d_3} \right)^2 + \left[\left(g_R^{H_p \bar{d}_3 d_1} \right)^* \right]^2 \right] \frac{1}{m_{H_p}^2} \right. \\ &- \sum_{p=3}^8 \left[\left(g_R^{\mathcal{A}_p \bar{d}_1 d_3} \right)^2 + \left[\left(g_R^{\mathcal{A}_p \bar{d}_3 d_1} \right)^* \right]^2 \right] \frac{1}{m_{\mathcal{A}_p}^2} \left. \right\} \left(\frac{m_{B_d}}{m_b + m_d} \right)^2 m_{B_d} f_{B_d}^2 \\ &- \frac{1}{4} \text{Re} \left\{ \sum_{p=1}^8 \left(g_R^{H_p \bar{d}_3 d_1} \right)^* \left(g_R^{H_p \bar{d}_1 d_3} \right) \frac{1}{m_{H_p}^2} + \sum_{p=3}^8 \left(g_R^{\mathcal{A}_p \bar{d}_3 d_1} \right)^* \left(g_R^{\mathcal{A}_p \bar{d}_1 d_3} \right) \frac{1}{m_{\mathcal{A}_p}^2} \right\} \left(\frac{1}{6} + \frac{m_{B_d}^2}{(m_b + m_d)^2} \right) m_{B_d} f_{B_d}^2. \quad (91) \end{aligned}$$

We want to remark that the new interactions in the considering model also generate a contribution to another meson mixing parameter of the Kaon system, named CP-violating parameters ϵ_K . By using the formula in Ref. [72], we find that the NP contribution to the ϵ_K parameter in the model can naively be expressed as $\epsilon_K^{H_p} \sim \text{Re}[g_R^{H_p \bar{s} d}] \text{Im}[g_R^{H_p \bar{s} d}]$ for the neutral Higgs contribution, and as $\epsilon_K^{Z'} \sim \text{Re}[g_L^{Z' \bar{s} d}] \text{Im}[g_L^{Z' \bar{s} d}]$ for the Z' contribution, with $g_L^{Z' \bar{s} d} = \frac{g_X}{3} (V_{uL}^*)_{31} (V_{uL})_{32}$. Using the numerical inputs shown below, we approximately estimate these contributions as $\epsilon_K^{H_p} \sim \mathcal{O}(10^{-19})$ whereas $\epsilon_K^{Z'} \sim \mathcal{O}(10^{-11})$. These values are remarkably tiny compared with the SM predictions [73] and the experimental values of $\epsilon_K^{\text{SM,exp}} \sim \mathcal{O}(10^{-3})$ [13], thus we ignore the NP contribution for this observable. On the other hand, we also do not consider NP contributions to the meson mixing observables in the up-type quark sector $\bar{D}^0 - D^0$ such as mass difference Δm_D . This is justified because $\Delta m_D \sim \text{Re}[(g_R^{H_p \bar{u} c})^2 + ((g_R^{H_p \bar{c} u})^*)^2] \sim \mathcal{O}(10^{-26})$ GeV for neutral Higgs contributions H_p , and $\Delta m_D^{Z'} \sim \text{Re}[(g_L^{Z' \bar{u} c})^2] \sim \mathcal{O}(10^{-19})$ GeV for Z' , which are significantly smaller compared with the current experimental constraints $\Delta m_D^{\text{exp}} = x \Gamma_D \in [5.78, 7.38] \times 10^{-16}$ GeV [74]. Besides, for the theoretical calculation in SM, the double Cabibbo and GIM suppression, makes the short-distance box diagrams

contributing to Δm_D much smaller by several orders compared with long-distance diagrams [75, 76], responsible for the large theoretical uncertainty for this observable. We cannot get the SM prediction with high precision for Δm_D . This is not like the case of $\Delta m_{B_s, B_d}$ which is mostly affected by short-distance box diagrams. For instance, we currently have that the magnitude Δm_D in the SM is much large than the corresponding NP contribution, i.e., $\Delta m_D^{\text{SM}} \sim \mathcal{O}(10^{-16} - 10^{-15}) \gg \Delta m_D^{\text{NP}}$. Consequently, the NP contributions of the model are significantly suppressed, and thus we do not consider the $\bar{D}^0 - D^0$ meson mixing in our analysis.

2. FCCC $b \rightarrow c$ observables

The effective Hamiltonian that induces the $b \rightarrow c$ transition reads

$$\mathcal{H}_{\text{eff}}^{b \rightarrow c} = \frac{4G_F}{\sqrt{2}} V_{cb} [\tilde{C}_V^I \tilde{\mathcal{O}}_V^I(\mu) + \tilde{C}_S^I(\mu) \tilde{\mathcal{O}}_S^I(\mu) + \tilde{C}'_S^I(\mu) \tilde{\mathcal{O}}_S^{\prime I}(\mu)], \quad (92)$$

where index I denotes the lepton flavor, and the operators are given as follows

$$\tilde{\mathcal{O}}_V^I = (\bar{c} \gamma_\mu P_L b) (\bar{l}_I \gamma^\mu P_L \nu_I), \quad \tilde{\mathcal{O}}_S^{\prime I} = (\bar{c} P_{L(R)} b) (\bar{l}_I P_L \nu_I). \quad (93)$$

Here the operator $\tilde{\mathcal{O}}_V$ is generated via the exchange of the SM charged gauge boson W_μ^\pm . In the SM, the WC of this operator is $\tilde{C}_V^{\text{SM}} = 1$ for all lepton flavor. However, as pointed out in the $b \rightarrow s$ observables sector and there is mixing in lepton sector, the WCs \tilde{C}_V will be modified as $\tilde{C}_V^I = \frac{(V_q)_{23}}{V_{cb}} (V_l^*)_{II}$. Here V_l is the leptonic mixing matrix defined by $V_l = V_{e_L}^\dagger V_{\nu_L}$ (shown below). Furthermore, the new charged Higgs bosons $H^\pm, H_{1,2}^\pm$ cause the operators $\tilde{\mathcal{O}}_S^{\prime I}$. Their corresponding WCs are given as follows

$$\tilde{C}_S^{\prime I} = \tilde{C}_S^{H^+ \bar{u}_2 d_3}(\mu_H) + \tilde{C}_S^{H_{1,2}^+ \bar{u}_2 d_3}(\mu_H), \quad (94)$$

with

$$\tilde{C}_S^{H^+ \bar{u}_2 d_3}(\mu_H) = \frac{\sqrt{2}}{4G_F V_{cb}} \frac{g_{L(R)}^{H^+ \bar{u}_2 d_3} (g_R^{H^+ \bar{\nu}_1 l_I})^*}{m_{H^\pm}^2}, \quad \tilde{C}_S^{H_{1,2}^+ \bar{u}_2 d_3}(\mu_H) = \frac{\sqrt{2}}{4G_F V_{cb}} \frac{g_{L(R)}^{H_{1,2}^+ \bar{u}_2 d_3} (g_R^{H_{1,2}^+ \bar{\nu}_1 l_I})^*}{m_{H_{1,2}^\pm}^2}. \quad (95)$$

Regarding the observables related to the $b \rightarrow c$ transition, we consider LFUV ratios $R_{D^{(*)}}$ which are defined by

$$R_{D^{(*)}} = \frac{\int_{m_\tau^2}^{(m_B - m_{D^{(*)}})^2} \frac{d\Gamma(\bar{B} \rightarrow D^{(*)} \tau \bar{\nu}_\tau)}{dq^2} dq^2}{\int_{m_l^2}^{(m_B - m_{D^{(*)}})^2} \frac{d\Gamma(\bar{B} \rightarrow D^{(*)} l \bar{\nu}_l)}{dq^2} dq^2}, \quad (96)$$

with q^2 is the squared transfer momentum, and l denotes either to e or μ . The differential decay widths of $\bar{B} \rightarrow D l \bar{\nu}_l$ and $\bar{B} \rightarrow D^* l \bar{\nu}_l$ are given as follows

$$\begin{aligned} \frac{d\Gamma(\bar{B} \rightarrow D l \bar{\nu}_l)}{dq^2} &= \frac{\eta_{\text{EW}}^2 G_F^2 |V_{cb}|^2 m_B \sqrt{\lambda}}{192\pi^3} \left(1 - \frac{m_l^2}{q^2}\right)^2 \left\{ \left[\frac{\lambda}{m_B^4} \left(1 + \frac{m_l^2}{2q^2}\right) (f_+(q^2))^2 + \frac{3m_l^2}{2q^2} \left(1 - \frac{m_D^2}{m_B^2}\right) (f_0(q^2))^2 \right] |C_V|^2 \right. \\ &+ \frac{3q^2}{2(m_b - m_c)^2} \left(1 - \frac{m_D^2}{m_B^2}\right)^2 (f_0(q^2))^2 |\tilde{C}_S + \tilde{C}'_S|^2 \\ &\left. + \frac{3m_l}{m_b - m_c} \text{Re}[\tilde{C}_V (\tilde{C}'_S + \tilde{C}_S^*)] \left(1 - \frac{m_D^2}{m_B^2}\right) (f_0(q^2))^2 \right\}, \quad (97) \end{aligned}$$

$$\begin{aligned} \frac{d\Gamma(\bar{B} \rightarrow D^* l \bar{\nu}_l)}{dq^2} &= \frac{\eta_{\text{EW}}^2 G_F^2 |V_{cb}|^2 m_B \sqrt{\lambda^3}}{192\pi^3} \left(1 - \frac{m_l^2}{q^2}\right)^2 \left\{ \left(1 + \frac{m_l^2}{5q^2}\right) \frac{5q^2(m_B + m_{D^*})^2}{2\lambda^*} (A_1(q^2))^2 + \frac{64m_B^2 m_{D^*}^2}{\lambda^*} (A_{12}(q^2))^2 \right. \\ &\left. + \frac{3m_l^2}{2q^2} (A_0(q^2))^2 |C_V|^2 + \frac{3q^2}{2(m_b + m_c)^2} (A_0(q^2))^2 |\tilde{C}_S - \tilde{C}'_S|^2 + \frac{m_l}{\sqrt{q^2}} \text{Re}[\tilde{C}_V (\tilde{C}_S^* - \tilde{C}'_S^*)] (A_0(q^2))^2 \right\} \quad (98) \end{aligned}$$

where $\eta_{\text{EW}} \simeq 1.0066$ is the QED correction [77]. $f_{+,0}(q^2)$ are the vector and scalar form factors (FFs) of $B \rightarrow D$ transition, whereas $A_{12}(q^2), A_0(q^2), A_1(q^2)$ are FFs for $B \rightarrow D^*$ transition. All FFs are depend on the squared

momentum transfer $q^2 = (m_B - m_D)^2$, and defined explicitly in Refs. [78, 79]. Otherwise, $\lambda^{(*)}$ is the Kallen function $\lambda = m_B^4 + m_{D^{(*)}}^4 + q^4 - 2(m_B^2 m_{D^{(*)}}^2 + m_B^2 q^2 + m_{D^{(*)}}^2 q^2)$, m_l is the mass of daughter lepton l . Taking integral, we obtain the following expressions for $R_{D^{(*)}}$ ratios as functions of WCs $\tilde{C}_{V_L}, \tilde{C}_S^{(\prime)}$

$$\begin{aligned} R_D &\simeq R_D^{\text{SM}} \frac{|\tilde{C}_{V_L}^\tau|^2 + 1.46\text{Re}[\tilde{C}_{V_L}^\tau (\tilde{C}_S^{\prime*\tau} + \tilde{C}_S^{*\tau})] + 0.98|\tilde{C}_S^{\prime\tau} + \tilde{C}_S^\tau|^2}{|\tilde{C}_{V_L}^\mu|^2 + 0.14\text{Re}[\tilde{C}_{V_L}^\mu (\tilde{C}_S^{\prime*\mu} + \tilde{C}_S^{*\mu})] + 0.95|\tilde{C}_S^{\prime\mu} + \tilde{C}_S^\mu|^2}, \\ R_{D^*} &\simeq R_{D^*}^{\text{SM}} \frac{|\tilde{C}_{V_L}^\tau|^2 + 0.127\text{Re}[\tilde{C}_{V_L}^\tau (\tilde{C}_S^{\prime*\tau} - \tilde{C}_S^{*\tau})] + 0.035|\tilde{C}_S^{\prime\tau} - \tilde{C}_S^\tau|^2}{|\tilde{C}_{V_L}^\mu|^2 + 0.037\text{Re}[\tilde{C}_{V_L}^\mu (\tilde{C}_S^{\prime*\mu} - \tilde{C}_S^{*\mu})] + 0.05|\tilde{C}_S^{\prime\mu} - \tilde{C}_S^\mu|^2}. \end{aligned} \quad (99)$$

It is important to note that the above expression of LFU ratios $R_{D^{(*)}}$ are written in the most general form and different than Refs [80–82] for the following reasons. Firstly, in the considering model, the charged Higgs bosons $H^\pm, H_{1,2}^\pm$ couplings to different lepton flavors are distinguishable, as given explicitly in Sec. A. As a result, this enables our predicted ratios $R_{D^{(*)}}$ to depend explicitly on both couplings of NP with τ and μ flavor. Secondly, the SM WC \tilde{C}_V is modified since the CKM matrix in the model has different entries $(V_q)_{ij}$ compared to CKM ones defined by the standard parameterization [13] as well as there are mixing between charged lepton and neutrino flavors. Thirdly, there are several charged Higgs contributions $H^\pm, H_{1,2}^\pm$ to these observables. Combining above mentions, $R_{D^{(*)}}$ in our model are differences compared to Refs. [80–82] which assume one charged Higgs contribution coupling to only τ flavor. Therefore, the below numerical studies about these observables will demonstrate differences from such works.

3. $t \rightarrow u(c)$ transitions

In terms of the observables related to the up type quark transitions $t \rightarrow u(c)$, we consider the branching ratios for the FCNC top quark decays $t \rightarrow u(c)h, t \rightarrow u(c)\gamma$. The branching ratios for the $t \rightarrow u(c)h$ decay are given by:

$$\text{BR}(t \rightarrow u(c)h) = \frac{(|g_R^{h\bar{u}_{1(2)}u_3}|^2 + |(g_R^{h\bar{u}_3u_{1(2)})^*}|^2) (m_t^2 - m_h^2)^2}{16\pi\Gamma_t m_t^3}, \quad (100)$$

where $\Gamma_t = 1.42_{-0.15}^{+0.19}$ GeV is the total decay width of top quark [13]. On the other hand, the branching ratios for the radiative decays $t \rightarrow u(c)\gamma i$ have the following expressions

$$\text{BR}(t \rightarrow u_i\gamma) = \frac{\Gamma(t \rightarrow u(c)\gamma)}{\Gamma_t^{\text{total}}} = \frac{m_t^3 (|C_L^{tu_i\gamma}|^2 + |C_R^{tu_i\gamma}|^2)}{16\pi\Gamma_t^{\text{total}}}, \quad i = 1, 2, \quad (101)$$

with $C_{L,R}^t$ are the coefficients combining by different contributions

$$\begin{aligned}
C_R^{tu_i\gamma} &= \frac{iem_t}{16\pi^2 m_{H^\pm}^2} \left[(g_L^{H^- \bar{D}_1 u_i})^* g_L^{H^- \bar{D}_1 u_3} f_\gamma''' \left(\frac{m_{D_1}^2}{m_{H^\pm}^2} \right) + (g_L^{H^- \bar{D}_1 u_i})^* g_R^{H^- \bar{D}_1 u_3} \frac{m_{D_1}}{m_t} h_\gamma''' \left(\frac{m_{D_1}^2}{m_{H^\pm}^2} \right) \right] \\
&+ \frac{iem_t}{16\pi^2 m_{H_{1(2)}^\pm}^2} \left[(g_L^{H_{1(2)}^- \bar{D}_1 u_i})^* g_L^{H_{1(2)}^- \bar{D}_1 u_3} f_\gamma''' \left(\frac{m_{D_1}^2}{m_{H_{1(2)}^\pm}^2} \right) + (g_L^{H_{1(2)}^- \bar{D}_1 u_i})^* g_R^{H_{1(2)}^- \bar{D}_1 u_3} \frac{m_{D_1}}{m_t} h_\gamma''' \left(\frac{m_{D_1}^2}{m_{H_{1(2)}^\pm}^2} \right) \right] \\
&+ \frac{iem_t}{24\pi^2} \sum_{p=1}^8 \frac{1}{m_{H_p}^2} \left[(g_L^{H_p \bar{U} u_i})^* g_L^{H_p \bar{U} u_3} f_\gamma' \left(\frac{m_U^2}{m_{H_p}^2} \right) + (g_L^{H_p \bar{U} u_i})^* g_R^{H_p \bar{U} u_3} \frac{m_U}{m_t} h_\gamma' \left(\frac{m_U^2}{m_{H_p}^2} \right) \right] \\
&+ \frac{iem_t}{24\pi^2} \sum_{p=3}^8 \frac{1}{m_{A_p}^2} \left[(g_L^{A_p \bar{U} u_i})^* g_L^{A_p \bar{U} u_3} f_\gamma' \left(\frac{m_U^2}{m_{A_p}^2} \right) + (g_L^{A_p \bar{U} u_i})^* g_R^{A_p \bar{U} u_3} \frac{m_U}{m_t} h_\gamma' \left(\frac{m_U^2}{m_{A_p}^2} \right) \right], \\
C_L^{tu_i\gamma} &= \frac{iem_t}{16\pi^2 m_{H^\pm}^2} \left[(g_R^{H^- \bar{D}_1 u_i})^* g_R^{H^- \bar{D}_1 u_3} f_\gamma''' \left(\frac{m_{D_1}^2}{m_{H^\pm}^2} \right) + (g_R^{H^- \bar{D}_1 u_i})^* g_L^{H^- \bar{D}_1 u_3} \frac{m_{D_1}}{m_t} h_\gamma''' \left(\frac{m_{D_1}^2}{m_{H^\pm}^2} \right) \right] \\
&+ \frac{iem_t}{16\pi^2 m_{H_{1(2)}^\pm}^2} \left[(g_R^{H_{1(2)}^- \bar{D}_1 u_i})^* g_R^{H_{1(2)}^- \bar{D}_1 u_3} f_\gamma''' \left(\frac{m_{D_1}^2}{m_{H_{1(2)}^\pm}^2} \right) + (g_R^{H_{1(2)}^- \bar{D}_1 u_i})^* g_L^{H_{1(2)}^- \bar{D}_1 u_3} \frac{m_{D_1}}{m_t} h_\gamma''' \left(\frac{m_{D_1}^2}{m_{H_{1(2)}^\pm}^2} \right) \right] \\
&+ \frac{iem_t}{24\pi^2} \sum_{p=1}^8 \frac{1}{m_{H_p}^2} \left[(g_R^{H_p \bar{U} u_i})^* g_R^{H_p \bar{U} u_3} f_\gamma' \left(\frac{m_U^2}{m_{H_p}^2} \right) + (g_R^{H_p \bar{U} u_i})^* g_L^{H_p \bar{U} u_3} \frac{m_U}{m_t} h_\gamma' \left(\frac{m_U^2}{m_{H_p}^2} \right) \right] \\
&+ \frac{iem_t}{24\pi^2} \sum_{p=3}^8 \frac{1}{m_{A_p}^2} \left[(g_L^{A_p \bar{U} u_i})^* g_L^{A_p \bar{U} u_3} f_\gamma' \left(\frac{m_U^2}{m_{A_p}^2} \right) + (g_R^{A_p \bar{U} u_i})^* g_L^{A_p \bar{U} u_3} \frac{m_U}{m_t} h_\gamma' \left(\frac{m_U^2}{m_{A_p}^2} \right) \right] \\
&+ \frac{iem_t}{24\pi^2} \left[\sum_{p=1}^8 \sum_{a=1}^3 \frac{1}{m_{H_p}^2} (g_R^{H_p \bar{u}_a u_i})^* g_R^{H_p \bar{u}_a u_3} f_\gamma' \left(\frac{m_{u_a}^2}{m_{H_p}^2} \right) + \sum_{p=3}^8 \sum_{a=1}^3 \frac{1}{m_{A_p}^2} (g_R^{A_p \bar{u}_a u_i})^* g_R^{A_p \bar{u}_a u_3} f_\gamma' \left(\frac{m_{u_a}^2}{m_{A_p}^2} \right) \right], \quad (102)
\end{aligned}$$

where the loop functions are shown in Appendix B. Similarly to the mentioned decays $b \rightarrow s\gamma$, we should consider the QCD corrections in $t \rightarrow u(c)\gamma$ decays. However, the QCD effects at next-to-leading order (NLO) to $t \rightarrow u(c)\gamma$ are negligible and modify the branching ratios of such decays around 0.2% compared to the LO contribution [83]. Moreover, both the measurements and theoretical predictions for such decays are currently not precisely known, as compared to the $b \rightarrow s\gamma$ decay⁴. Thus the role of QCD corrections is insignificant, and we can ignore the QCD effects in such observables.

4. Constraints on quark flavor processes

All the predicted observables should be compared with the corresponding experimental values shown in the last column in Table V. It is worth mentioning that the central values of SM prediction and the measurement results of some "clean" observables are quite close, including $\text{BR}(B_s \rightarrow \mu^+ \mu^-)$, $\text{BR}(\bar{B} \rightarrow X_s \gamma)$, LFUV ratios $R_{D^{(*)}}$ and $\text{BR}(B_i^- \rightarrow \tau \bar{\nu}_\tau)$. However, we should take into account the effect of both SM and experimental uncertainties. Therefore, it is better to consider the ratios between SM and respective experimental values on each clean observable since the uncertainties can be reduced via the numerator and denominator of these ratios. Moreover, considering ratios like that also causes the overall factors to be canceled. For instance, with the branching ratios $\text{BR}(B_s \rightarrow \mu^+ \mu^-)$ and $\text{BR}(\bar{B} \rightarrow X_s \gamma)$, we have the following constraints at 3σ range as follows

$$\frac{\text{BR}(B_s \rightarrow \mu^+ \mu^-)_{\text{exp}}}{\text{BR}(B_s \rightarrow \mu^+ \mu^-)_{\text{SM}}} = \frac{1}{1 - y_s} \frac{\left(1 - \frac{4m_\mu^2}{m_{B_s}^2}\right) |\tilde{S}|^2 + |\tilde{P}|^2}{|C_{10}^{\text{SM}}|^2} = 0.9426(1 \pm 0.2772), \quad (103)$$

⁴ These decays currently just have the experimental upper limits for branching ratios, which are indicated in Table V

with

$$\tilde{P} = C_{10} + \frac{m_{B_s}^2}{2m_\mu(m_b + m_s)}(C_P - C'_P), \quad \tilde{S} = \frac{m_{B_s}^2}{2m_\mu(m_b + m_s)}(C_S - C'_S), \quad (104)$$

$$\begin{aligned} \frac{\text{BR}(\bar{B} \rightarrow X_s \gamma)_{\text{exp}}}{\text{BR}(\bar{B} \rightarrow X_s \gamma)_{\text{SM}}} &= 1 + \frac{|C_7^{\text{NP}}|^2 + |C_7'^{\text{NP}}|^2 + 2C_7^{\text{SM}}\text{Re}[C_7^{\text{NP}}]}{|C_7^{\text{SM}}|^2 + N(E_\gamma)} \\ &= 1.0265(1 \pm 0.2217). \end{aligned} \quad (105)$$

For constraint of LFV ratios $R_{D^{(*)}}$, we also obtain

$$\frac{R_D^{\text{exp}}}{R_D^{\text{SM}}} = 1.106(1 \pm 0.109), \quad \frac{R_D^{*\text{exp}}}{R_D^{*\text{SM}}} = 1.48(1 \pm 0.203). \quad (106)$$

In addition, we obtain constraints for $B_{s,d}^0 - \bar{B}_{s,d}^0$ meson systems as

$$\frac{(\Delta m_{B_d})_{\text{SM}}}{(\Delta m_{B_d})_{\text{exp}}} = 1.0721(1 \pm 0.1605), \quad \frac{(\Delta m_{B_s})_{\text{SM}}}{(\Delta m_{B_s})_{\text{exp}}} = 1.0566(1 \pm 0.1374). \quad (107)$$

However, in $K^0 - \bar{K}^0$ meson system, the lattice QCD calculations for long-distance effect are not well-controlled. Therefore, we assume the present theory contributes about 30% to Δm_K , it reads

$$\frac{(\Delta m_K)_{\text{SM}}}{(\Delta m_K)_{\text{exp}}} = 1(1 \pm 0.3), \quad (108)$$

and then translates to the following constraint

$$\frac{(\Delta m_K)_{\text{NP}}}{(\Delta m_K)_{\text{exp}}} \in [-0.3, 0.3], \quad (109)$$

in agreement with [84].

For other observables such as branching ratios of FCNC top quark decays $t \rightarrow hu(c), t \rightarrow u(c)\gamma, B_s \rightarrow \tau^+\mu^-, B^+ \rightarrow K^+\tau^+\mu^-$ and $B^+ \rightarrow K^+\tau^+\tau^-$, we will compare their theory predictions with corresponding upper experimental limits.

Observables	SM predictions	Experimental constraints
Δm_K	$0.467 \times 10^{-2} \text{ ps}^{-1}$ [13]	$0.5293(9) \times 10^{-2} \text{ ps}^{-1}$ [13]
Δm_{B_s}	$18.77(86) \text{ ps}^{-1}$ [85]	$17.765(6) \text{ ps}^{-1}$ [74]
Δm_{B_d}	$0.543(29) \text{ ps}^{-1}$ [85]	$0.5065(19) \text{ ps}^{-1}$ [74]
$\text{BR}(B_s \rightarrow \mu^+\mu^-)$	$(3.66 \pm 0.14) \times 10^{-9}$ [65]	$(3.45 \pm 0.29) \times 10^{-9}$ [74]
$\text{BR}(\bar{B} \rightarrow X_s \gamma)$	$(3.40 \pm 0.17) \times 10^{-4}$ [64]	$(3.49 \pm 0.19) \times 10^{-4}$ [74]
R_D	0.298 ± 0.004 [86–88]	$0.441 \pm 0.060 \pm 0.066$ [22]
R_{D^*}	0.254 ± 0.005 [89, 90]	$0.281 \pm 0.018 \pm 0.024$ [22]
$\text{BR}(t \rightarrow hu)$	2×10^{-17} [91, 92]	$< 1.9 \times 10^{-4}$ [13]
$\text{BR}(t \rightarrow hc)$	3×10^{-15} [91, 92]	$< 7.3 \times 10^{-4}$ [13]
$\text{BR}(t \rightarrow u\gamma)$	4×10^{-16} [91, 92]	$< 0.85 \times 10^{-5}$ [93]
$\text{BR}(t \rightarrow c\gamma)$	5×10^{-14} [91, 92]	$< 4.2 \times 10^{-5}$ [93]
$\text{BR}(B_s \rightarrow \tau^+\mu^-)$	0 [13]	$< 4.2 \times 10^{-5}$ [94]
$\text{BR}(B^+ \rightarrow K^+\tau^+\mu^-)$	0 [13]	$< 3.3 \times 10^{-5}$ [95]
$\text{BR}(B^+ \rightarrow K^+\tau^+\tau^-)$	$(1.4 \pm 0.2) \times 10^{-7}$ [96]	$< 2.25 \times 10^{-3}$ [13]

Table V: The SM predictions and experimental values for flavor-changing observables related to quark sectors.

VI. NUMERICAL RESULTS

A. Set up input parameters

In this section, we perform a numerical analysis of all observables above mentioned in the lepton and quark sectors. We first provide some comments about the input parameters. In the quark sector, we use the benchmark points satisfying the observed quark spectrum, given in the Ref. [46] and then we obtain the numerical forms of the mixing matrices $V_{(u,d)_{L,R}}$ for the left- and right-handed SM up (type) quarks, respectively, as follows

$$\begin{aligned}
 V_{u_L} &\simeq \begin{pmatrix} -0.691643 & & -0.72224 & & -3.4606 \times 10^{-5} \\ -0.03477 - 0.7214i & & 0.03331 + 0.69084i & & 5.4627 \times 10^{-5} + 2.987 \times 10^{-5}i \\ 2.4033 \times 10^{-5} + 2.99143 \times 10^{-5}i & & -5.9984 \times 10^{-5} + 1.835 \times 10^{-5} & & 0.77155 - 0.63617i \end{pmatrix}, \\
 V_{d_L} &\simeq \begin{pmatrix} 0.59424 & & -0.80365 & & -0.03216 \\ 0.33464 + 0.73129i & & 0.24752 + 0.53964i & & -0.001978 + 0.02746i \\ -0.00852 - 0.006394i & & 0.01665 - 0.03739i & & -0.57436 + 0.817511i \end{pmatrix}, \tag{110}
 \end{aligned}$$

$$\begin{aligned}
 V_{u_R} &\simeq \begin{pmatrix} 0.062774 + 0.0789265i & -0.772558 + 0.217704i & 0.45357 - 0.373982i \\ -0.324679 - 0.404588i & 0.444546 - 0.124976i & 0.555116 - 0.45771i \\ -0.531888 - 0.661678i & -0.363214 + 0.102927i & -0.285327 + 0.235261i \end{pmatrix}, \\
 V_{d_R} &\simeq \begin{pmatrix} -0.615248 - 0.345117i & 0.152051 + 0.37215i & -0.33544 + 0.477733i \\ 0.0635554 - 0.064921i & -0.158241 - 0.795923i & -0.332068 + 0.47217i \\ -0.56473 - 0.418558i & -0.00509284 - 0.424059i & 0.328169 - 0.467272i \end{pmatrix}. \tag{111}
 \end{aligned}$$

We would like to note that the obtained quark mixing matrix is defined as follows

$$V_q = V_{u_L}^\dagger V_{d_L} = \begin{pmatrix} -0.950192 + 0.215979i & 0.157931 + 0.159795i & 0.00248254 - 0.00234475i \\ 0.0871643 - 0.206829i & 0.961472 - 0.153024i & 0.0421355 + 0.00223271i \\ -0.00248469 - 0.0103215i & 0.0366984 - 0.0182365i & -0.96322 + 0.26536i \end{pmatrix}, \tag{112}$$

is unitary and its magnitude $|V|$ is in agreement with the constraints of absolute values of the CKM matrix given in [13]. However, the entries themselves V_{ij} are different than the corresponding CKM ones.

Additionally, the exotic up (down) type quarks U, T (D_1, B) are nearly degenerate with masses at the TeV scale, i.e $m_U \simeq m_T \sim \mathcal{O}(1)$ TeV, $m_{D_1} \simeq m_B \sim \mathcal{O}(1)$ TeV. Moreover, they barely mix with ordinary quarks $u(d)$, as stated in [46]. Therefore, we ignore their mixing with the SM quarks and consider these new quarks as physical fields.

Similarly, in the lepton sector, we have found the numerical forms for the charged leptonic mixing matrices $V_{e_{L(R)}}$ obtained from the benchmark points in Eq. (7). These mixing matrices are given by

$$V_{e_L} \simeq \begin{pmatrix} 0.120049 & 0.0789769 & -0.989622 \\ -0.35756 & 0.933372 & 0.0311129 \\ -0.926142 & -0.350114 & -0.140289 \end{pmatrix}, \quad V_{e_R} \simeq \begin{pmatrix} -0.472389 & 0.871878 & -0.129139 \\ -0.88139 & -0.467177 & 0.0699824 \\ -0.000685472 & -0.14688 & -0.989154 \end{pmatrix}. \tag{113}$$

The mixing matrix of active neutrinos V_{ν_L} is given by:

$$V_{\nu_L} \simeq \begin{pmatrix} -0.331797 - 0.0666808i & 0.64392 - 0.0408052i & -0.684818 + 0.0137822i \\ -0.598615 + 0.0635722i & 0.420741 + 0.0389029i & 0.676312 - 0.0410494i \\ -0.722483 - 0.0331869i & -0.636202 - 0.0203087i & -0.24586 - 0.106325i \end{pmatrix}, \tag{114}$$

such the leptonic mixing matrix $V_l = V_{e_L}^\dagger V_{\nu_L}$ is unitary and agrees with the constraints imposed by the allowed ranges of the absolute values of the PMNS mixing matrix entries, given in [13, 97].

On the one hand, the masses and eigenstates of exotic charged leptons $E_{1,2}$ are supposed to be the same exotic quarks, i.e they do not mix with SM charged leptons and are nearly degenerate in mass ($m_{E_1} \sim m_{E_2} \sim \mathcal{O}(1)$ TeV). On the

other hand, the mixing matrices of right-handed neutrinos ν_R and neutral leptons N_R are assumed to be diagonal, i.e $V_{\nu_R} = I, V_{N_R} = I$, for simplicity. The active neutrino masses are chosen in the normal hierarchy as follows

$$m_{\nu_{1L}} = 0.5 \text{ eV}, \quad m_{\nu_{2L}}^2 = m_{\nu_{1L}}^2 + \Delta m_{21}^2, \quad m_{\nu_{3L}}^2 = m_{\nu_{1L}}^2 + \Delta m_{31}^2, \quad (115)$$

where $\Delta m_{21}^2, \Delta m_{31}^2$ are given in [97]. Besides, the masses of heavy neutral lepton N_R and right-handed neutrinos ν_R are obtained from the inverse seesaw mechanism as $m_{N_{aR}} \simeq m_{\nu_{aR}} = \frac{v_\sigma}{\sqrt{2}}$ [46]. With the remaining SM parameters used in our numerical study, we list them in Table VI.

Table VI: The numerical values of input parameters.

Input parameters	Values	Input parameters	Values
f_{B_s}	230.3(1.3) MeV [98]	m_{B_s}	5366.88(11) MeV [13]
m_u	1.24(22) MeV [47]	m_d	2.69(19) MeV [47]
m_c	0.63(2) GeV [47]	m_s	53.5(4.6) MeV [47]
m_t	172.9(4) GeV [47]	m_b	2.86(3) GeV [47]
$N(E_\gamma)$	3.3×10^{-3} [64]	$C_7^{\text{SM}}(\mu_b = 2.0 \text{ GeV})$	-0.3636[63, 64, 99]
$C_9^{\text{SM}}(\mu_b = 5.0 \text{ GeV})$	4.344 [100]	$C_{10}^{\text{SM}}(\mu_b = 5.0 \text{ GeV})$	-4.198 [100]
y_s	0.0645(3) [74]	κ_7	0.408 [70]
κ_7	0.408 [70]	κ_8	0.129
m_W	80.385 GeV [101]	m_Z	91.1876 GeV [101]
G_F	$1.166379 \times 10^{-5} \text{ GeV}^{-2}$ [13]	s_W^2	0.2312 [13]
λ	0.22519(83) [102]	A	0.828(11) [102]
$\bar{\rho}$	0.1609(95) [102]	$\bar{\eta}$	0.347(10) [102]

With all specified setup of input parameters, the free parameters used in the analysis of the observables are only the couplings f, B appearing in the scalar potential, the masses of charged exotic fermions m_{E_1}, m_{D_1}, m_U , the charged Higgs boson masses $m_{H^\pm}, m_{H_{1,2}^\pm}$, the mixing angle θ between $m_{H_{1,2}^\pm}$. For our numerical analysis, we will randomly vary these unknown parameters in the following ranges

$$-f \in [10^{-3}, 10^{-1}], \quad \theta \in [0, \pi/2], \quad B \in [10^{-3}, 10^{-2}] \text{ TeV}, \quad m_{E_1} \in [1, 4] \text{ TeV}, \quad m_{H^\pm, H_{1,2}^\pm} \in [0.5, 1.5] \text{ TeV}. \quad (116)$$

Below, we provide a justification for the choice of these ranges. The ranges of f and B are chosen based on the assumptions used in the diagonalization of the scalar mass matrices, whereas the mass ranges of exotic fermions and charged Higgs bosons are obtained from the experimental exclusion limits arising from collider searches [103, 104]. Additionally, the mass range of charged Higgs bosons also satisfies the experimental constraints resulting from the experimentally allowed ranges of the anomalous magnetic moments of the electron and muon $\Delta a_{e,\mu}$, as shown in [46].

B. SM-like Higgs boson decays $h \rightarrow \bar{f}f$ and $h \rightarrow \bar{f}f'$

Firstly, we are interesting in the deviations factors $a_{h\bar{f}f}$ from the couplings of SM like Higgs boson h with fermions f as follows

$$a_{h\tau\tau} = \frac{(g_{h\tau\tau})_{\text{theory}}}{(g_{h\tau\tau})_{\text{SM}}}, \quad a_{h\mu\mu} = \frac{(g_{h\mu\mu})_{\text{theory}}}{(g_{h\mu\mu})_{\text{SM}}}, \quad a_{h\bar{b}b} = \frac{(g_{h\bar{b}b})_{\text{theory}}}{(g_{h\bar{b}b})_{\text{SM}}}, \quad a_{h\bar{t}t} = \frac{(g_{h\bar{t}t})_{\text{theory}}}{(g_{h\bar{t}t})_{\text{SM}}}, \quad (117)$$

where $(g_{h\bar{f}f})_{\text{theory}}$ are the couplings predicted by the model and are obtained from the last lines of Eq. (A2) and Eq. (A3). The $(g_{h\bar{f}f})_{\text{SM}} = m_f/v$ are the SM predictions. With the help of input parameters given in Sec. (VIA), we find the predicted values of the model for these factors and are shown them in the Table (VII). We see that factors $a_{h\tau+\tau-}, a_{h\bar{b}b}$ and $a_{h\bar{t}t}$ are in agreement with the 1σ experimentally allowed range reported by ATLAS and CMS [93, 105], whereas the model estimates $a_{h\mu+\mu-}$ is in the 3σ experimentally allowed range of the ATLAS result. This can be understood because the second and first SM fermion families receive tree and one loop level masses from the inverse seesaw mechanism, whereas the masses for the third generation of SM fermions are generated at tree level by Yukawa interactions involving the Higgs doublets $\phi_{1,2}$ (ϕ_1 for the top and ϕ_2 for the bottom and tau lepton).

Therefore, the couplings of the SM-like Higgs boson h with the first and second SM fermion generations are smaller than the coupling of the 125 GeV SM-like Higgs boson h with the third family of the SM fermions.

Table VII: The comparison between predicted values and experimental limits of deviation factors. $a_{h\bar{f}f}$

Observables $a_{h\bar{f}f}$	$a_{h\mu\mu}$	$a_{h\tau\tau}$	a_{hbb}	a_{htt}
Predicted values	$\simeq 0.143$	$\simeq 0.86$	$\simeq 1.01$	$\simeq 0.997$

Besides, the model also predicts the LFV decays of SM like Higgs boson h , namely $\text{BR}(h \rightarrow \bar{l}_{b_1} l_{b_2})$, which are demonstrated in the below Table (VIII)

Table VIII: The comparison between predicted values and experimental limits of $\text{BR}(h \rightarrow \bar{l}_{b_1} l_{b_2})$.

Branching ratios	Predicted values	Experimental upper limits
$h \rightarrow e\mu$	$\simeq 2.7 \times 10^{-10}$	4.4×10^{-5} [106]
$h \rightarrow e\tau$	$\simeq 3.0 \times 10^{-8}$	2.0×10^{-3} [107]
$h \rightarrow \mu\tau$	$\simeq 1.2 \times 10^{-3}$	1.8×10^{-3} [107]

We see that all predicted branching ratios of LFV decays of SM like Higgs boson $h \rightarrow e\mu, e\tau, \mu\tau$ satisfy the current upper experimental bounds [106, 107]. Specifically, the decays $h \rightarrow e\mu, e\tau$ are significantly lower by several orders of magnitudes compared with corresponding experiment results, whereas $h \rightarrow \mu\tau$ channel is quite close to its measurement limit. This behavior of the branching ratio for the $h \rightarrow \mu\tau$ decay can be interpreted similarly as in Table VII, where the couplings of SM-like 125 GeV Higgs boson h with the third generation of SM charged fermions arise at tree-level, which are much larger than the couplings of h with the remaining SM fermions resulting from the inverse seesaw mechanisms at tree and one-loop levels. It is worth mentioning that the flavor changing leptonic Yukawa interactions in our model are dynamically generated at one loop level below the scale of spontaneous breaking of the $U(1)_X \times Z_4$ symmetry, after we integrate out the heavy neutral leptonic seesaw messengers and the charged scalars running in the internal lines of the loop. Such interactions give rise to flavor changing Higgs decays $h \rightarrow e\mu, h \rightarrow e\tau$ and $h \rightarrow \mu\tau$ whose corresponding rates do depend on the corresponding flavor changing Yukawa couplings. As a consequence of our particular benchmark in the charged lepton sector, we find rates for the $h \rightarrow e\mu$ and $h \rightarrow e\tau$ decays, very well below their current experimental limits, whereas for the $h \rightarrow \mu\tau$ decay, we find that its corresponding rate is below and very close to its upper experimental bound. This makes the $h \rightarrow \mu\tau$ decay one example of a smoking gun signature which can be used to assess the viability of our model.

On the other hand, it is important to note that the model contains a $Z - Z'$ mixing, which is controlled by the small mixing angle $\tan \theta_{ZZ'} \sim \mathcal{O}\left(\frac{v^2}{\Lambda_{new}^2}\right) \sim \mathcal{O}(10^{-4})$ (whose exact expression is given in Appendix D), then implying the existence of additional contributions to Z boson decays including both flavor-conserving $Z \rightarrow \bar{f}f$ and flavor-violating ones $Z \rightarrow \bar{f}_a f_b$ ($a \neq b$). The flavor-violating Z decays are originated by the non-universal $U(1)_X$ gauge symmetry assignments of the SM left handed quark fields, as well as to the $Z - Z'$ mixing. The branching ratios for the flavor-violating $Z \rightarrow \bar{f}_a f_b$ decays read

$$\text{BR}(Z \rightarrow \bar{f}_a f_b) = \frac{M_Z}{12\pi\Gamma_Z} \left(|(g_L^Z)_{ab}|^2 + |(g_R^Z)_{ab}|^2 \right) = \frac{M_Z}{6\pi\Gamma_Z} \left(|(g_V^Z)_{ab}|^2 + |(g_A^Z)_{ab}|^2 \right), \quad (118)$$

where the vector (axial) couplings of Z gauge boson are provided in Appendix D. As follows from the expression given above as well as from the expressions of the Z couplings given in Appendix D, the non-SM contributions to the Z flavor-conserving couplings with SM fermions will be of the order of $\sim s_{\theta_{ZZ'}} \sim \mathcal{O}(10^{-4})$, which implies that the branching ratios of Z decays into SM fermions will be very close to the SM predictions and thus consistent with the current experimental constraints [13]. For quark flavor-violating decays $Z \rightarrow bs, bd, cu$, the model predicts these processes can happen at the tree-level due to non-universal assignments of the quark fields under $U(1)_X$ gauge group and the $Z - Z'$ mixing. As seen from Appendix D, we can estimate New Physics (NP) contributions to $\text{BR}(Z \rightarrow \bar{s}b) \sim s_{\theta_{ZZ'}}^2 |(V_{dL}^*)_{32}(V_{dL})_{33}|^2 \sim (10^{-4})^2 \times 10^{-3} \sim 10^{-11}$, $\text{BR}(Z \rightarrow \bar{d}b) \sim s_{\theta_{ZZ'}}^2 |(V_{dL}^*)_{31}(V_{dL})_{33}|^2 \sim (10^{-4})^2 \times 10^{-4} \sim 10^{-12}$, $\text{BR}(Z \rightarrow \bar{u}c) \sim s_{\theta_{ZZ'}}^2 |(V_{uL}^*)_{31}(V_{uL})_{32}|^2 \sim (10^{-4})^2 \times 10^{-18} \sim 10^{-26}$. These ones are much smaller than the upper experimental limits $\text{BR}(Z \rightarrow \{bs, bd, cu\})_{\text{exp}} < 2.9 \times 10^{-3}$ as well as SM prediction $\text{BR}(Z \rightarrow \{bs, bd, cu\})_{\text{SM}} = \{4.2(7) \times 10^{-8}, 1.8(3) \times 10^{-9}, 1.4(2) \times 10^{-18}\}$ [108], therefore the NP impact to quark flavor-violating decays of Z boson are very weak and thus can be ignored.

On the other hand, we would also like to note that there are lepton flavor-violating Z decays induced at one-loop level including the virtual exchange of charged Higgses $H^\pm, H_{1,2}^\pm$, neutral CP even (odd) Higgses $H(\mathcal{A})$ running in the internal lines of the loop. For instance, the branching ratio for the $Z \rightarrow e\mu$ decay is approximately estimated as follows

$$\text{BR}(Z \rightarrow e\mu) \sim \frac{1}{16\pi^2} \left\{ \left| \sum_{F,\phi} (g_R^{\phi^+ F l_1})^* g_R^{H^+ F l_2} + \sum_{p=1}^8 [(g_L^{H_p \bar{E}_1 l_1} + g_R^{H_p \bar{E}_1 l_1})^* (g_L^{H_p \bar{E}_1 l_2} + g_R^{H_p \bar{E}_1 l_2}) + (g_R^{H_p \bar{A} l_1})^* g_R^{H_p \bar{A} l_2}] \right. \right. \\ \left. \left. + \sum_{p=3}^8 [(g_L^{A_p \bar{E}_1 l_1} + g_R^{A_p \bar{E}_1 l_1})^* (g_L^{A_p \bar{E}_1 l_2} + g_R^{A_p \bar{E}_1 l_2}) + (g_R^{A_p \bar{A} l_1})^* g_R^{A_p \bar{A} l_2}] \right|^2 \right\} \sim \mathcal{O}(10^{-14}), \quad (119)$$

where $1/(16\pi^2)$ is a loop factor, and $\phi = H^+, H_{1,2}^+, F = \nu_{aL}, \nu_{aR}, N_a$. Similarly, we find $\text{BR}(Z \rightarrow \mu\tau) \sim \mathcal{O}(10^{-8})$ and $\text{BR}(Z \rightarrow e\tau) \sim \mathcal{O}(10^{-13})$. These predicted values are very suppressed in comparison with the order of magnitude of the upper experimental limits $\mathcal{O}(10^{-6} - 10^{-7})$ [13]. This shows the NP constraints for the lepton-flavor violating Z decays are very weak and thus can also be skipped.

C. Leptonic flavor observables

In what follows we perform a numerical study of the constraints imposed by the upper limits of the branching ratios of cLFV decays $\text{BR}(l_{b_1} \rightarrow l_{b_2} \gamma)$ as well as by the allowed experimental ranges of the anomalous magnetic moments $\Delta a_{e(\mu)}$ via the Figs (3, 4).

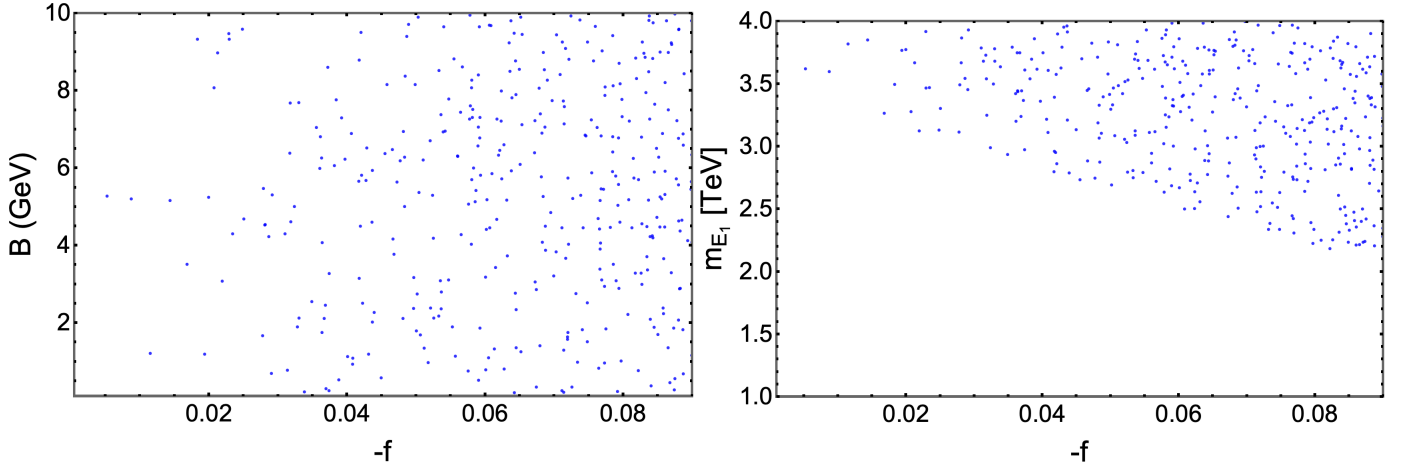


Figure 3: The left and right panels respectively show the correlations of couplings $B - f$ and $m_{E_1} - f$ satisfying the experimental limits of cLFV and anomalous magnetic moments $\Delta a_{e(\mu)}$.

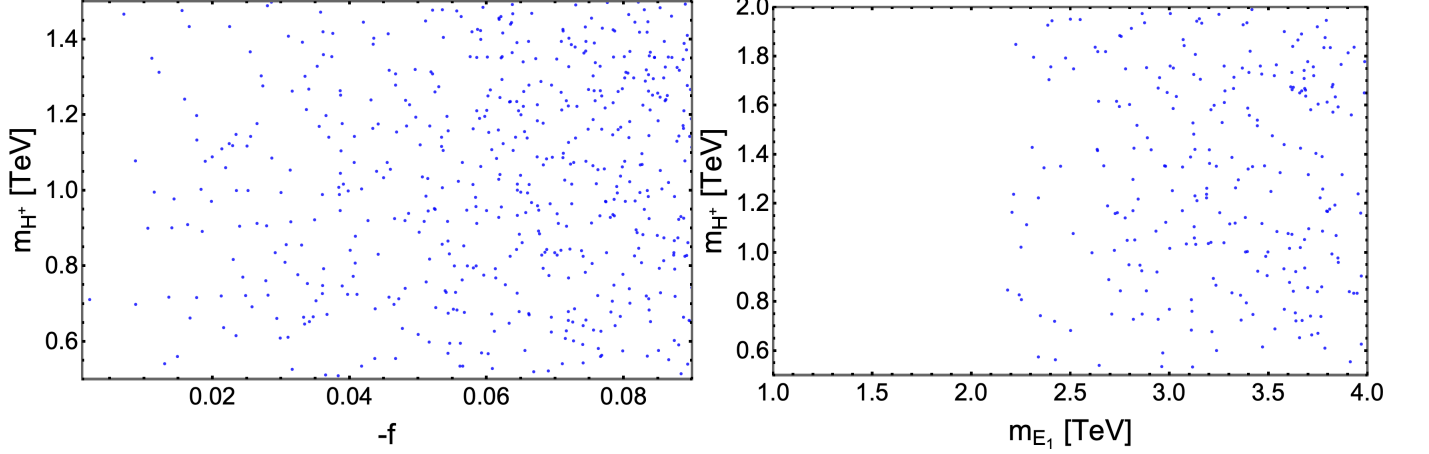


Figure 4: The left and right panels respectively show the correlations of couplings $-f$ vs $m_{H_1^\pm}$ and m_{E_1} vs $m_{H_1^\pm}$ satisfying the experimental limits of cLFV and anomalous magnetic moments $\Delta a_{e(\mu)}$.

The left panel in Fig. (3) illustrates the correlation between couplings of the scalar potential, denoted as $-f$ and B . There is almost no dependence between these parameters; in other words, the change of B does not affect f , especially for $-f \geq 0.04$. This indicates that the values of the B coupling are insignificant to the leptonic observables. From the left panel, the values of $-f$ mainly range from $-f \geq 0.04$. On the other hand, the right panel demonstrates stronger correlations between the $-f$ parameter and the mass of exotic charged lepton E_1 . We notice that the behavior of m_{E_1} and $-f$ is reversed; in other words, an increase of the charged exotic lepton mass m_{E_1} leads to a decrease of the $-f$ parameter and vice versa. From the right panel, we find the limit $m_{E_1} \geq 2.2$ TeV.

Turning to Fig. (4), we illustrate the correlations between $-f$ or m_{E_1} and mass of charged Higgs $m_{H_1^\pm}$ in the left and right panel, respectively. We observe that both panels indicate the irrelevance of $m_{H_1^\pm}$ to leptonic observables. Moreover, this behavior is similar if we consider other charged Higgs bosons $H_{1,2}^\pm$. Additionally, the Figs. (3,4) demonstrate the remarkable impacts of the loop diagrams involving the exotic charged lepton E_1 and neutral Higgs bosons $H(A)$ on cLFV and anomalous magnetic moments $\Delta a_{e(\mu)}$.

Moreover, we consider the branching ratios of three body leptonic decays $\text{BR}(l \rightarrow 3l')$, $\text{Mu}-\overline{\text{Mu}}$ transition, and coherent conversion $\mu \rightarrow e$ in a muonic atom, which only depends on the coupling f , as shown in Fig. (5) and Fig (6). We observe that the model predicts these observables to be much lower by several orders of magnitude than their corresponding upper experimental bounds, as given in Table (IV). Therefore, the new physics contributions in the considering model for these observables are negligible and can be ignored.

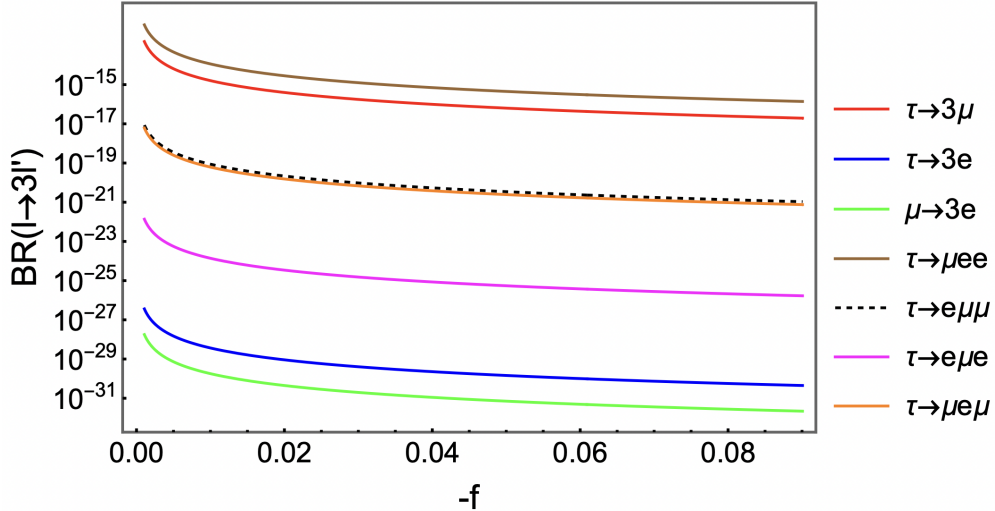


Figure 5: The figure shows the dependence of branching ratios of three body leptonic decays as the function of coupling $-f$.

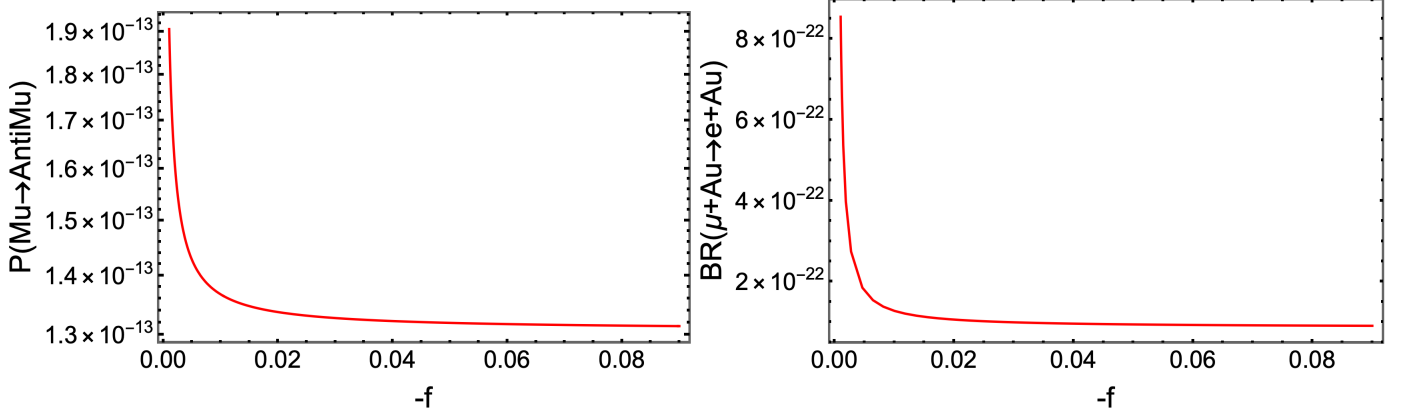


Figure 6: The left and right panels respectively show the dependence of $\text{Mu}-\overline{\text{Mu}}$ transition in Eq. (59) and branching ratio $\text{BR}(\mu^+ \text{Au} \rightarrow e^+ \text{Au})$ in Eq. (64) as the function of coupling $-f$.

D. Quark flavor observables

Let's now focus on the phenomenology of flavor quark observables. First, we will consider the FCNC observables in down type quark transitions $d_a \rightarrow d_b$. It is important to note that only meson mass splittings, such as $\Delta m_{K, B_s, B_d}$, $\text{BR}(B_s \rightarrow \mu^+ \mu^-)$ and $\text{BR}(B^+ \rightarrow K^+ \tau^+ \tau^-)$ do depend on the new neutral gauge boson mass $m_{Z'}$ and the coupling g_X of $U(1)_X$ symmetry. Other quark flavor observables, however, are independent of these parameters. Thus, our initial focus is to analyze the constraints on $m_{Z'}$ and g_X that satisfy the experimental limits of $\Delta m_{K, B_s, B_d}$, $\text{BR}(B_s \rightarrow \mu^+ \mu^-)$ and $\text{BR}(B^+ \rightarrow K^+ \tau^+ \tau^-)$ by the Fig. 7

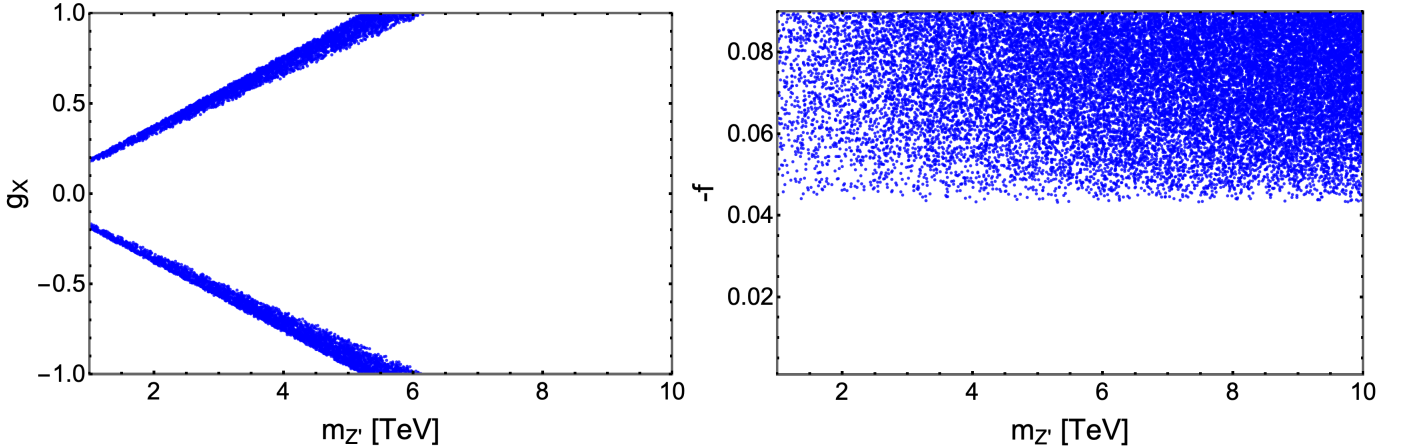


Figure 7: The left and right panels respectively show the correlations of $m_{Z'} - g_X$ and $m_{Z'} - f$ satisfying the constraints given in Eq. (103) for $\text{BR}(B_s \rightarrow \mu^+ \mu^-)$, Eqs. (107, 109) for $\Delta m_{K, B_s, B_d}$, and [13] for $\text{BR}(B^+ \rightarrow K^+ \tau^+ \tau^-)$

In the left panel, we observe that the range of $m_{Z'}$ varies with the values of g_X . For instance, with $|g_X| \simeq 0.2$, the mass of Z' boson is about $\simeq [1, 1.4]$ TeV. However, if $|g_X| > 0.2$, $m_{Z'}$ increases and can reach up to 6.5 TeV for $|g_X| \simeq 1$. However, it should be noted that the LHC searches of the Z' gauge boson set a lower mass limit of $m_{Z'} \geq 4$ TeV [13], implying the coupling g_X should satisfy $|g_X| \geq 0.65$. These constraints for g_X and $m_{Z'}$ are stronger than those ones obtained from studying meson oscillations in [46].

On the one hand, both observables are also affected by the f coupling and we depict the right panel to demonstrate the correlations between f and $m_{Z'}$. We observe that the correlation here is weaker compared to the left panel. This suggests that the (pseudo)scalar WCs $C_{S(P)}^{(\prime)\mu\mu}$, which involve CP-even or CP-odd Higgs bosons provide very small and subleading contributions to these observables. This can be understood because when we impose the limit, $-f \geq 0.04$ obtained from the analysis of leptonic flavor observables, such WCs become $C_{S(P)}^{(\prime)\mu\mu} \sim \mathcal{O}(10^{-2} - 10^{-4})$, which are

extremely small compared to WCs $C_{9,10} \sim \mathcal{O}(1)$. It is worth noting that the lower bound $-f \geq 0.045$ obtained in the right panel is relatively higher than that obtained in Fig. (3).

On the other hand, for the branching ratios of (semi)leptonic decays $\text{BR}(B^+ \rightarrow K^+ \tau^+ \mu^-)$, $\text{BR}(B_s \rightarrow \tau^+ \mu^-)$ influenced by (pseudo)scalar WCs $C_{S(P)}^{(\prime)\tau\mu}$ depending on the parameter f , we plot the Fig. 8 and realize that the model evaluates $\text{BR}(B^+ \rightarrow K^+ \tau^+ \mu^-)_{\text{theory}} \sim 10^{-10}$, $\text{BR}(B_s \rightarrow \tau^+ \mu^-)_{\text{theory}} \sim 10^{-9} - 10^{-8}$. Compared with relative experimental bounds given in Table V, the predicted values are much lower by several orders of magnitude.

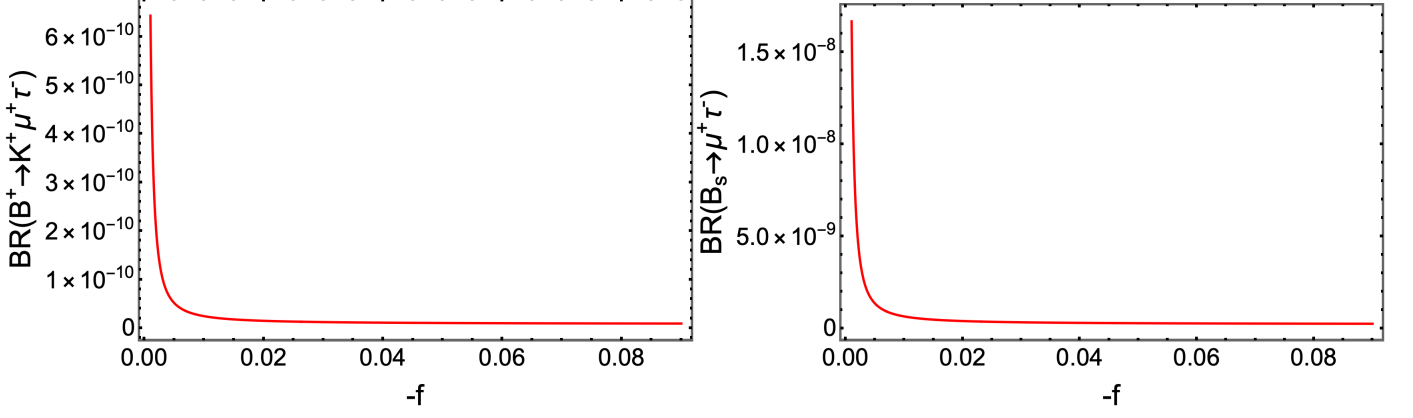


Figure 8: The left and right panels respectively show the dependence of $\text{BR}(B^+ \rightarrow K^+ \tau^+ \mu^-)$ and $\text{BR}(B_s \rightarrow \tau^+ \mu^-)$ as the function of coupling $-f$.

For remaining observables related to the FCNC $d_a \rightarrow d_b$ transitions, namely $\text{BR}(\bar{B} \rightarrow X_s)\gamma$, which are contributed by WCs induced by charged Higgs $H^\pm, H_{1,2}^\pm$, and neutral Higgs bosons $H(\mathcal{A})$, we plot the Fig. 9 to demonstrate the relationship between parameters fulfilling the constraints given in Eq. (105).

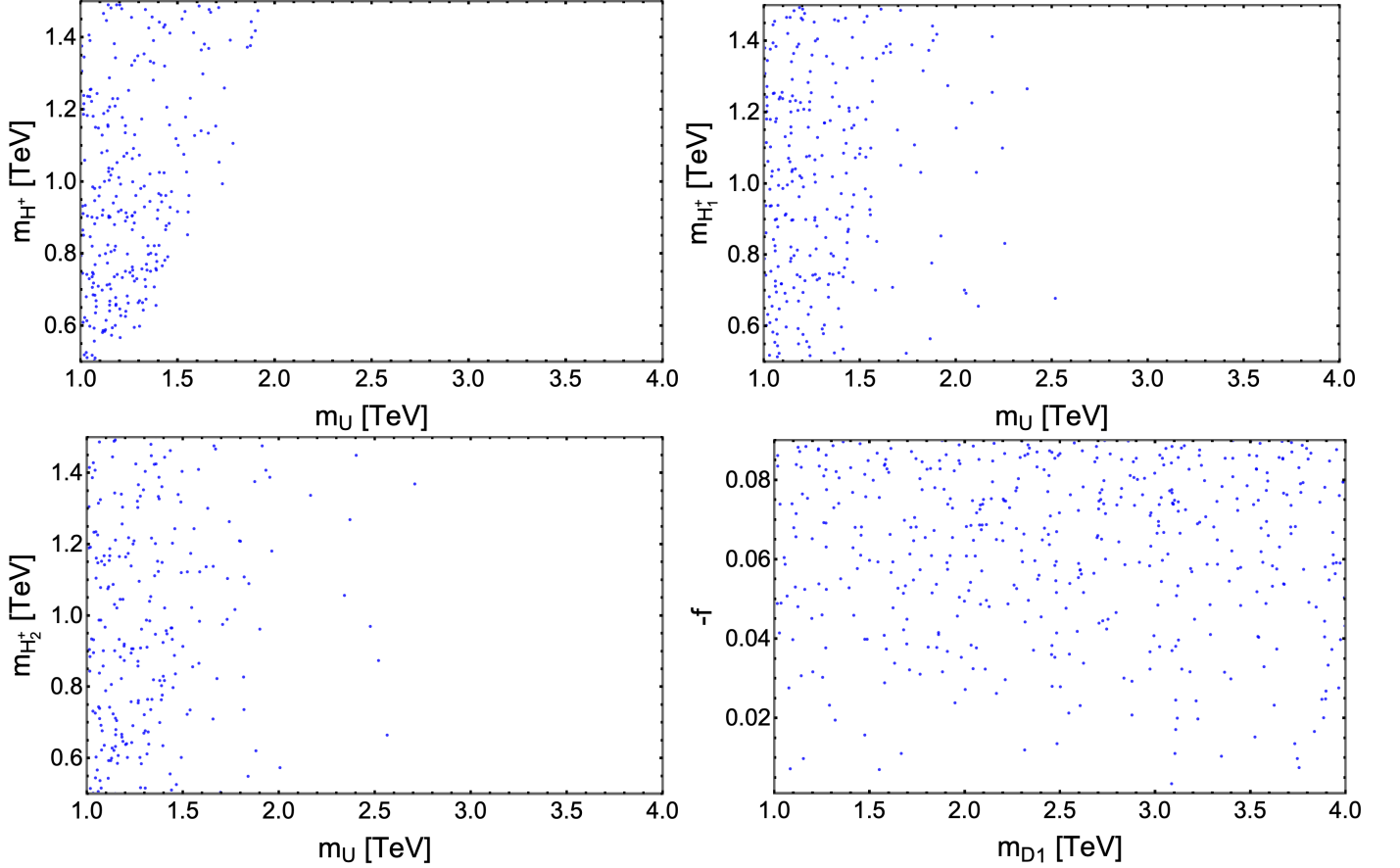


Figure 9: The first three panels (from left to right) and last panel respectively show the correlations between mass of exotic up type quark m_U with masses of charged Higgs bosons H^\pm , $H_{1,2}^\pm$ and coupling $-f$ satisfying the constraints of $\text{BR}(\bar{B} \rightarrow X_s \gamma)$ in Eq. (105).

In the first three panels (from left to right) of Fig. 9, we illustrate the correlation between the mass of new up quark m_U and the masses of three charged Higgs bosons m_{H^\pm} , $m_{H_{1,2}^\pm}$ satisfying the constraint of $\text{BR}(\bar{B} \rightarrow X_s \gamma)$ in Eq. (103). We observe that the entire ranges of m_{H^\pm} , $m_{H_{1,2}^\pm}$ in all panels meet the constraint, whereas the range of m_U is more stringent, ranging up to approximately $\simeq 2.5$ TeV but dominantly distribute with the ranges $m_U \in [1, 2]$ TeV. It is worth noting that this observable also depends on f through the WCs induced by the neutral CP even (odd) Higgs bosons such as $C_7^{(')H(A)\bar{D}_1 d}$. We plot the correlation between $-f$ and mass of down type quark m_{D_1} in the fourth panel of Fig. (9). We observe that this correlation is not as strong compared to the others. This can be understood because with $-f \geq 0.04$ and $m_{D_1} \sim \mathcal{O}(1)$ TeV, we numerically estimate the magnitude of WCs as $|C_{7,8}^{H(A)\bar{D}_1 d}| \sim \mathcal{O}(10^{-6} - 10^{-4}) \ll 1$, which is much lower by 3 to 5 orders of magnitude than the corresponding SM predictions $|C_7^{\text{SM}}| \sim \mathcal{O}(10^{-1})$. Consequently, this implies that WCs induced by new quark U and charged Higgs bosons H^\pm , $H_{1,2}^\pm$ dominantly contribute compared to those containing D_1 and H_p , and therefore we can ignore these latter contributions in such observables.

Turning to up quark transition observables $t \rightarrow u(c)$, we first study branching ratios of tree-level top quark decays $\text{BR}(t \rightarrow u(c)h)$, as the couplings of these observables are fixed and do not depend on free parameters. The comparison between the predictions of the model and the upper experimental bounds for such decays is shown in Table IX

Table IX: The comparison between predicted values and experimental limits of $\text{BR}(t \rightarrow u(c)h)$.

Branching ratios	Predicted values	Experimental limits [109]
$t \rightarrow uh$	$\simeq 3.97 \times 10^{-10}$	$< 3.8 \times 10^{-4}$
$t \rightarrow ch$	$\simeq 9.71 \times 10^{-10}$	$< 4.3 \times 10^{-4}$

We observe that the obtained branching ratios $\text{BR}(t \rightarrow u(c)h)$ in the model are on the order of $10^{-9} - 10^{-10}$, significantly larger by several orders of magnitude than the corresponding SM values. Besides that, these results for the decays satisfy the upper experimental bounds, notably as they are lower than 5 to 6 orders of magnitude than the measurement ones. Thus, the NP contributions of NP in these decays are small and safe under the experimental constraints.

On the one hand, with branching ratios of radiative decays $\text{BR}(t \rightarrow u(c)\gamma)$ are induced by loop diagrams containing charged Higgs bosons $H^\pm, H_{1,2}^\pm$ and exotic down-type quark D_1 , as well as by neutral CP even(odd) Higgs bosons $H(A)$ with up-type quark U or SM quarks u, c, t . The Figs. (10) are plotted using parameters obtained from $b \rightarrow s$ studies, enhancing the understanding of these transitions.

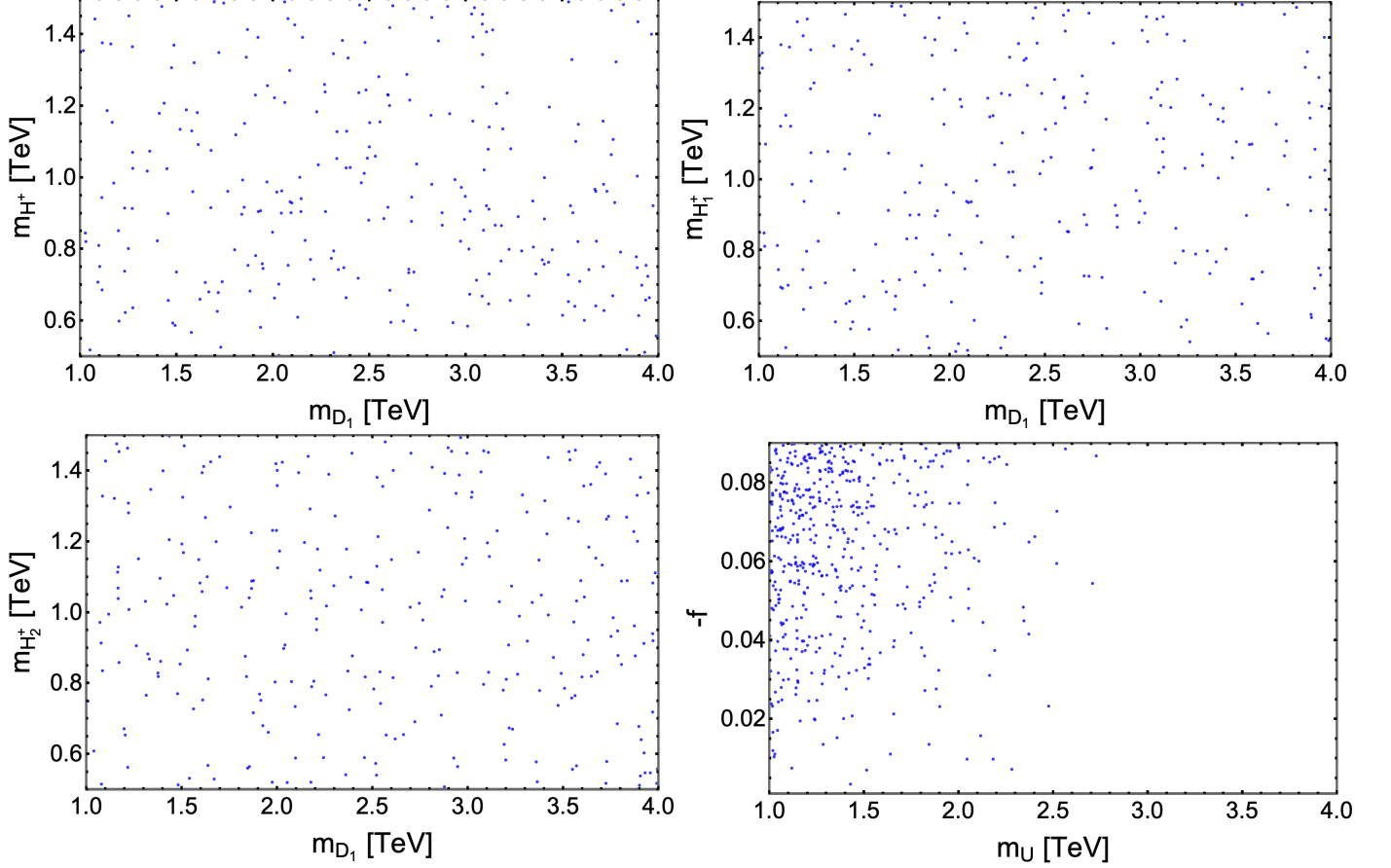


Figure 10: The first three panels (from left to right) and last panel respectively show the correlations between mass of exotic down type quark m_{D_1} with masses of charged Higgs bosons $H^\pm, H_{1,2}^\pm$ and coupling $-f$ satisfying the constraints of $\text{BR}(t \rightarrow u(c)\gamma)$ [93].

Comparing the two panels, we observe that almost the entire range of the first three panels satisfies the constraint, whereas the last panel demonstrates a tighter correlation. This indicates that, for this kind of observable, the contribution of WCs associated with charged Higgs bosons is not as strong as those associated with neutral CP even (odd) Higgs bosons. This behavior is opposite to the governing $\text{BR}(\bar{B} \rightarrow X_s \gamma)$.

Finally, we examine the LFUV ratios $R_{D^{(*)}}$, which are generated at the tree level via the exchange of the SM charged gauge boson W_μ^\pm and the charged Higgs bosons $H^\pm, H_{1,2}^\pm$. In Fig. (11), we plot the correlation between the mass of the charged Higgs bosons that satisfy the constraint of $R_{D^{(*)}}$ in Eq. (106) with input parameters enhanced by the above studies. The figure shows that satisfied points are dominantly linearly distributed which can be interpreted for the following reasons. Firstly, the ratios are depend on WCs $\tilde{C}_S^{(\prime)}$ induced by charged Higgs $H_{1,2}^\pm$ which are proportional $g_{L,R}^{H_{1,2}^+ \bar{u}_2 d_3}$. In addition, these couplings respectively relate to elements of mixing charged scalar matrix $(U_c^\dagger)_{13(14)}$ and $(U_c^\dagger)_{23(24)} \sim \frac{1}{\epsilon_{1(2)}} \sim \frac{1}{m_{H_{1,2}^\pm}^2 - m_{H^\pm}^2}$ given in Eq. (23). Therefore, the WCs induced by $H_{1,2}^\pm$ will be

enhanced significantly if there is slight degeneration in charged Higgs masses $m_{H_{1,2}^\pm} \sim m_{H^\pm}$. This results in almost all points being distributed linearly in Fig. (11). For $m_{H_{1,2}^\pm} \simeq m_{H^\pm} + \mathcal{O}(10^1)$ GeV, and with obtained parameter in above studies, we can estimate the magnitude of these scalar WCs which can attain the maximum value $|\tilde{C}_S^{(\prime)}| \sim \mathcal{O}(10^{-4})$, which is much smaller than WC of SM \tilde{C}_V . This suggests that the charged Higgs boson contributes insignificantly compared to the SM contributions. It is worth mentioning that this scenario of nearly degenerate charged scalar masses is favored by the constraints arising from electroweak precision observables, which is a generic feature of multi-Higgs doublet models [110], like the one analyzed in this work.

To close this section, we want to remark that our obtained constraint of charged Higgs masses satisfying $R_{D^{(*)}}$ is different than Refs. [80, 82, 111] for the following reasons. In these works, the charged Higgs interpretation for $R_{D^{(*)}}$ anomalies is indirectly constrained by $\tau\nu$ resonance search at LHC via fast collider simulation $pp \rightarrow bc \rightarrow \tau\nu$. For instance, the obtained bound of charged Higgs mass is $m_{H^\pm} \leq 400$ GeV when the charged resonance H^+ decays only to final states $bc/\tau\nu$. However, the considering model provides not only $bc/\tau\nu$ decays by H^+ but also more channels due to the existence of couplings of charged Higgs with both SM and exotic fermions, as can be seen in Eqs. (65,66). Particularly, we estimate $\Gamma(H^+ \rightarrow \bar{b}c) \sim |g_L^{H^+\bar{u}_2d_3}|^2 + |g_R^{H^+\bar{u}_2d_3}|^2 \sim 6.3 \times 10^{-11} \ll \Gamma(H^+ \rightarrow \bar{b}t) \sim 3.23 \times 10^{-2}$, showing that bc mode is not the dominant one. Moreover, as mentioned above, the ratios $R_{D^{(*)}}$ in our model contain explicitly the dependence on τ and μ flavor, as well as there are multi-charged Higgs contributions to $R_{D^{(*)}}$, which are not like [80, 82, 111]. To conclude, the $R_{D^{(*)}}$ in this model is different than previous references, thus the bound for charged Higgs mass in these work is not applied in our case. We also would like to note that since the charged Higgs contributions in our model are shown to be insignificant, the predicted branching ratio $\text{BR}(B_c \rightarrow \tau\bar{\nu})_{\text{model}} \simeq \text{BR}(B_c \rightarrow \tau\bar{\nu})_{\text{SM}} \simeq 2.2\%$, thus the constraint by $\text{BR}(B_c \rightarrow \tau\bar{\nu}) \leq 63\%$ [112] in this model is also relaxed.

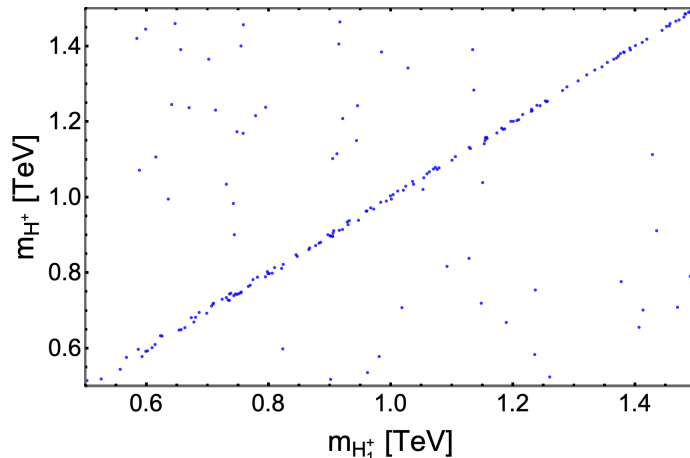


Figure 11: The figure shows the correlations between mass of charged Higgs bosons H^\pm , H_1^\pm satisfying the constraints of $R_{D^{(*)}}$ in Eq. (106).

VII. CONCLUSIONS

In this paper, we have investigated in great detail several flavor observables in both the lepton and quark sectors within the context of an extended 2HDM with the inverse seesaw mechanism. We have performed a detailed analysis of the scalar mass spectrum using the perturbation method, based on certain assumptions for the Higgs potential couplings. Additionally, we have obtained the benchmark points fulfilling the SM lepton masses and mixing parameters. Due to the couplings of both Higgs (charged, CP-even and CP-odd) and Z' gauge boson with SM and new fermions at tree-level, the model contains a rich flavor phenomenology in lepton and quark sectors. This model has been demonstrated that it may theoretically account for discrepancies between SM and experiment in flavor observables. In particular, we found that the contributions to cLFV decays and anomalous magnetic moments observables, resulting from loop diagrams involving the virtual exchange of CP even (odd) Higgs bosons $H(\mathcal{A})$ and charged exotic leptons, are significantly larger than those arising from the exchange of charged Higgs boson. In addition, the constraints for coupling f and m_{E_1} are derived as $-f \geq 0.04$ and $m_{E_1} \geq 2.2$ TeV. With the obtained bound on f , the new physics contributions to the branching ratios of three-body leptonic decays $\text{BR}(l \rightarrow 3l')$, $\text{Mu}-\overline{\text{Mu}}$ transition, as well as $\text{BR}(\mu\text{Au} \rightarrow e\text{Au})$ conversion, are shown to be remarkably smaller than upper experimental limits. On the other

hand, the study of quark flavor observables is more complicated. Specifically, for the FCNC $d_a \rightarrow d_b$ observables, the WCs induced by charged Higgs bosons $H^\pm, H_{1,2}^\pm$ and exotic quark U exchange contribute the most to $\text{BR}(\bar{B}_s \rightarrow X_s \gamma)$, whereas the remaining WCs of $H(\mathcal{A})$ are insignificant. The range of $m_U \geq [1, 2]$ TeV is obtained. Furthermore, the meson oscillations are revisited with all contributions and comprehensive quark couplings, combining with studies for $\text{BR}(B_s \rightarrow \mu^+ \mu^-)$ and $\text{BR}(B^+ \rightarrow K^+ \tau^+ \mu^-)$, we obtain tighter constraints on the $U(1)_X$ coupling g_X and on the Z' gauge boson which read $|g_X| \geq 0.65$ and $m_{Z'} \geq 4$ TeV, respectively. The obtained lower bound of $m_{Z'}$ is consistent with LHC searches of the Z' gauge boson [13].

The numerical values for the up-type quark flavor observables corresponding to FCNC decays $t \rightarrow u(c)h$ are found to be much lower than their corresponding upper experimental limits [109], but several orders of magnitude larger than SM predictions [91, 92]. Concerning radiative decays $t \rightarrow u(c)\gamma$, their obtained branching ratios are primarily influenced by WCs induced by CP even (odd) Higgs bosons interacting with exotic up-type quark U compared to WCs containing charged Higgs bosons. This behavior is opposite to that governing $\text{BR}(\bar{B} \rightarrow X_s \gamma)$. The FCCC $b \rightarrow s$ LFUV ratios $R_{D^{(*)}}$ are calculated to agree with their experimental constraints, with the new physics contributions arising from charged Higgs bosons at the tree-level shown to be negligible.

The properties of the SM-like Higgs boson h are also discussed. Particularly, the model predicts the deviation factors $a_{h\tau\bar{\tau}}, a_{hb\bar{b}}$ and $a_{ht\bar{t}}$ of the SM Higgs couplings to $\tau\bar{\tau}, b\bar{b}$ and $t\bar{t}$ pairs, which are found to agree with their 1σ experimentally allowed ranges [105, 113]. Furthermore, the factor $a_{h\mu\bar{\mu}}$ of the SM Higgs coupling to $\mu\bar{\mu}$ pair is estimated to agree with its corresponding 3σ bound. This is because the first and second fermion generations acquire masses via the tree and one-loop inverse seesaw mechanisms, respectively. Additionally, the obtained values for the branching ratios for the LFV decays of h such as $h \rightarrow e\mu, h \rightarrow e\tau, h \rightarrow \mu\tau$, are shown to be consistent with their corresponding experimental upper limits [13, 107].

The model accommodates dark matter due to the presence of the unbroken Z_2 symmetry. Assuming that dark matter is represented by a scalar field, which has to be the lightest among the particles having a non trivial charge under the preserved Z_2 symmetry, which can be denoted as φ_2 , that scalar dark matter candidate mainly annihilates into $WW, ZZ, t\bar{t}, b\bar{b}$ and SS , via a Higgs portal scalar interaction $\lambda_S SS(\varphi_2^\dagger \varphi_2)$, where S stands for any of scalars of the model, including the 125 GeV SM like Higgs boson. Consequently, the constraints arising from the DM relic density and DM direct detection experiments lead to restrictions on the DM mass as well as on its coupling between φ_2 and the Higgs scalars, including the Standard Model-like Higgs bosons as well as non SM scalars, similarly as, for instance in [46, 114, 115]. Thus, the scenario of scalar DM candidate has a good amount of parametric freedom that allows to successfully accommodate the Dark matter relic density while being compatible with the constraints arising from DM direct limits. Based on specific assumptions regarding these scalar coupling bosons, which closely resembles the parameter space used in this study as well as in [114, 115], we found that aligning with current DM data requires the scalar DM mass to be in the range of a few TeV, as illustrated in Refs. [46, 114, 115]. On the other hand, in the scenario of fermionic dark matter (DM) candidate, the DM candidate will corresponds to the lightest among the Z_2 odd neutral leptons Ψ_{1R} and Ψ_{2R} . Assuming that in that scenario, the DM candidate is Ψ_{1R} , it can annihilate into active and heavy neutrinos via the t channel exchange of Z_2 odd scalar singlets φ_1 and φ_2 . Besides that, the fermionic DM candidate can also annihilate into pairs of SM fermions and heavy fermions via the s channel exchange of the heavy Z' gauge boson. Consequently we expect that in the scenario of fermionic DM candidate, the DM constraints will impose limits on the masses of the new gauge boson and the DM itself, similarly as in [46, 114]. A detailed analysis of the Dark matter phenomenology goes beyond the scope of this work.

Acknowledgement

This research was funded by the Vietnam Academy of Science and Technology, Grant No.CBCLCA.03/25-27. N.T. Duy was funded by the Postdoctoral Scholarship Programme of Vingroup Innovation Foundation (VINIF), code VINIF.2023.STS.65; AECH was funded by Chilean grants ANID-Chile FONDECYT 1210378, FONDECYT 1241855, ANID PIA/APOYO AFB230003, ANID Programa Milenio code ICN2019-044. The authors thank Duong Van Loi for helpful discussions.

Appendix A: Coefficients in Lagrangian for lepton and quark flavor violating processes

The coefficients mentioned in Eq. (47) are given as follows

$$\begin{aligned}
g_R^{H^+ \bar{\nu}_a L b} &= (U_c^\dagger)_{22} \sum_{i=1}^3 y_i^{(l)} (V_{\nu_L}^*)_{ia} (V_{e_R})_{3b}, & g_R^{H_{1,2}^+ \bar{\nu}_a L b} &= (U_c^\dagger)_{23(24)} \sum_{i=1}^3 y_i^{(l)} (V_{\nu_L}^*)_{ia} (V_{e_R})_{3b}, \\
g_R^{H^+ \bar{N}_a l b} &= (U_c^\dagger)_{42} \sum_{i=1}^3 \sum_{n=1}^2 z_{in}^{(l)} (V_{N_R}^*)_{ia} (V_{e_R})_{nb}, & g_R^{H_{1,2}^+ \bar{N}_a l b} &= (U_c^\dagger)_{43(44)} \sum_{i=1}^3 \sum_{n=1}^2 z_{in}^{(l)} (V_{N_R}^*)_{ia} (V_{e_R})_{nb}, \\
g_L^{H^+ \bar{\nu}_a R l b} &= (U_c^\dagger)_{22} \sum_{i=1}^3 \sum_{j=1}^3 y_{ij}^{*(\nu)} (V_{\nu_R}^*)_{ja} (V_{e_L})_{ib}, & g_L^{H_{1,2}^+ \bar{\nu}_a R l b} &= (U_c^\dagger)_{23(24)} \sum_{i=1}^3 \sum_{j=1}^3 y_{ij}^{*(\nu)} (V_{\nu_R}^*)_{ja} (V_{e_L})_{ib}, \\
g_L^{H_p \bar{E}_1 l b} &= \frac{1}{\sqrt{2}} \sum_{i=1}^3 y_i^{*(E)} (V_{e_L})_{ib} (U_S^\dagger)_{2p}, & g_R^{H_p \bar{E}_1 l b} &= \frac{1}{\sqrt{2}} \sum_{n=1}^2 x_n^{(E)} (V_{e_R})_{nb} (U_S^\dagger)_{3p}, \\
g_L^{A_p \bar{E}_1 l b} &= -\frac{1}{\sqrt{2}} \sum_{i=1}^3 y_i^{*(E)} (V_{e_L})_{ib} (U_A^\dagger)_{2p}, & g_R^{A_p \bar{E}_1 l b} &= -\frac{1}{\sqrt{2}} \sum_{n=1}^2 x_n^{(E)} (V_{e_R})_{nb} (U_A^\dagger)_{3p}, \\
g_R^{H_p \bar{l}_a l b} &= \frac{1}{\sqrt{2}} \sum_{i=1}^3 y_i^{(l)} (V_{e_L}^*)_{ia} (V_{e_R})_{3b} (U_S^\dagger)_{2p}, & g_R^{A_p \bar{l}_a l b} &= \frac{1}{\sqrt{2}} \sum_{i=1}^3 y_i^{(l)} (V_{e_L}^*)_{ia} (V_{e_R})_{3b} (U_A^\dagger)_{2p}.
\end{aligned} \tag{A1}$$

Otherwise, the coefficients used in Eq. (68) and Eq. (69) read

$$\begin{aligned}
g_L^{H^+ \bar{u}_a d b} &= -(U_c^\dagger)_{12} \sum_{i=1}^3 y_i^{*(u)} (V_{u_R}^*)_{ia} (V_{d_L})_{3b}, & g_R^{H^+ \bar{u}_a d b} &= (U_c^\dagger)_{22} \sum_{i=1}^3 y_i^{(d)} (V_{u_L}^*)_{3a} (V_{d_R})_{ib}, \\
g_L^{H_{1(2)}^+ \bar{u}_a d b} &= -(U_c^\dagger)_{13(14)} \sum_{i=1}^3 y_i^{*(u)} (V_{u_R}^*)_{ia} (V_{d_L})_{3b}, & g_R^{H_{1(2)}^+ \bar{u}_a d b} &= (U_c^\dagger)_{23(24)} \sum_{i=1}^3 y_i^{(d)} (V_{u_L}^*)_{3a} (V_{d_R})_{ib}, \\
g_L^{H^+ \bar{U} d b} &= -(U_c^\dagger)_{22} \sum_{n=1}^2 x_n^{*(U)} (V_{d_L})_{nb}, & g_R^{H^+ \bar{U} d b} &= (U_c^\dagger)_{32} \sum_{i=1}^3 [w_k^{(d)} i (V_{d_R})_{ib}], \\
g_L^{H_{1(2)}^+ \bar{U} d b} &= -(U_c^\dagger)_{23(24)} \sum_{n=1}^2 x_n^{*(U)} (V_{d_L})_{nb}, & g_R^{H_{1(2)}^+ \bar{U} d b} &= (U_c^\dagger)_{33(34)} \sum_{i=1}^3 [w_k^{(d)} i (V_{d_R})_{ib}], \\
g_L^{H_p \bar{D}_1 d b} &= \frac{1}{\sqrt{2}} \sum_{n=1}^2 [x_n^{*(D)} (V_{d_L})_{nb}] (U_S^\dagger)_{1p}, & g_R^{H_p \bar{D}_1 d b} &= \frac{1}{\sqrt{2}} \sum_{i=1}^3 [x_i^{(d)} (V_{d_R})_{ib}] (U_S^\dagger)_{3p}, \\
g_L^{A_p \bar{D}_1 d b} &= -\frac{1}{\sqrt{2}} \sum_{n=1}^2 [x_n^{*(D)} (V_{d_L})_{nb}] (U_A^\dagger)_{1p}, & g_R^{A_p \bar{D}_1 d b} &= \frac{1}{\sqrt{2}} \sum_{i=1}^3 [x_i^{(d)} (V_{d_R})_{ib}] (U_A^\dagger)_{3p}, \\
g_R^{H_p \bar{d}_a d b} &= \frac{1}{\sqrt{2}} \sum_{i=1}^3 [y_i^{(d)} (V_{d_L}^*)_{3a} (V_{d_R})_{ib}] (U_S^\dagger)_{2p}, & g_R^{A_p \bar{d}_a d b} &= \frac{1}{\sqrt{2}} \sum_{i=1}^3 [y_i^{(d)} (V_{d_L}^*)_{3a} (V_{d_R})_{ib}] (U_A^\dagger)_{2p},
\end{aligned} \tag{A2}$$

$$\begin{aligned}
g_L^{H^- \bar{D}_1 u_b} &= (U_c^\dagger)_{12} \sum_{n=1}^2 x_n^{*(D)} (V_{u_L})_{nb}, & g_R^{H^- \bar{D}_1 u_b} &= (U_c^\dagger)_{32} \sum_{i=1}^3 [w_i^{(U)} (V_{u_R})_{ib}], \\
g_L^{H_{1(2)}^- \bar{D}_1 u_b} &= (U_c^\dagger)_{13(14)} \sum_{n=1}^2 x_n^{*(D)} (V_{u_L})_{nb}, & g_R^{H_{1(2)}^- \bar{D}_1 u_b} &= (U_c^\dagger)_{33(34)} \sum_{i=1}^3 [w_i^{(U)} (V_{u_R})_{ib}], \\
g_L^{H_p \bar{U} u_b} &= \frac{1}{\sqrt{2}} \sum_{n=1}^2 [x_n^{*(U)} (V_{u_L})_{nb}] (U_S^\dagger)_{1p}, & g_R^{H_p \bar{U} u_b} &= \frac{1}{\sqrt{2}} \sum_{i=1}^3 [x_i^{*(u)} (V_{u_R})_{ib}] (U_S^\dagger)_{3p}, \\
g_L^{A_p \bar{U} u_b} &= -\frac{1}{\sqrt{2}} \sum_{n=1}^2 [x_n^{*(U)} (V_{u_L})_{nb}] (U_A^\dagger)_{1p}, & g_R^{A_p \bar{U} u_b} &= -\frac{1}{\sqrt{2}} \sum_{i=1}^3 [x_i^{*(u)} (V_{u_R})_{ib}] (U_A^\dagger)_{3p}, \\
g_R^{H_p \bar{u}_a u_b} &= \frac{1}{\sqrt{2}} \sum_{i=1}^3 [y_i^{(u)} (V_{u_L}^*)_{3a} (V_{u_R})_{ib}] (U_S^\dagger)_{1p}, & g_R^{A_p \bar{u}_a u_b} &= \frac{1}{\sqrt{2}} \sum_{i=1}^3 [y_i^{(u)} (V_{u_L}^*)_{3a} (V_{u_R})_{ib}] (U_A^\dagger)_{1p} \quad (A3)
\end{aligned}$$

Appendix B: Loop functions

The loop functions used in Eq. (76) are given as follow

$$\begin{aligned}
f_\gamma^W(x) &= \frac{-4x^3 + 45x^2 - 33x + 10}{12(x-1)^3} - \frac{3x^3}{2(x-1)^4} \ln x \\
f_\gamma(x) &= \frac{(-1 + 5x + 2x^2)}{12(x-1)^3} - \frac{x^2}{2(x-1)^4} \ln x, & f'_\gamma(x) &= \frac{-2 - 5x + x^2}{12(x-1)^3} + \frac{x}{2(x-1)^4} \ln x, \\
f''_\gamma(x) &= \frac{-7 + 5x + 8x^2}{36(x-1)^3} + \frac{(2-3x)x}{6(x-1)^4} \ln x, & f'''_\gamma(x) &= \frac{5 - 10x - 7x^2}{36(x-1)^3} + \frac{x(3x-1)}{6(x-1)^4} \ln x, \\
h'_\gamma(x) &= \frac{x-3}{2(x-1)^2} + \frac{1}{(x-1)^3} \ln x, & h''_\gamma(x) &= \frac{-3+5x}{6(x-1)^2} + \frac{(2-3x)}{3(x-1)^3} \ln x, & h'''_\gamma(x) &= -\frac{2x}{3(x-1)^2} + \frac{3x-1}{3(x-1)^3} \ln x, \\
f'_g(x) = f''_g(x) &= \frac{-2-5x+x^2}{12(x-1)^3} + \frac{x}{2(x-1)^4} \ln x, & h'_g(x) = h''_g(x) &= \frac{x-3}{2(x-1)^2} + \frac{1}{(x-1)^3}. \quad (B1)
\end{aligned}$$

Appendix C: Anomaly checking

In this appendix, we show explicitly how the anomaly cancellation is satisfied with fermion content given in Tables II and III.

$$\begin{aligned}
[SU(3)_C]^2 U(1)_X &= \sum_{\text{quarks}} X_{qL} - X_{qR} \\
&= 2 \times 2X_{q_{nL}} + 2X_{q_{3L}} + X_{U_L} + X_{D_{1L}} + X_{D_{2L}} - 3X_{u_{iR}} - 3X_{d_{iR}} - X_{U_R} - X_{D_{1R}} - X_{D_{2R}} \\
&= 2 \times 0 + 2 \times 1/3 + 1/3 + 0 + 0 - 3 \times 2/3 - 3 \times (-1/3) - 2/3 - (-1/3) - (-1/3) = 0, \quad (C1)
\end{aligned}$$

$$\begin{aligned}
[SU(3)_C]^2 U(1)_Y &= \sum_{\text{quarks}} Y_{qL} - Y_{qR} \\
&= 2 \times 2Y_{q_{nL}} + 2Y_{q_{3L}} + Y_{U_L} + Y_{D_{1L}} + Y_{D_{2L}} - 3Y_{u_{iR}} - 3Y_{d_{iR}} - Y_{T_R} - Y_{D_{1R}} - Y_{D_{2R}} \\
&= 2 \times 2(1/6) + 2(1/6) + 2/3 - 1/3 - 1/3 - 3(2/3) - 3(-1/3) - 2/3 - (-1/3) - (-1/3) = 0, \quad (C2)
\end{aligned}$$

$$\begin{aligned}
[SU(2)_L]^2 U(1)_X &= \sum_{\text{doublets}} X_{fL} = 2 \times 3X_{q_{nL}} + 3X_{q_{3L}} + 3 \times X_{l_{iL}} \\
&= 2 \times 0 + 3 \times 1/3 + 3 \times -1/3 = 0, \quad (C3)
\end{aligned}$$

$$\begin{aligned}
[SU(2)_L]^2 U(1)_Y &= \sum_{\text{doublets}} Y_{fL} - X_{qR} = 2 \times 3Y_{q_{nL}} + 3Y_{q_{3L}} + 3Y_{l_{iL}} \\
&= 2 \times 3 \times 1/6 + 3 \times 1/6 + 1/3 + 3 \times -1/2 = 0, \quad (C4)
\end{aligned}$$

$$\begin{aligned}
[\text{Gravity}]^2 U(1)_X &\sim \sum_{\text{fermions}} X_{f_L} - X_{f_R} \\
&= 2 \times 3 \times 2X_{q_{nL}} + 3 \times 2X_{q_{3L}} + 3 \times 2X_{l_{iL}} + 3X_{U_L} + 3X_{D_{1L}} + 3X_{D_{2L}} + X_{E_{1L}} - 3 \times 3X_{u_{iR}} - 3 \times 3X_{d_{iR}} \\
&\quad - 3X_{U_R} - 3X_{D_{1R}} - 3X_{D_{2R}} - 2X_{l_{nR}} - X_{l_{3R}} - X_{E_{1R}} - 3X_{\nu_{iR}} - 3X_{N_{iR}} - 2X_{\psi_{nR}} - 2X_{\Omega_{nR}} \\
&= 2 \times 3 \times 0 + 3 \times 2(1/3) + 3 \times 2(-1/3) + 3(1/3) + 3(0) + 3(0) + 1(-1) - 3 \times 3(2/3) - 3 \times 3(-1/3) \\
&\quad - 2/3 - (-1/3) - (-1/3) - 2(-1) - (-1) - (-1) - 3(1/3) - 3(0) - 2(1) - 2(-1) = 0 \tag{C5}
\end{aligned}$$

$$\begin{aligned}
[\text{Gravity}]^2 U(1)_Y &\sim \sum_{\text{fermions}} Y_{f_L} - Y_{f_R} \\
&= 2 \times 3 \times 2Y_{q_{nL}} + 3 \times 2Y_{q_{3L}} + 3 \times 2Y_{l_{iL}} + 3Y_{U_L} + 3Y_{D_{1L}} + 3Y_{D_{2L}} + Y_{E_{1L}} - 3 \times 3Y_{u_{iR}} - 3 \times 3Y_{d_{iR}} \\
&\quad - 3Y_{U_R} - 3Y_{D_{1R}} - 3Y_{D_{2R}} - 2Y_{l_{nR}} - Y_{l_{3R}} - Y_{E_{1R}} - 3Y_{\nu_{iR}} - 3Y_{N_{iR}} - 2Y_{\psi_{nR}} - 2Y_{\Omega_{nR}} \\
&= 2 \times 3 \times 2(1/6) + 3 \times 2(1/6) + 3 \times 2(-1/2) + 3(2/3) + 3(-1/3) + 3(-1/3) + (-1) - 3 \times 3(2/3) \\
&\quad - 3 \times 3(-1/3) - 3(2/3) - 3(-1/3) - 3(-1/3) - 2(-1) - (-1) - (-1) \\
&\quad - 3(0) - 3(0) - 2(0) - 2(0) = 0 \tag{C6}
\end{aligned}$$

$$\begin{aligned}
[U(1)_Y]^2 U(1)_X &= \sum_{\text{fermions}} (Y_{f_L}^2 X_{f_L} - Y_{f_R}^2 X_{f_R}) \\
&= 3 \times 2 \times 2Y_{q_{nL}}^2 X_{q_{nL}} + 3 \times 2Y_{q_{3L}}^2 X_{q_{3L}} + 3Y_{U_L}^2 X_{U_L} + 3Y_{D_{1L}}^2 X_{D_{1L}} + 3Y_{D_{2L}}^2 X_{D_{2L}} + 3 \times 2Y_{l_{iL}}^2 X_{l_{iL}} \\
&\quad + Y_{E_{1L}}^2 X_{E_{1L}} - 3 \times 3Y_{u_{iR}}^2 X_{u_{iR}} - 3 \times 3Y_{d_{iR}}^2 X_{d_{iR}} - 3Y_{U_R}^2 X_{U_R} - 3Y_{D_{1R}}^2 X_{D_{1R}} - 3Y_{D_{2R}}^2 X_{D_{2R}} - 2Y_{l_{nR}}^2 X_{l_{nR}} \\
&\quad - Y_{l_{3R}}^2 X_{l_{3R}} - Y_{E_{1R}}^2 X_{E_{1R}} - 3Y_{\nu_{iR}}^2 X_{\nu_{iR}} - 3Y_{N_{iR}}^2 X_{N_{iR}} - 2Y_{\psi_{nR}}^2 X_{\psi_{nR}} - 2Y_{\Omega_{nR}}^2 X_{\Omega_{nR}} \\
&= 3 \times 2 \times 2(1/6)^2(0) + 3 \times 2(1/6)^2(1/3) + 3(2/3)^2(1/3) + 3(-1/3)^2(0) + 3(-1/3)^2(0) \\
&\quad + 3 \times 2(-1/2)^2(-1/3) + (-1)^2(-1) - 3 \times 3(2/3)^2(2/3) - 3 \times 3(-1/3)^2(-1/3) - 3(2/3)^2(2/3) \\
&\quad - 3(-1/3)^2(-1/3) - 3(-1/3)^2(-1/3) - 2(-1)^2(-1) - (-1)^2(-1) - (-1)^2(-1) - 3(0)^2(1/3) \\
&\quad - 3(0)^2(0) - 2(0)^2(1) - 2(0)^2(-1) = 0 \tag{C7}
\end{aligned}$$

$$\begin{aligned}
[U(1)_X]^2 U(1)_Y &= \sum_{\text{fermions}} (X_{f_L}^2 Y_{f_L} - X_{f_R}^2 Y_{f_R}) \\
&= 3 \times 2 \times 2X_{q_{nL}}^2 Y_{q_{nL}} + 3 \times 2X_{q_{3L}}^2 Y_{q_{3L}} + 3X_{U_L}^2 Y_{U_L} + 3X_{D_{1L}}^2 Y_{D_{1L}} + 3X_{D_{2L}}^2 Y_{D_{2L}} + 3 \times 2X_{l_{iL}}^2 Y_{l_{iL}} \\
&\quad + X_{E_{1L}}^2 Y_{E_{1L}} - 3 \times 3X_{u_{iR}}^2 Y_{u_{iR}} - 3 \times 3X_{d_{iR}}^2 Y_{d_{iR}} - 3X_{U_R}^2 Y_{U_R} - 3X_{D_{1R}}^2 Y_{D_{1R}} - 3X_{D_{2R}}^2 Y_{D_{2R}} - 2X_{l_{nR}}^2 Y_{l_{nR}} \\
&\quad - X_{l_{3R}}^2 Y_{l_{3R}} - X_{E_{1R}}^2 Y_{E_{1R}} - 3X_{\nu_{iR}}^2 Y_{\nu_{iR}} - 3X_{N_{iR}}^2 Y_{N_{iR}} - 2X_{\psi_{nR}}^2 Y_{\psi_{nR}} - 2X_{\Omega_{nR}}^2 Y_{\Omega_{nR}} \\
&= 3 \times 2 \times 2(0)^2(1/6) + 3 \times 2(1/3)^2(1/6) + 3(1/3)^2(2/3) + 3(0)^2(-1/3) + 3(0)^2(-1/3) \\
&\quad + 3 \times 2(-1/3)^2(-1/2) + (-1)^2(-1) - 3 \times 3(2/3)^2(2/3) - 3 \times 3(-1/3)^2(-1/3) - 3(2/3)^2(2/3) \\
&\quad - 3(-1/3)^2(-1/3) - 3(-1/3)^2(-1/3) - 2(-1)^2(-1) - (-1)^2(-1) - (-1)^2(-1) - 3(-1/3)^2(0) \\
&\quad - 3(0)^2(0) - 2(1)^2(0) - 2(-1)^2(0) = 0 \tag{C8}
\end{aligned}$$

$$\begin{aligned}
[U(1)_Y]^3 &= \sum_{\text{fermions}} (Y_{f_L}^3 - Y_{f_R}^3) \\
&= 3 \times 2Y_{q_{3L}}^3 + 3 \times 2 \times 2Y_{q_{nL}}^3 + 3Y_{U_L}^3 + 3Y_{D_{1L}}^3 + 3Y_{D_{2L}}^3 + 3 \times 2Y_{l_{iL}}^3 + Y_{E_{1L}}^3 - 3 \times 3Y_{u_{iR}}^3 - 3 \times 3Y_{d_{iR}}^3 \\
&\quad - 3Y_{U_R}^3 - 3Y_{D_{1R}}^3 - 3Y_{D_{2R}}^3 - 2Y_{l_{nR}}^3 - Y_{l_{3R}}^3 - Y_{E_{1R}}^3 - 3Y_{\nu_{iR}}^3 - 3Y_{N_{iR}}^3 - 2Y_{\psi_{nR}}^3 - 2Y_{\Omega_{nR}}^3 \\
&= 3 \times 2(1/6)^3 + 3 \times 2 \times 2(1/6)^3 + 3(2/3)^3 + 3(-1/3)^3 + 3(-1/3)^3 + 3 \times 2(-1/2)^3 + (-1)^3 \\
&\quad - 3 \times 3(2/3)^3 - 3 \times (-1/3)^3 - 3(2/3)^2 - 3(-1/3)^3 - 3(-1/3)^3 - 2(-1)^3 - (-1)^3 - (-1)^3 \\
&\quad - 3(0)^3 - 3(0)^3 - 2(0)^2 - 2(0)^2 = 0 \tag{C9}
\end{aligned}$$

$$\begin{aligned}
[U(1)_X]^3 &= \sum_{\text{fermions}} (X_{f_L}^3 - X_{f_R}^3) \\
&= 3 \times 2X_{q_{3L}}^3 + 3 \times 2 \times 2X_{q_{nL}}^3 + 3X_{U_L}^3 + 3X_{D_{1L}}^3 + 3X_{D_{2L}}^3 + 3 \times 2X_{l_{iL}}^3 + X_{E_{1L}}^3 - 3 \times 3X_{u_{iR}}^3 - 3 \times 3X_{d_{iR}}^3 \\
&\quad - 3X_{U_R}^3 - 3X_{D_{1R}}^3 - 3X_{D_{2R}}^3 - 2X_{l_{nR}}^3 - X_{l_{3R}}^3 - X_{E_{1R}}^3 - 3X_{\nu_{iR}}^3 - 3X_{N_{iR}}^3 - 2X_{\psi_{nR}}^3 - 2X_{\Omega_{nR}}^3 \\
&= 3 \times 2(0)^3 + 3 \times 2 \times 2(1/3)^3 + 3(1/3)^3 + 3(0)^3 + 3(0)^3 + 3 \times 2(-1/3)^3 + (-1)^3 \\
&\quad - 3 \times 3(2/3)^3 - 3 \times (-1/3)^3 - 3(2/3)^3 - 3(-1/3)^3 - 3(-1/3)^3 - 2(-1)^3 - (-1)^3 - (-1)^3 \\
&\quad - 3(1/3)^3 - 3(0)^3 - 2(1)^3 - 2(-1)^3 = 0
\end{aligned} \tag{C10}$$

Here we ignore the contribution from vector-like fermions $T_{L,R}$, $B_{L,R}$ and $E_{2L,R}$ since they have identical quantum numbers for both chiral parts.

Appendix D: The couplings of neutral bosons, Z_μ, Z'_μ , to SM fermions $\bar{f}_a - f_b$

Interactions of neutral currents with fermions are written in the mass eigenstates have the following form

$$\mathcal{L}^{\text{NC}} = \bar{f}_a \gamma^\mu \left\{ g_V^{Z,(Z')} (f_a f_b) - g_A^{Z,(Z')} (f_a f_b) \gamma_5 \right\} f_b Z_\mu (Z'_\mu), \tag{D1}$$

where the expressions of $g_V^Z (f_a f_b)$; $g_A^Z (f_a f_b)$ are given in Table X.

Here, we define the following notations: $c_W = \cos \theta_W$, $s_W = \sin \theta_W$, $t_W = \frac{g'}{g}$, $t_X = \frac{g_X}{g}$, $c_{\theta_{ZZ'}}$ = $\cos \theta_{ZZ'}$ and

$\bar{f}_a f_b$	$12 \frac{g_V^Z(f_a f_b)}{g}$	$-12 \frac{g_A^Z(f_a f_b)}{g}$
$\bar{\nu}_a \nu_b$	$\left(3 \frac{c_{\theta_{ZZ'}}}{c_W} + 2t_X s_{\theta_{ZZ'}} \right) \delta_{ab}$	$\left(3 \frac{c_{\theta_{ZZ'}}}{c_W} + 2t_X s_{\theta_{ZZ'}} \right) \delta_{ab}$
$\bar{e}_a e_b$	$(-3c_{\theta_{ZZ'}} c_W + 9c_{\theta_{ZZ'}} s_W t_W + 8t_X s_{\theta_{ZZ'}}) \delta_{ab}$	$\left(3 \frac{c_{\theta_{ZZ'}}}{c_W} + 4t_X s_{\theta_{ZZ'}} \right) \delta_{ab}$
$\bar{u}_a u_b$	$\delta_{ab} (-1 + 4c_{2\theta_W}) \frac{c_{\theta_{ZZ'}}}{c_W} - 4\delta_{ab} t_X s_{\theta_{ZZ'}} - 2t_X s_{\theta_{ZZ'}} (V_{u_L}^*)_{3a} (V_{u_L})_{3b}$	$\left(3 \frac{c_{\theta_{ZZ'}}}{c_W} + 4t_X s_{\theta_{ZZ'}} \right) \delta_{ab} + 2t_X s_{\theta_{ZZ'}} (V_{u_L}^*)_{3a} (V_{u_L})_{3b}$
$\bar{d}_a d_b$	$-\delta_{ab} (1 + 2c_{2\theta_W}) \frac{c_{\theta_{ZZ'}}}{c_W} - 2\delta_{ab} t_X s_{\theta_{ZZ'}} - 2t_X s_{\theta_{ZZ'}} (V_{d_L}^*)_{3a} (V_{d_L})_{3b}$	$\left(3 \frac{c_{\theta_{ZZ'}}}{c_W} + 2t_X s_{\theta_{ZZ'}} \right) \delta_{ab} + 2t_X s_{\theta_{ZZ'}} (V_{d_L}^*)_{3a} (V_{d_L})_{3b}$

Table X: The couplings of Z_μ - bosons to SM fermions

$s_{\theta_{ZZ'}} = \sin \theta_{ZZ'}$. The mixing angle $\theta_{ZZ'}$ is determined by the following equation:

$$\tan \theta_{ZZ'} = \frac{12\sqrt{1 + t_X^2} t_X (v_1^2 + 2v_2^2)}{(9 + 9t_X^2 - 4t_X^2)v_1^2 + (9 + 9t_X^2 - 16t_X^2)v_2^2 - 4t_X^2 \Lambda_{\text{new}}^2}, \tag{D2}$$

where $\Lambda_{\text{new}}^2 = v_\sigma^2 + 4v_\chi^2 + 9v_\eta^2 + 36v_\rho^2 + 36v_\kappa^2$. The vector coupling of new gauge boson Z' $g_V^{Z'} (f_a f_b)$ is related to $g_V^Z (f_a f_b)$ by a rotation in the Z - Z' basis, specifically through the transformation $s_{\theta_{ZZ'}} \rightarrow -c_{\theta_{ZZ'}}$ and $c_{\theta_{ZZ'}} \rightarrow s_{\theta_{ZZ'}}$. The axial-vector coupling $g_A^{Z'} (f_i f_j)$ undergoes a similar rotation, with the substitutions $s_{\theta_{ZZ'}} \rightarrow c_{\theta_{ZZ'}}$ and $c_{\theta_{ZZ'}} \rightarrow -s_{\theta_{ZZ'}}$.

REFERENCES

-
- [1] **Super-Kamiokande** Collaboration, Y. Fukuda *et al.*, “Evidence for oscillation of atmospheric neutrinos,” *Phys. Rev. Lett.* **81** (1998) 1562–1567, [arXiv:hep-ex/9807003](#).
- [2] **Super-Kamiokande** Collaboration, Y. Fukuda *et al.*, “Measurements of the solar neutrino flux from Super-Kamiokande’s first 300 days,” *Phys. Rev. Lett.* **81** (1998) 1158–1162, [arXiv:hep-ex/9805021](#). [Erratum: *Phys.Rev.Lett.* 81, 4279 (1998)].
- [3] **Super-Kamiokande** Collaboration, Y. Fukuda *et al.*, “Measurement of the flux and zenith angle distribution of upward through going muons by Super-Kamiokande,” *Phys. Rev. Lett.* **82** (1999) 2644–2648, [arXiv:hep-ex/9812014](#).
- [4] **Super-Kamiokande** Collaboration, S. Fukuda *et al.*, “Tau neutrinos favored over sterile neutrinos in atmospheric muon-neutrino oscillations,” *Phys. Rev. Lett.* **85** (2000) 3999–4003, [arXiv:hep-ex/0009001](#).
- [5] **Super-Kamiokande** Collaboration, S. Fukuda *et al.*, “Solar B-8 and hep neutrino measurements from 1258 days of Super-Kamiokande data,” *Phys. Rev. Lett.* **86** (2001) 5651–5655, [arXiv:hep-ex/0103032](#).
- [6] **Super-Kamiokande** Collaboration, Y. Ashie *et al.*, “Evidence for an oscillatory signature in atmospheric neutrino oscillation,” *Phys. Rev. Lett.* **93** (2004) 101801, [arXiv:hep-ex/0404034](#).
- [7] **KamLAND** Collaboration, K. Eguchi *et al.*, “First results from KamLAND: Evidence for reactor anti-neutrino disappearance,” *Phys. Rev. Lett.* **90** (2003) 021802, [arXiv:hep-ex/0212021](#).
- [8] **KamLAND** Collaboration, T. Araki *et al.*, “Measurement of neutrino oscillation with KamLAND: Evidence of spectral distortion,” *Phys. Rev. Lett.* **94** (2005) 081801, [arXiv:hep-ex/0406035](#).
- [9] **SNO** Collaboration, Q. R. Ahmad *et al.*, “Measurement of day and night neutrino energy spectra at SNO and constraints on neutrino mixing parameters,” *Phys. Rev. Lett.* **89** (2002) 011302, [arXiv:nucl-ex/0204009](#).
- [10] **SNO** Collaboration, Q. R. Ahmad *et al.*, “Direct evidence for neutrino flavor transformation from neutral current interactions in the Sudbury Neutrino Observatory,” *Phys. Rev. Lett.* **89** (2002) 011301, [arXiv:nucl-ex/0204008](#).
- [11] **SNO** Collaboration, S. N. Ahmed *et al.*, “Measurement of the total active B-8 solar neutrino flux at the Sudbury Neutrino Observatory with enhanced neutral current sensitivity,” *Phys. Rev. Lett.* **92** (2004) 181301, [arXiv:nucl-ex/0309004](#).
- [12] **SNO** Collaboration, B. Aharmim *et al.*, “Electron energy spectra, fluxes, and day-night asymmetries of B-8 solar neutrinos from measurements with NaCl dissolved in the heavy-water detector at the Sudbury Neutrino Observatory,” *Phys. Rev. C* **72** (2005) 055502, [arXiv:nucl-ex/0502021](#).
- [13] **Particle Data Group** Collaboration, R. L. Workman and Others, “Review of Particle Physics,” *PTEP* **2022** (2022) 083C01.
- [14] **WMAP** Collaboration, D. N. Spergel *et al.*, “Wilkinson Microwave Anisotropy Probe (WMAP) three year results: implications for cosmology,” *Astrophys. J. Suppl.* **170** (2007) 377, [arXiv:astro-ph/0603449](#).
- [15] **Planck** Collaboration, P. A. R. Ade *et al.*, “Planck 2013 results. I. Overview of products and scientific results,” *Astron. Astrophys.* **571** (2014) A1, [arXiv:1303.5062 \[astro-ph.CO\]](#).
- [16] **Planck** Collaboration, N. Aghanim *et al.*, “Planck 2018 results. VI. Cosmological parameters,” *Astron. Astrophys.* **641** (2020) A6, [arXiv:1807.06209 \[astro-ph.CO\]](#). [Erratum: *Astron.Astrophys.* 652, C4 (2021)].
- [17] **LHCb** Collaboration, R. Aaij *et al.*, “Angular Analysis of the $B^+ \rightarrow K^{*+} \mu^+ \mu^-$ Decay,” *Phys. Rev. Lett.* **126** no. 16, (2021) 161802, [arXiv:2012.13241 \[hep-ex\]](#).
- [18] **LHCb** Collaboration, R. Aaij *et al.*, “Measurement of CP -Averaged Observables in the $B^0 \rightarrow K^{*0} \mu^+ \mu^-$ Decay,” *Phys. Rev. Lett.* **125** no. 1, (2020) 011802, [arXiv:2003.04831 \[hep-ex\]](#).
- [19] **LHCb** Collaboration, R. Aaij *et al.*, “Branching Fraction Measurements of the Rare $B_s^0 \rightarrow \phi \mu^+ \mu^-$ and $B_s^0 \rightarrow f_2'(1525) \mu^+ \mu^-$ Decays,” *Phys. Rev. Lett.* **127** no. 15, (2021) 151801, [arXiv:2105.14007 \[hep-ex\]](#).
- [20] **LHCb** Collaboration, R. Aaij *et al.*, “Measurements of the S-wave fraction in $B^0 \rightarrow K^+ \pi^- \mu^+ \mu^-$ decays and the $B^0 \rightarrow K^*(892)^0 \mu^+ \mu^-$ differential branching fraction,” *JHEP* **11** (2016) 047, [arXiv:1606.04731 \[hep-ex\]](#). [Erratum: *JHEP* 04, 142 (2017)].
- [21] **LHCb** Collaboration, R. Aaij *et al.*, “Angular analysis of the rare decay $B_s^0 \rightarrow \phi \mu^+ \mu^-$,” *JHEP* **11** (2021) 043, [arXiv:2107.13428 \[hep-ex\]](#).
- [22] **LHCb** Collaboration, “Measurement of the ratios of branching fractions $\mathcal{R}(D^*)$ and $\mathcal{R}(D^0)$,” *Phys. Rev. Lett.* **131** (2023) 111802, [arXiv:2302.02886 \[hep-ex\]](#).
- [23] **LHCb** Collaboration, R. Aaij *et al.*, “Test of lepton universality in $b \rightarrow s \ell^+ \ell^-$ decays,” *Phys. Rev. Lett.* **131** no. 5, (2023) 051803, [arXiv:2212.09152 \[hep-ex\]](#).
- [24] **LHCb** Collaboration, R. Aaij *et al.*, “Measurement of lepton universality parameters in $B^+ \rightarrow K^+ \ell^+ \ell^-$ and $B^0 \rightarrow K^{*0} \ell^+ \ell^-$ decays,” *Phys. Rev. D* **108** no. 3, (2023) 032002, [arXiv:2212.09153 \[hep-ex\]](#).
- [25] A. Greljo, J. Salko, A. Smolkovič, and P. Stangl, “Rare b decays meet high-mass Drell-Yan,” *JHEP* **05** (2023) 087, [arXiv:2212.10497 \[hep-ph\]](#).
- [26] S. M. Boucenna, A. Celis, J. Fuentes-Martin, A. Vicente, and J. Virto, “Non-abelian gauge extensions for B-decay anomalies,” *Phys. Lett. B* **760** (2016) 214–219, [arXiv:1604.03088 \[hep-ph\]](#).
- [27] P. H. Frampton, “Chiral dilepton model and the flavor question,” *Phys. Rev. Lett.* **69** (1992) 2889–2891.
- [28] R. Foot, O. F. Hernandez, F. Pisano, and V. Pleitez, “Lepton masses in an $SU(3)$ -L x $U(1)$ -N gauge model,” *Phys. Rev. D* **47** (1993) 4158–4161, [arXiv:hep-ph/9207264](#).

- [29] M. Singer, J. W. F. Valle, and J. Schechter, “Canonical Neutral Current Predictions From the Weak Electromagnetic Gauge Group $SU(3) \times U(1)$,” *Phys. Rev. D* **22**.
- [30] P. V. Dong, H. N. Long, D. T. Nhung, and D. V. Soa, “ $SU(3)(C) \times SU(3)(L) \times U(1)(X)$ model with two Higgs triplets,” *Phys. Rev. D* **73** (2006) 035004, [arXiv:hep-ph/0601046](#).
- [31] P. V. Dong, H. T. Hung, and T. D. Tham, “3-3-1-1 model for dark matter,” *Phys. Rev. D* **87** no. 11, (2013) 115003, [arXiv:1305.0369 \[hep-ph\]](#).
- [32] P. V. Dong and H. N. Long, “ $U(1)(Q)$ invariance and $SU(3)(C) \times SU(3)(L) \times U(1)(X)$ models with beta arbitrary,” *Eur. Phys. J. C* **42** (2005) 325–329, [arXiv:hep-ph/0506022](#).
- [33] P. V. Dong, D. T. Huong, F. S. Queiroz, J. W. F. Valle, and C. A. Vaquera-Araujo, “The Dark Side of Flipped Trinification,” *JHEP* **04** (2018) 143, [arXiv:1710.06951 \[hep-ph\]](#).
- [34] I. Doršner, S. Fajfer, A. Greljo, J. F. Kamenik, and N. Košnik, “Physics of leptoquarks in precision experiments and at particle colliders,” *Phys. Rept.* **641** (2016) 1–68, [arXiv:1603.04993 \[hep-ph\]](#).
- [35] M. Bauer and M. Neubert, “Minimal Leptoquark Explanation for the $R_{D^{(*)}}$, R_K , and $(g-2)_\mu$ Anomalies,” *Phys. Rev. Lett.* **116** no. 14, (2016) 141802, [arXiv:1511.01900 \[hep-ph\]](#).
- [36] S. Fajfer and N. Košnik, “Vector leptoquark resolution of R_K and $R_{D^{(*)}}$ puzzles,” *Phys. Lett. B* **755** (2016) 270–274, [arXiv:1511.06024 \[hep-ph\]](#).
- [37] R. Barbieri, G. Isidori, A. Pattori, and F. Senia, “Anomalies in B -decays and $U(2)$ flavour symmetry,” *Eur. Phys. J. C* **76** no. 2, (2016) 67, [arXiv:1512.01560 \[hep-ph\]](#).
- [38] D. Bećirević, S. Fajfer, N. Košnik, and O. Sumensari, “Leptoquark model to explain the B -physics anomalies, R_K and R_{D^*} ,” *Phys. Rev. D* **94** no. 11, (2016) 115021, [arXiv:1608.08501 \[hep-ph\]](#).
- [39] G. Hiller, D. Loose, and K. Schönwald, “Leptoquark Flavor Patterns & B Decay Anomalies,” *JHEP* **12** (2016) 027, [arXiv:1609.08895 \[hep-ph\]](#).
- [40] A. Crivellin, D. Müller, and T. Ota, “Simultaneous explanation of $R(D^{(*)})$ and $b \rightarrow s\mu^+\mu^-$: the last scalar leptoquarks standing,” *JHEP* **09** (2017) 040, [arXiv:1703.09226 \[hep-ph\]](#).
- [41] R. Alonso, B. Grinstein, and J. Martin Camalich, “Lepton universality violation and lepton flavor conservation in B -meson decays,” *JHEP* **10** (2015) 184, [arXiv:1505.05164 \[hep-ph\]](#).
- [42] T. D. Lee, “A Theory of Spontaneous T Violation,” *Phys. Rev. D* **8** (1973) 1226–1239.
- [43] G. C. Branco, P. M. Ferreira, L. Lavoura, M. N. Rebelo, M. Sher, and J. P. Silva, “Theory and phenomenology of two-Higgs-doublet models,” *Phys. Rept.* **516** (2012) 1–102, [arXiv:1106.0034 \[hep-ph\]](#).
- [44] A. Crivellin, D. Müller, and C. Wiegand, “ $b \rightarrow s\ell^+\ell^-$ transitions in two-Higgs-doublet models,” *JHEP* **06** (2019) 119, [arXiv:1903.10440 \[hep-ph\]](#).
- [45] H. B. Camara, R. G. Felipe, and F. R. Joaquim, “Minimal inverse-seesaw mechanism with Abelian flavour symmetries,” *JHEP* **05** (2021) 021, [arXiv:2012.04557 \[hep-ph\]](#).
- [46] A. E. C. Hernández, D. T. Huong, and I. Schmidt, “Universal inverse seesaw mechanism as a source of the SM fermion mass hierarchy,” *Eur. Phys. J. C* **82** no. 1, (2022) 63, [arXiv:2109.12118 \[hep-ph\]](#).
- [47] Z.-z. Xing, “Flavor structures of charged fermions and massive neutrinos,” *Phys. Rept.* **854** (2020) 1–147, [arXiv:1909.09610 \[hep-ph\]](#).
- [48] M. Jung and A. Pich, “Electric Dipole Moments in Two-Higgs-Doublet Models,” *JHEP* **04** (2014) 076, [arXiv:1308.6283 \[hep-ph\]](#).
- [49] H. E. Logan, S. Moretti, D. Rojas-Ciofalo, and M. Song, “CP violation from charged Higgs bosons in the three Higgs doublet model,” *JHEP* **07** (2021) 158, [arXiv:2012.08846 \[hep-ph\]](#).
- [50] **ACME** Collaboration, V. Andreev *et al.*, “Improved limit on the electric dipole moment of the electron,” *Nature* **562** no. 7727, (2018) 355–360.
- [51] J. O. Eeg, “Electric dipole moment of the neutron in two-Higgs-doublet models with flavor changing couplings,” *Phys. Rev. D* **102** no. 9, (2020) 095009, [arXiv:1911.07291 \[hep-ph\]](#).
- [52] J. O. Eeg, “Electric dipole moment of the neutron from a flavor changing Higgs boson,” *Eur. Phys. J. C* **78** no. 12, (2018) 998, [arXiv:1611.07778 \[hep-ph\]](#).
- [53] T. Fukuyama, Y. Mimura, and Y. Uesaka, “Models of the muonium to antimuonium transition,” *Phys. Rev. D* **105** no. 1, (2022) 015026, [arXiv:2108.10736 \[hep-ph\]](#).
- [54] L. Willmann *et al.*, “New bounds from searching for muonium to anti-muonium conversion,” *Phys. Rev. Lett.* **82** (1999) 49–52, [arXiv:hep-ex/9807011](#).
- [55] R. Kitano, M. Koike, and Y. Okada, “Detailed calculation of lepton flavor violating muon electron conversion rate for various nuclei,” *Phys. Rev. D* **66** (2002) 096002, [arXiv:hep-ph/0203110](#). [Erratum: *Phys.Rev.D* 76, 059902 (2007)].
- [56] H.-Y. Cheng and C.-W. Chiang, “Revisiting Scalar and Pseudoscalar Couplings with Nucleons,” *JHEP* **07** (2012) 009, [arXiv:1202.1292 \[hep-ph\]](#).
- [57] T. Suzuki, D. F. Measday, and J. P. Roalsvig, “Total Nuclear Capture Rates for Negative Muons,” *Phys. Rev. C* **35** (1987) 2212.
- [58] **SINDRUM II** Collaboration, W. H. Bertl *et al.*, “A Search for muon to electron conversion in muonic gold,” *Eur. Phys. J. C* **47** (2006) 337–346.
- [59] **BaBar** Collaboration, B. Aubert *et al.*, “Searches for Lepton Flavor Violation in the Decays $\tau^+ \rightarrow e^+\gamma$ and $\tau^+ \rightarrow \mu^+\gamma$,” *Phys. Rev. Lett.* **104** (2010) 021802, [arXiv:0908.2381 \[hep-ex\]](#).
- [60] **MEG** Collaboration, A. M. Baldini *et al.*, “Search for the lepton flavour violating decay $\mu^+ \rightarrow e^+\gamma$ with the full dataset of the MEG experiment,” *Eur. Phys. J. C* **76** no. 8, (2016) 434, [arXiv:1605.05081 \[hep-ex\]](#).
- [61] **Muon g-2** Collaboration, D. P. Aguillard *et al.*, “Measurement of the Positive Muon Anomalous Magnetic Moment to

- 0.20 ppm,” *Phys. Rev. Lett.* **131** no. 16, (2023) 161802, [arXiv:2308.06230 \[hep-ex\]](#).
- [62] A. J. Buras, F. De Fazio, J. Girrbach, and M. V. Carlucci, “The Anatomy of Quark Flavour Observables in 331 Models in the Flavour Precision Era,” *JHEP* **02** (2013) 023, [arXiv:1211.1237 \[hep-ph\]](#).
- [63] M. Misiak and M. Steinhauser, “NNLO QCD corrections to the $\bar{B} \rightarrow X_s \gamma$ matrix elements using interpolation in m_c ,” *Nucl. Phys. B* **764** (2007) 62–82, [arXiv:hep-ph/0609241](#).
- [64] M. Misiak, A. Rehma, and M. Steinhauser, “Towards $\bar{B} \rightarrow X_s \gamma$ at the NNLO in QCD without interpolation in m_c ,” *JHEP* **06** (2020) 175, [arXiv:2002.01548 \[hep-ph\]](#).
- [65] M. Beneke, C. Bobeth, and R. Szafron, “Power-enhanced leading-logarithmic QED corrections to $B_q \rightarrow \mu^+ \mu^-$,” *JHEP* **10** (2019) 232, [arXiv:1908.07011 \[hep-ph\]](#). [Erratum: *JHEP* **11**, 099 (2022)].
- [66] LHCb Collaboration, R. Aaij *et al.*, “Search for the Rare Decays $B_s^0 \rightarrow e^+ e^-$ and $B^0 \rightarrow e^+ e^-$,” *Phys. Rev. Lett.* **124** no. 21, (2020) 211802, [arXiv:2003.03999 \[hep-ex\]](#).
- [67] R. Mohanta, “Implications of the non-universal Z boson in FCNC mediated rare decays,” *Phys. Rev. D* **71** (2005) 114013, [arXiv:hep-ph/0503225](#).
- [68] K. De Bruyn, R. Fleischer, R. Kneijens, P. Koppenburg, M. Merk, and N. Tuning, “Branching Ratio Measurements of B_s Decays,” *Phys. Rev. D* **86** (2012) 014027, [arXiv:1204.1735 \[hep-ph\]](#).
- [69] P. Gambino and M. Misiak, “Quark mass effects in anti-B \rightarrow X(s gamma),” *Nucl. Phys. B* **611** (2001) 338–366, [arXiv:hep-ph/0104034](#).
- [70] A. J. Buras, L. Merlo, and E. Stamou, “The Impact of Flavour Changing Neutral Gauge Bosons on $\bar{B} \rightarrow X_s \gamma$,” *JHEP* **08** (2011) 124, [arXiv:1105.5146 \[hep-ph\]](#).
- [71] C. Cornella, D. A. Faroughy, J. Fuentes-Martin, G. Isidori, and M. Neubert, “Reading the footprints of the B-meson flavor anomalies,” *JHEP* **08** (2021) 050, [arXiv:2103.16558 \[hep-ph\]](#).
- [72] J. Aebischer, A. J. Buras, and J. Kumar, “Kaon physics without new physics in ϵ_K ,” *Eur. Phys. J. C* **83** no. 5, (2023) 368, [arXiv:2302.00013 \[hep-ph\]](#).
- [73] J. Brod, M. Gorbahn, and E. Stamou, “Standard-Model Prediction of ϵ_K with Manifest Quark-Mixing Unitarity,” *Phys. Rev. Lett.* **125** no. 17, (2020) 171803, [arXiv:1911.06822 \[hep-ph\]](#).
- [74] HFLAV Collaboration, Y. Amhis *et al.*, “Averages of b -hadron, c -hadron, and τ -lepton properties as of 2021,” [arXiv:2206.07501 \[hep-ex\]](#).
- [75] G. Isidori, J. F. Kamenik, Z. Ligeti, and G. Perez, “Implications of the LHCb Evidence for Charm CP Violation,” *Phys. Lett. B* **711** (2012) 46–51, [arXiv:1111.4987 \[hep-ph\]](#).
- [76] E. Franco, S. Mishima, and L. Silvestrini, “The Standard Model confronts CP violation in $D^0 \rightarrow \pi^+ \pi^-$ and $D^0 \rightarrow K^+ K^-$,” *JHEP* **05** (2012) 140, [arXiv:1203.3131 \[hep-ph\]](#).
- [77] A. Sirlin, “Large $m(W)$, $m(Z)$ Behavior of the $O(\alpha)$ Corrections to Semileptonic Processes Mediated by W,” *Nucl. Phys. B* **196** (1982) 83–92.
- [78] M. Bordone, M. Jung, and D. van Dyk, “Theory determination of $\bar{B} \rightarrow D^{(*)} \ell^- \bar{\nu}$ form factors at $\mathcal{O}(1/m_c^2)$,” *Eur. Phys. J. C* **80** no. 2, (2020) 74, [arXiv:1908.09398 \[hep-ph\]](#).
- [79] F. U. Bernlochner, Z. Ligeti, M. Papucci, and D. J. Robinson, “Combined analysis of semileptonic B decays to D and D^* : $R(D^{(*)})$, $|V_{cb}|$, and new physics,” *Phys. Rev. D* **95** no. 11, (2017) 115008, [arXiv:1703.05330 \[hep-ph\]](#). [Erratum: *Phys.Rev.D* **97**, 059902 (2018)].
- [80] S. Iguro, Y. Omura, and M. Takeuchi, “Test of the $R(D^{(*)})$ anomaly at the LHC,” *Phys. Rev. D* **99** no. 7, (2019) 075013, [arXiv:1810.05843 \[hep-ph\]](#).
- [81] M. Blanke, A. Crivellin, S. de Boer, T. Kitahara, M. Moscati, U. Nierste, and I. Nišandžić, “Impact of polarization observables and $B_c \rightarrow \tau \nu$ on new physics explanations of the $b \rightarrow c \tau \nu$ anomaly,” *Phys. Rev. D* **99** no. 7, (2019) 075006, [arXiv:1811.09603 \[hep-ph\]](#).
- [82] S. Iguro, “Revival of H- interpretation of $RD^{(*)}$ anomaly and closing low mass window,” *Phys. Rev. D* **105** no. 9, (2022) 095011, [arXiv:2201.06565 \[hep-ph\]](#).
- [83] J. J. Zhang, C. S. Li, J. Gao, H. Zhang, Z. Li, C. P. Yuan, and T.-C. Yuan, “Next-to-leading order QCD corrections to the top quark decay via model-independent FCNC couplings,” *Phys. Rev. Lett.* **102** (2009) 072001, [arXiv:0810.3889 \[hep-ph\]](#).
- [84] A. J. Buras and F. De Fazio, “ ϵ'/ϵ in 331 Models,” *JHEP* **03** (2016) 010, [arXiv:1512.02869 \[hep-ph\]](#).
- [85] A. Lenz and G. Tetlalmatzi-Xolocotzi, “Model-independent bounds on new physics effects in non-leptonic tree-level decays of B-mesons,” *JHEP* **07** (2020) 177, [arXiv:1912.07621 \[hep-ph\]](#).
- [86] D. Bigi and P. Gambino, “Revisiting $B \rightarrow D \ell \nu$,” *Phys. Rev. D* **94** no. 9, (2016) 094008, [arXiv:1606.08030 \[hep-ph\]](#).
- [87] S. Jaiswal, S. Nandi, and S. K. Patra, “Extraction of $|V_{cb}|$ from $B \rightarrow D^{(*)} \ell \nu$ and the Standard Model predictions of $R(D^{(*)})$,” *JHEP* **12** (2017) 060, [arXiv:1707.09977 \[hep-ph\]](#).
- [88] G. Martinelli, S. Simula, and L. Vittorio, “ $|V_{cb}|$ and $R(D^{(*)})$ using lattice QCD and unitarity,” *Phys. Rev. D* **105** no. 3, (2022) 034503, [arXiv:2105.08674 \[hep-ph\]](#).
- [89] BaBar Collaboration, J. P. Lees *et al.*, “Extraction of form Factors from a Four-Dimensional Angular Analysis of $\bar{B} \rightarrow D^* \ell^- \bar{\nu}_\ell$,” *Phys. Rev. Lett.* **123** no. 9, (2019) 091801, [arXiv:1903.10002 \[hep-ex\]](#).
- [90] P. Gambino, M. Jung, and S. Schacht, “The V_{cb} puzzle: An update,” *Phys. Lett. B* **795** (2019) 386–390, [arXiv:1905.08209 \[hep-ph\]](#).
- [91] G. Eilam, J. L. Hewett, and A. Soni, “Rare decays of the top quark in the standard and two Higgs doublet models,” *Phys. Rev. D* **44** (1991) 1473–1484. [Erratum: *Phys.Rev.D* **59**, 039901 (1999)].
- [92] J. A. Aguilar-Saavedra, “Top flavor-changing neutral interactions: Theoretical expectations and experimental

- detection,” *Acta Phys. Polon. B* **35** (2004) 2695–2710, [arXiv:hep-ph/0409342](#).
- [93] **ATLAS** Collaboration, G. Aad *et al.*, “Search for flavour-changing neutral-current couplings between the top quark and the photon with the ATLAS detector at $\sqrt{s}=13$ TeV,” *Phys. Lett. B* **842** (2023) 137379, [arXiv:2205.02537 \[hep-ex\]](#). [Erratum: *Phys.Lett.B* 847, 138286 (2024)].
- [94] **LHCb** Collaboration, R. Aaij *et al.*, “Search for the lepton-flavour-violating decays $B_s^0 \rightarrow \tau^\pm \mu^\mp$ and $B^0 \rightarrow \tau^\pm \mu^\mp$,” *Phys. Rev. Lett.* **123** no. 21, (2019) 211801, [arXiv:1905.06614 \[hep-ex\]](#).
- [95] **BaBar** Collaboration, J. P. Lees *et al.*, “A search for the decay modes $B^{+-} \rightarrow h^{+-} \tau^+ l^-$,” *Phys. Rev. D* **86** (2012) 012004, [arXiv:1204.2852 \[hep-ex\]](#).
- [96] C. Cornella, J. Fuentes-Martin, and G. Isidori, “Revisiting the vector leptoquark explanation of the B-physics anomalies,” *JHEP* **07** (2019) 168, [arXiv:1903.11517 \[hep-ph\]](#).
- [97] M. C. Gonzalez-Garcia, M. Maltoni, and T. Schwetz, “NuFIT: Three-Flavour Global Analyses of Neutrino Oscillation Experiments,” *Universe* **7** no. 12, (2021) 459, [arXiv:2111.03086 \[hep-ph\]](#).
- [98] **Flavour Lattice Averaging Group (FLAG)** Collaboration, Y. Aoki *et al.*, “FLAG Review 2021,” *Eur. Phys. J. C* **82** no. 10, (2022) 869, [arXiv:2111.09849 \[hep-lat\]](#).
- [99] M. Czakon, U. Haisch, and M. Misiak, “Four-Loop Anomalous Dimensions for Radiative Flavour-Changing Decays,” *JHEP* **03** (2007) 008, [arXiv:hep-ph/0612329](#).
- [100] M. Beneke, C. Bobeth, and R. Szafron, “Enhanced electromagnetic correction to the rare B -meson decay $B_{s,d} \rightarrow \mu^+ \mu^-$,” *Phys. Rev. Lett.* **120** no. 1, (2018) 011801, [arXiv:1708.09152 \[hep-ph\]](#).
- [101] M. Czakon, P. Fiedler, T. Huber, M. Misiak, T. Schutzmeier, and M. Steinhauser, “The $(Q_7, Q_{1,2})$ contribution to $\bar{B} \rightarrow X_s \gamma$ at $\mathcal{O}(\alpha_s^2)$,” *JHEP* **04** (2015) 168, [arXiv:1503.01791 \[hep-ph\]](#).
- [102] **UTfit** Collaboration, M. Bona *et al.*, “New UTfit Analysis of the Unitarity Triangle in the Cabibbo-Kobayashi-Maskawa scheme,” *Rend. Lincei Sci. Fis. Nat.* **34** (2023) 37–57, [arXiv:2212.03894 \[hep-ph\]](#).
- [103] P. Sanyal, “Limits on the Charged Higgs Parameters in the Two Higgs Doublet Model using CMS $\sqrt{s} = 13$ TeV Results,” *Eur. Phys. J. C* **79** no. 11, (2019) 913, [arXiv:1906.02520 \[hep-ph\]](#).
- [104] **CMS** Collaboration, A. M. Sirunyan *et al.*, “Search for a light charged Higgs boson in the $H^\pm \rightarrow cs$ channel in proton-proton collisions at $\sqrt{s} = 13$ TeV,” *Phys. Rev. D* **102** no. 7, (2020) 072001, [arXiv:2005.08900 \[hep-ex\]](#).
- [105] **CMS** Collaboration, A. Tumasyan *et al.*, “A portrait of the Higgs boson by the CMS experiment ten years after the discovery,” *Nature* **607** no. 7917, (2022) 60–68, [arXiv:2207.00043 \[hep-ex\]](#).
- [106] **CMS** Collaboration, A. Hayrapetyan *et al.*, “Search for the lepton-flavor violating decay of the Higgs boson and additional Higgs bosons in the $e\mu$ final state in proton-proton collisions at $\sqrt{s} = 13$ TeV,” *Phys. Rev. D* **108** no. 7, (2023) 072004, [arXiv:2305.18106 \[hep-ex\]](#).
- [107] **ATLAS** Collaboration, G. Aad *et al.*, “Searches for lepton-flavour-violating decays of the Higgs boson into $e\tau$ and $\mu\tau$ in $\sqrt{s} = 13$ TeV pp collisions with the ATLAS detector,” *JHEP* **07** (2023) 166, [arXiv:2302.05225 \[hep-ex\]](#).
- [108] J. F. Kamenik, A. Korajac, M. Szewc, M. Tammario, and J. Zupan, “Flavor-violating Higgs and Z boson decays at a future circular lepton collider,” *Phys. Rev. D* **109** no. 1, (2024) L011301, [arXiv:2306.17520 \[hep-ph\]](#).
- [109] **ATLAS** Collaboration, G. Aad *et al.*, “Search for flavour-changing neutral tqH interactions with $H \rightarrow \gamma\gamma$ in pp collisions at $\sqrt{s} = 13$ TeV using the ATLAS detector,” *JHEP* **12** (2023) 195, [arXiv:2309.12817 \[hep-ex\]](#).
- [110] A. E. Cárcamo Hernández, S. Kovalenko, and I. Schmidt, “Precision measurements constraints on the number of Higgs doublets,” *Phys. Rev. D* **91** (2015) 095014, [arXiv:1503.03026 \[hep-ph\]](#).
- [111] M. Blanke, S. Iguro, and H. Zhang, “Towards ruling out the charged Higgs interpretation of the $R_{D^{(*)}}$ anomaly,” *JHEP* **06** (2022) 043, [arXiv:2202.10468 \[hep-ph\]](#).
- [112] J. Aebischer and B. Grinstein, “Standard Model prediction of the B_c lifetime,” *JHEP* **07** (2021) 130, [arXiv:2105.02988 \[hep-ph\]](#).
- [113] **ATLAS** Collaboration, G. Aad *et al.*, “A detailed map of Higgs boson interactions by the ATLAS experiment ten years after the discovery,” *Nature* **607** no. 7917, (2022) 52–59, [arXiv:2207.00092 \[hep-ex\]](#). [Erratum: *Nature* 612, E24 (2022)].
- [114] A. Abada, N. Bernal, A. E. C. Hernández, X. Marcano, and G. Piazza, “Gauged inverse seesaw from dark matter,” *Eur. Phys. J. C* **81** no. 8, (2021) 758, [arXiv:2107.02803 \[hep-ph\]](#).
- [115] C. Bonilla, A. E. Carcamo Hernandez, S. Kovalenko, H. Lee, R. Pasechnik, and I. Schmidt, “Fermion mass hierarchy in an extended left-right symmetric model,” *JHEP* **12** (2023) 075, [arXiv:2305.11967 \[hep-ph\]](#).